Study of radiotherapy resistance associated to EGFR/MAPK signaling pathway and its application in the rational design of a treatment with simvastatin in combination with cetuximab and radiotherapy (in experimental models of carcinoma)

Lara Isabel de Llobet Cucalón

UNIVERSITAT DE BARCELONA

STUDY OF RADIOTHERAPY RESISTANCE ASSOCIATED TO EGFR/MAPK SIGNALING PATHWAY AND ITS APPLICATION IN THE RATIONAL DESIGN OF A TREATMENT WITH SIMVASTATIN IN COMBINATION WITH CETUXIMAB AND RADIOTHERAPY (IN EXPERIMENTAL MODELS OF CARCINOMA)

Lara Isabel de Llobet Cucalón

2013

IDIBELL
Institut d'Investigació Biomèdica de Bellvitge

ICO
Institut Català d'Oncologia
Hospital Duran i Reynals

STUDY OF RADIOTHERAPY RESISTANCE ASSOCIATED TO EGFR/MAPK SIGNALING PATHWAY AND ITS APPLICATION IN THE RATIONAL DESIGN OF A TREATMENT WITH SIMVASTATIN IN COMBINATION WITH CETUXIMAB AND RADIOTHERAPY (IN EXPERIMENTAL MODELS OF CARCINOMA)

Memoria presentada por
Lara Isabel de Llobet Cucalón

Para optar al título de
Doctor por la **Universidad de Barcelona**

Este proyecto se ha realizado bajo la dirección del Dr. Josep Balart Serra, en el grupo de **Radiobiología Aplicada y Radioterapia Experimental** del **Laboratorio de Investigación Translacional** del *Instituto Catalán de Oncología – IDIBELL*.

Tesis adscrita al Programa de Doctorado en **Biomedicina**
de la **Facultad de Medicina** de la **Universidad de Barcelona**.
Tutor: Dr. Francesc Viñals Canals

Dr. Josep Balart Serra **Dr. Francesc Viñals Canals** **Lara I. de Llobet Cucalón**

Barcelona, 2013

A mis padres Mª Pilar y Paco

A mis hermanos Saúl, Andrea, David y Uli

Qué rápido han pasado estos 4 años en el laboratorio. Es difícil entender la importancia de los agradecimientos de una tesis doctoral hasta que no se ha terminado. En este momento te das cuenta de cuánto tienes que agradecer a tanta gente. Intentaré resumir en unas líneas la gratitud que siento hacia todas las personas que han estado presentes durante esta etapa, haciendo posible que hoy concluya esta tesis.

Quisiera dar las gracias en primer lugar a **Josep**, director de esta tesis, por acogerme en su grupo y permitirme llevar a cabo este trabajo. Por apoyarme siempre, por seguir en el barco pese a las adversidades que nos hemos ido encontrando y haber llegado juntos a buen puerto.

A **Pepe, Mila** y los técnicos de Radioterapia del ICO por su amabilidad a la hora de hacerme huecos entre pacientes para poder irradiar mis células y ratones adaptándose a mis horarios.

Agradecer sobre todo al grupo de angio por permitirme participar en sus seminarios y por haberme ayudado en el laboratorio. Gracias a **Francesc, Oriol, Mar, Agnès, Laura, Alba, Nicklas, Susana, Lidia, Gaby, Mercé**, **Marta V. y Marta B**. A **Mariona G**. y sus niñas **Helena, Adri, Ana A., Magali** y **Ana F**. Mención especial a **Mariona** y **Eli** por todos los buenos ratos y risas que hemos compartido dentro y fuera del laboratorio y por sus ánimos y apoyo. I a tu **Eli** en catalá i en majúscules: GRÀCIES! Ja saps que sense tu…

A todos los compañeros del laboratorio. Al grupo del comedor, por esas risas y temas variopintos: **Curro, Mireia**, **Natalia** y **Gorka**. Gracias a mis niñas que son 3 soles como 3 casas: **Sarita, Clara** y **Mónica** por todas esas risas y momentos compartidos. Y a **María** especialmente por su paciencia y amabilidad y su incalculable ayuda con todo. Al grupo de virus: **Raúl, Alba** (por ser un cielo), **Marta, Cris, Edu, Rafa, Luis, Miriam, Marcel, Ahmed** y **Carlos**. A mi bruixa **Helena**. A **Jack** por los buenos ratos. A **Alberto** por haber estado pendiente. A **Dori, Nadia, Gemma, Laura, Natalia, Thais** y **Olga**. Gracias a todos por estar ahí.

A **Samu**. Por sempre me arrancar um sorriso. Por me fazer desconcetar. Pelo curso intensivo de pelotense. Por me ajudar em tudo que pôde. Por sua alegria. Por me animar e estar sempre alí. Obrigada!!

A mis amigos de siempre **María Eugenia, Astrid, María Inés, Anita**, **Javi, Susana** e **Inés** que de alguna forma también han sufrido un poquito con esta tesis.

A mis compañeras de piso de los últimos meses **Ana, Mari** y **Kari** por hacerme la vida fácil en casa.

A las personas que, aunque no aparecen aquí con nombres y apellidos, han estado presentes de alguna forma durante el desarrollo de este trabajo y han hecho posible que hoy vea la luz.

A mi yayo y mi abuela, que tanto me enseñaron y a los que admiraré siempre.

A mi familia. A mis hermanos **Saúl, David, Andrea** y **Ángela**, por su ánimo y apoyo incondicional. Y a **Uli**, por haber existido.

En último lugar y muy especialmente, a mis padres **Mª Pilar** y **Paco**, por apoyarme siempre, por todos sus esfuerzos, por enseñarme que la vida es para los valientes, por su cariño, ternura y comprensión, por hacerme creer que podía hacerlo. Gracias por todo.

A todos mi más sincero agradecimiento.

INDEX

ABBREVIATIONS LIST

ABBREVIATIONS LIST

µ	Micro
AKT	Phosphatidylinositol 3-kinase/AKT-Protein Kinase B
APS	Ammonium persulfate
AR	Amphiregulin
ATCC	American Type Cell Collection
ATM	Ataxia telangiectasia mutated protein
ATP	Adenosine-5'-triphosphate
ATR	Ataxia telangiectasia and Rad-3 related protein
BrdU	5-Bromodeoxyuridine
BSA	Bovine serum albumin
BTR	Betacellulin
C225	Cetuximab
Cbl	Casitas B-lineage lymphoma
CD31	Cluster of Differentiation 31
CE	Clonogenic efficiency
CRC	Colorectal cancer
CSC	Cancer stem cell
D	Mean inactivation dose
DAPI	4',6-diamidino-2-phenylindole
DMEM	Dulbecco's Modified Eagle's Medium
DMSO	Dimethyl sulfoxide
DNA	Deoxyribonucleic acid
DNA-PK	DNA-dependent protein kinase
DNP	2,4-dinitrophenol
DSB	Double strand break
EDTA	Ethylenediaminetetraacetic acid
EGF	Epidermal growth factor
EGFR	Epidermal growth factor receptor
ELISA	Enzyme-linked immunoabsorbent assay
ER	Epiregulin
ERK 1/2	Extracellular-signal-regulated kinases 1 and 2
FACS	Fluorescence-activated cell sorting
FBS	Foetal Bovine Serum
g	Gram
Gy	Gray
h	Hour
HB-EGF	Heparin-binding EGF
HCl	Hydrochloric acid
HEPES	Hydroxyethyl piperazineethanesulfonic acid
HIF-1α	Hypoxia-inducible factor 1-alpha
HIV	Human immunodeficiency virus
HMG-CoA	3-hydroxy-3-methylglutaryl-coenzyme A

HNSCC	Head and neck squamous cell carcinoma
HPLC	High performance liquid chromatography
ICD-O-3	International Classification of Diseases for Oncology, 3rd Edition
IgG	Immunoglobulin G
iNOS	Inducible nitric oxide synthetase
IR	Ionizing radiation
JAK	Janus tyrosine kinase
kDa	Kilodaltons
KOH	Potassium hydroxide
KRAS	Ki- *Rat sarcoma*
LDL	Low density lipoprotein
LQ	Linear-Quadratic model
M	Molar
m	Metre
MAb	Monoclonal antibody
MAPK	Mitogen activated protein kinase
$MgCl_2$	Magnesium chloride
min	Minute
mL	Millilitre
mm^3	Square millimetre
MV	Megavolts
MW	Molecular weight
n	Nano
NADPH	Nicotinamide adenine dinucleotide phosphate
NaF	Sodium floride
NHEJ	Non homologous end joining repair
NO	Nitric oxide
NOS	Nitric oxide synthase
NR	Neuroregulins
NSCLC	non-small cell lung cancer
p	p-value
p	Phospho
PBS	Phosphate buffered saline
PCNA	Proliferating cell nuclear antigen
PCR	Polymerase chain reaction
PDGFR	Platelet-derived growth factor receptor
PECAM-1	Platelet endothelial cell adhesion molecule
PFGE	Pulsed-field gel electrophoresis
PI	Propidium iodine
PI3K	Phosphatidylinositol-3-kinase
Plc	Phospholipase C
PMMA	Poly-methyl methacrylate
PMSF	Phenylmethanesulfonyl fluoride
R	Resistant

RB	Retinoblastoma
RNA	Ribonucleic acid
RNAse	Ribonuclease
RNS	reactive nitrogen species
ROS	reactive oxygen species
RTK	Receptor tyrosine kinase
SCR	Tyrosine protein kinase
SDS	Sodium dodecyl sulfate
SDS-PAGE	Sodium dodecyl sulfate polyacrylamide gel electrophoresis
SEM	Standard error of the mean
Ser	Serine
SF	Surviving fractions
SF2	Surviving fraction at 2 Gy
Simva	simvastatin
SNAP	S-nitroso-N-acethylpenicillamine
SPF	Specific Pathogen Free
SSB	Single strand break
STAT3	Signal transducer and activator of transcription number 3
TBE	Tris-Borate-EDTA buffer
TBS	Tris Buffered Saline
TE	Tris-EDTA (Ethylenediaminetetraacetic acid) buffer
TEMED	N, N, N', N'-tetrametiletilenodiamine
TGF	Transforming growth factor
Thr	Threonine
TK	Tyrosine kinase
TNF	Tumor necrosis factor
TR	Tomoregulin
Tyr	Tyrosine
UV	Ultraviolet light
VEGF	Vascular endothelial growth factor
VEGFR	Vascular endothelial growth factor receptor
WT	Wild type
XRT	Radiation/radiotherapy

SUMMARY

1. INTRODUCCIÓN

Las células de nuestro organismo están programadas para seguir un patrón definido y ordenado de crecimiento y división celular. Una multiplicación descontrolada de éstas dará lugar al cáncer.

El cáncer es la primera causa de muerte en países desarrollados y la segunda causa, por detrás de las enfermedades cardiovasculares, en países en vías de desarrollo. Alrededor de 12,7 millones de individuos son diagnosticados cada año, de los cuales 7,6 millones mueren a causa del cáncer.

Cuando el ADN sufre daños, las células poseen mecanismos de reparación que se ponen en marcha. Sin embargo, si el daño no es reparable, puede inducirse la muerte de la célula o darse una mutación. La edad, la acumulación de sustancias químicas en el organismo, la radiación ionizante, algunos virus como los del papiloma, el SIDA o la Hepatitis B/C (entre otros), junto con otros factores que afecten al sistema inmunitario, incrementan la probabilidad de desarrollar cáncer.

La radioterapia es uno de los pilares del tratamiento del cáncer. De forma individual o combinada, es junto con la cirugía y la quimioterapia uno de los tratamientos en los que se basa la curación del cáncer. Aproximadamente un 60 % de los pacientes oncológicos reciben radioterapia en algún momento de la enfermedad. Las células pueden presentar resistencia a la radioterapia. Uno de los mecanismos más relevantes para la radiorresistencia depende de la activación de la vía de transducción de señales del EGFR y de las proteínas efectoras de esta vía, principalmente ERK1/2 y AKT. La resistencia celular mediada por EGFR se caracteriza por una mayor mitogénesis y habilidad de reparación del ADN, una sobreexpresión de proteínas anti-apoptóticas, estimulación de la angiogénesis y cambios en la motilidad y capacidad infiltrativa de las células (funciones determinadas por las proteínas ERK y Akt). Las células pueden activar la vía de señalización del EGFR en respuesta a distintas agresiones, reacción que evolutivamente se habría visto favorecida como mecanismo de supervivencia. La radioterapia puede

activar el EGFR independientemente de la presencia de ligandos del receptor, mecanismo que explica la repoblación acelerada durante la radioterapia (típica en tumores de cabeza y cuello). A la complicación que supone la aceleración de la proliferación de las células tumorales durante la radioterapia, viene a sumársele el hecho de que puede producirse una selección positiva de las células supervivientes tras la radioterapia basada en la hiperactividad de la señalización dependiente del EGFR. Para los cánceres que presentan sobreexpresión del EGFR, la actividad del EGFR conferiría resistencia a la radioterapia, por lo que el bloqueo de esta vía podría radiosensibilizar y ser una terapia eficiente.

El cetuximab es un potente anticuerpo monoclonal que se une específicamente al EGFR con una afinidad superior a la de los ligandos naturales, bloqueando la emisión de señales pro-supervivencia procedentes del EGFR. Este mecanismo de acción explica por qué el tratamiento concomitante con radioterapia y cetuximab mejora significativamente la supervivencia en pacientes con cáncer de cabeza y cuello (en los que EGFR suele estar sobreexpresado) y se ha convertido en una indicación estándar.

La eficacia de los tratamientos dirigidos contra dianas integradas en rutas de señalización molecular frecuentemente se ve ensombrecida por la resistencia intrínseca o adquirida. La existencia de vías alternativas, a través de las cuales las células escapan al bloqueo de una diana, es un mecanismo común de resistencia; este mecanismo ha inspirado tratamientos basados en el bloqueo simultáneo de distintas dianas.

Las estatinas inhiben la enzima 3-hidroxi-3-metilglutaril coenzima A (HMG-CoA) reductasa necesaria para catalizar la síntesis de mevalonato, precursor esencial de la molécula de colesterol. Son uno de los fármacos más utilizados en atención primaria, indicado en la prevención y tratamiento de la aterosclerosis secundaria a hipercolesterolemia. La reducción de los niveles de colesterol explica el efecto beneficioso de las estatinas sobre las placas de ateroma. Sin embargo, en pacientes con niveles normales de colesterol las estatinas mejoran la mortalidad y la morbilidad cardiovascular, sugiriendo que otros mecanismos de acción, además del de una disminución de la hipercolesterolemia, intervienen en este beneficio. La reducción de la

síntesis de colesterol puede influir en la composición de la membrana plasmática, especialmente en las regiones de máxima concentración de colesterol. Se ha relacionado funcionalmente la fluidez de estas regiones con la eficiencia en la emisión de señales celulares a partir de los receptores transmembrana. Asimismo, las estatinas inhiben la biosíntesis de isopreno y de sus derivados geranilpirofosfato y farnesilpirofosfato, productos intermediarios fundamentales para una señalización celular eficiente. Proteínas clave para ejecutar la transducción de señales que imprime EGFR, como son las proteínas G (proteínas RAS) y la proteína quinasa B/AKT, requieren de los derivados del isopreno para su relocalización funcional en la cara interna de la membrana plasmática. La inhibición de la proliferación celular (en la pared arterial) mediada por las estatinas reduciría la proliferación celular en la placa de ateroma y contribuiría a mejorar la evolución de la arteriosclerosis incluso en pacientes con niveles de colesterol normales. Si se tiene en cuenta que la proliferación descontrolada es una de las características esenciales del cáncer, parece razonable hipotetizar que una disminución en la proliferación o un incremento de la apoptosis inducido por estatinas sería una posible estrategia para el tratamiento del cáncer. Esta idea es todavía una hipótesis de trabajo, pero algunos datos epidemiológicos indican que la toma de estatinas se asocia con una mejor evolución tras un tratamiento con radioterapia o quimioterapia.

2. OBJETIVOS

Este proyecto de tesis doctoral consta de 3 objetivos específicos:

1- Desarrollo y caracterización de una línea celular radiorresistente para emplearla en la identificación de cambios asociados a la resistencia adquirida a radiación.

2- Implementación de un procedimiento para administrar radioterapia fraccionada a tumores xenoimplantados en ratones inmunodeprimidos usando un acelerador lineal de un hospital (como alternativa a la falta de instalaciones destinadas a la investigación con radiación).

3- Evaluar si la simvastatina incrementa el efecto antitumoral de la combinación de radioterapia y cetuximab en modelos derivados de carcinoma escamoso.

3. RESULTADOS

3.1. Generación y caracterización de una línea celular radiorresistente

Para el estudio de los posibles mecanismos implicados en la resistencia a radioterapia, se generó una línea celular resistente a radioterapia. Se utilizó la línea de carcinoma escamoso A431, la cual se sometió a dosis diarias crecientes de radiación ionizante hasta alcanzar una dosis total de 85 Gy en un periodo de 7 meses. Posteriormente se procedió a un proceso de selección celular a partir de las colonias con un crecimiento más vigoroso (selección clonal). Una subpoblación resistente denominada A431-R se expandió y se procedió a su caracterización comparándola con la parental A431-WT.

Se evaluó la radiosensibilidad de las células generadas A431-R y se observó que era ligeramente inferior a la de las parentales. Cuando se analizaron las curvas de supervivencia se observó que el hombro de la curva de las células A431-R era más pronunciado que el de las A431-WT y que el valor SF2 se incrementó de 0,62 a 0,75 ($p=0,024$). Adicionalmente, se calcularon los valores α y ß del modelo linear-cuadrático y la dosis media de inactivación (D). Se observó que la ratio $\alpha/ß$ se redujo de 12 Gy a 4,6 Gy para las células resistentes, como resultado principalmente de disminuir el componente α, lo que podría estar indicando que las células A431-R tendrían una mayor habilidad para reparar el daño radioinducido.

En vista de estos resultados, se determinó si las células A431-R habrían adquirido una mayor habilidad de reparación del ADN. Se observó que tras la fragmentación del ADN inducida por la irradiación, las células A431-R se mostraban más eficientes que las células parentales en el *rejoining* de los fragmentos de ADN. Se observó asimismo que

tras irradiación las células A431-R no sólo formaban más focos de H2AX (que indican complejos proteicos/ADN de reparación) que las células parentales, sino que además los resolvían más rápidamente. El incremento en la formación de focos de reparación junto con la rápida capacidad de eliminación de éstos, sugiere que las células A431-R podrían reparar las roturas de doble cadena de manera más eficaz que las parentales.

Se confirmó que las células A431-R habían adquirido una mayor motilidad durante el proceso de selección que les permitía migrar y reparar la herida del test de *wound healing* en un menor periodo de tiempo que las células parentales, comportamiento consistente con la adquisición de un fenotipo más agresivo.

Se evaluó el efecto de la radioterapia fraccionada en el crecimiento de tumores xenoimplantados en ratones atímicos. Los tumores que no recibieron tratamiento crecieron de forma similar para los dos tipos celulares, en cambio tras la radioterapia los tumores originados a partir de las células A431-R mostraban un crecimiento 1,8 veces mayor. Diferencia que se mantuvo o se incrementó al terminar la radioterapia durante el periodo de seguimiento. Se observó un mayor retraso del crecimiento y una menor tasa de recrecimiento en los tumores derivados de las células parentales, indicando que los tumores originados a partir de las células resistentes se veían menos afectados por la radiación.

Dado que las células A431 sobreexpresan el EGFR, se analizó esta vía de señalización para identificar posibles cambios originados durante el proceso de generación de las células A431-R. Se observó que las células A431-R mostraban niveles basales incrementados de pEGFR así como de pAKT y pERK1/2, proteínas implicadas en el crecimiento celular, la mitogénesis, la supervivencia, la reparación del ADN y la migración celular. Tras estímulo del receptor con el ligando EGF, ambos tipos celulares reaccionaron con un incremento de los niveles de oncoproteínas, destacando el incremento de pERK1/2. Tras irradiación, las células parentales incrementaron los niveles de pERK1/2; en cambio en las células A431-R no se observó un aumento en los niveles fosforilados de

EGFR, AKT o ERK1/2 sino que incluso se apreció una pequeña disminución respecto a los niveles basales.

Se analizaron los niveles del Factor de Crecimiento Endotelial Vascular (VEGF), factor crucial en la angiogénesis asociada a tumor y cuya secreción está también regulada por el EGFR y la radiación ionizante. Ambos tipos celulares respondieron a la radiación con un incremento de la secreción de VEGF, sin embargo la liberación de VEGF en respuesta a radiación fue más eficiente en las células A431-R, apoyando la teoría de que estas células estarían mejor adaptadas para resistir condiciones de estrés, como el estrés oxidativo inducido por radioterapia y serían capaces de promover la angiogénesis para facilitar su potencial oncogénico.

Recientemente se ha descrito el antígeno de superficie celular CD44 (marcador putativo para células madre cancerosas) como biomarcador para predecir el control local en el cáncer de laringe tratado con radioterapia, sugiriendo que este antígeno podría ser un indicador de radiorresistencia. Sin embargo, en las dos líneas celulares A431-WT y A431-R no se encontró expresión diferencial del antígeno CD44. Se observó que esta proteína se expresaba de forma constitutiva en la línea parental y en la línea derivada, independientemente de su grado de radiosensibilidad.

Se comparó la distribución de las fases del ciclo celular de ambas líneas celulares por si ésta podía haber influido en la radiosensibilidad, pero no se observaron diferencias relevantes.

Por último, se estudió si los dos tipos celulares mostraban un patrón de metilación diferente que pudiera estar relacionado con la diferente radiosensibilidad. Pese a encontrar diferencias importantes (más del 50%) en la metilación de 36 genes entre ambos tipos celulares, no pudimos vincular estas diferencias con la adquisición de radiorresistencia en las A431-R.

3.2. Descripción de la metodología utilizada para irradiar ratones.

Debido a la falta de literatura existente, se ideó e implementó un procedimiento para irradiar ratones inmunodeprimidos con xenoimplantes de tumores humanos utilizando un acelerador lineal en el departamento de oncología radioterápica del hospital.

Se inocularon células tumorales humanas por inyección subcutánea en la extremidad posterior derecha de ratones atímicos. Unos días antes de comenzar el tratamiento con radioterapia, los ratones se reubicaron en la zona de cuarentena de donde se podrían sacar del animalario y volver a estabularlos tras las sesiones de radioterapia diarias. A partir del primer día de tratamiento, cuando los tumores eran ya medibles y previamente al traslado al departamento de radioterapia, los ratones se anestesiaron en el animalario con el objetivo de inmobilizarlos para limitar la radiación al tumor. Tanto durante el transporte como durante la manipulación e irradiación de los ratones, se aplicaron medidas de asepsia. Tras las irradiaciones, se revertió la anestesia de los ratones en el animalario.

Junto con el departamento de medicina física se calcularon los parámetros para administrar la radioterapia siguiendo los mismos criterios que se utilizan para los pacientes. Se realizó una dosimetría para verificar la dosis que recibían los tumores así como la precisión del protocolo y se observó que existía una variación del 3% en las dosis de radiación que recibían los diferentes ratones en una misma sesión, y la variación era de 1,5% entre sesiones de diferentes días, confirmando que el procedimiento experimental empleado era homogéneo y reproducible.

Se sometió a los ratones controles a los mismos procedimientos que los que recibieron la radioterapia: anestesia, transporte fuera del animalario y reversión de la anestesia. Se apreció una ligera disminución de peso en los ratones que recibieron la radioterapia, pero ésta no fue significativa y se asumió que era debida a la exposición

parcial de la parte inferior derecha del hemiabdomen a la radiación, puesto que se encontraba demasiado próxima al tumor como para poder protegerla completamente del haz de radiación.

De esta forma se consiguió un diseño experimental en el que se minimizó la irradiación de los tejidos sanos de los ratones y se cumplió con los principios de irradiación estándar para el tratamiento humano.

3.3. Estudio de la combinación de simvastatina con cetuximab y radioterapia en modelos experimentales de carcinoma

Para evaluar si la simvastatina podría potenciar la combinación de cetuximab y radioterapia en carcinomas, se estudió en primer lugar si la adición de simvastatina al tratamiento estándar con cetuximab y radioterapia reducía la tasa a la que los cultivos celulares migraban para reparar la herida en los ensayos de *wound healing.* Se observó que la simvastatina dificultaba la cicatrización de las heridas en las células FaDu y A431-R.

Se evaluó si la simvastatina afectaba la proliferación de células tratadas con radioterapia y cetuximab en las líneas FaDu, A431-WT y A431-R. Se observó que tanto a las 48 como a las 72 horas, la proliferación se veía disminuida de forma significativa en las células tratadas con la triple combinación comparada con las células tratadas únicamente con cetuximab y radioterapia.

Se comprobó el efecto de los tratamientos en la supervivencia celular clonogénica y se vio que la triple combinación de simvastatina, cetuximab y radioterapia resultó en una menor supervivencia que la combinación de cetuximab y radioterapia para los tres tipos celulares analizados.

Para estudiar si el efecto de la simvastatina podría estar relacionado con la activación de la apoptosis o con un descenso en la proliferación, se estudió la incorporación de BrdU (marcador de células en fase de síntesis del ADN) en tumores

tratados durante 4 días con los esquemas: radiación y cetuximab o radiación, cetuximab y simvastatina. Con los 2 tipos de tratamientos se observó una disminución de la proliferación respecto a los tumores no tratados, sin embargo no se observaron diferencias entre la adición o no de simvastatina a la radioterapia y cetuximab en cuanto a la incorporación de BrdU en los 3 tipos celulares.

En cuanto a la apoptosis, se observó que el tratamiento con simvastatina, cetuximab y radioterapia incrementaba el número de células positivas para caspasa-3 activada (apoptosis) respecto al tratamiento de radioterapia y cetuximab sin simvastatina en cualquiera de los 3 tipos celulares. Además se comprobó mediante *western blot* en células FaDu que se incrementaron específicamente los niveles de la proteína caspasa-3 activada con dosis crecientes de simvastatina.

Se analizó el número de vasos en xenotumores tratados con la doble o la triple combinación y se observó que para las células FaDu la adición de simvastatina al tratamiento con cetuximab y radioterapia incrementaba el número de vasos, pero que éstos presentaban un diámetro menor comparado con los tumores tratados únicamente con cetuximab y radioterapia. En los tumores originados a partir de células A431-WT se apreció la misma tendencia al añadir simvastatina de observar un mayor número de vasos que con el tratamiento de cetuximab y radioterapia sin simvastatina, sin embargo en este caso el diámetro era similar con ambos tratamientos. En los tumores derivados de A431-R no se apreció este efecto sino que la adición de simvastatina al tratamiento con radiación y cetuximab tendía a reducir el número de vasos. En estos tumores, lo que sí se visualizó fue un mayor número de vasos (A431-R vs A431-WT) al tratar con radioterapia, resultado que encajaría con la mayor secreción de VEGF en las células A431-R tras irradiación (mencionado en el primer objetivo de este resumen).

Se estudió el efecto de la simvastatina sobre la vía de señalización del EGFR y se constató que la adición de la estatina al tratamiento con cetuximab y radioterapia reducía los niveles de ERK1/2, AKT y STAT3 fosforilados en las células FaDu. En las células A431-

WT se observó que la adición de simvastatina al tratamiento reducía significativamente los niveles de STAT3 fosforilado y se apreciaba una disminución en los niveles de ERK 1/2 aunque ésta no llegaba a ser significativa. En las células radiorresistentes A431-R se observó una disminución significativa en los niveles de EGFR, STAT3 y AKT fosforilados.

En último lugar se analizaron los niveles de colesterol de los xenotumores derivados de las células FaDu y se comprobó que los tumores tratados con simvastatina, cetuximab y radioterapia presentaban niveles de colesterol menores que los tumores no tratados y que los tumores tratados con cetuximab y radioterapia, pese a que las diferencias no llegaban a ser significativas.

4. DISCUSIÓN

El trabajo presentado se ha dividido en 3 partes. En la primera parte de este proyecto se desarrolló una línea celular resistente que utilizar para la identificación de cambios moleculares asociados a la adquisición de radiorresistencia. La identificación y comprensión de estos mecanismos es interesante no sólo a la hora de tratar la resistencia a radioterapia, sino también para la comprensión de las recurrencias tumorales que pueden darse tras la radioterapia.

La línea celular A431-R se desarrolló a partir de la parental A431-WT y se constató una disminución en la radiosensibilidad de ésta. En la radioterapia fraccionada una pequeña variación en la radiosensibilidad puede tener un mayor efecto en la respuesta posterior que la simple diferencia en una única fracción. El impacto clínico de este cambio es relevante ya que pequeños cambios en la ratio SF2 pasan de la radiocurabilidad del cáncer de mama a la resistencia del cáncer de melanoma.

Además de la resistencia a radiación, las células A431-R adquirieron una mayor eficiencia clonogénica y habilidades de crecimiento y de migración, propiedades asociadas con unos niveles basales incrementados de oncoproteínas y secreción de VEGF.

Estos hallazgos, al igual que otros publicados en la misma dirección, sugieren que las células tumorales desarrollarían respuestas adaptativas frente a agentes citotóxicos como la radiación ionizante, dirigidas a una ganancia de mecanismos moleculares para protegerse de dichos agentes. Diversas observaciones avalan esta idea: 1) la adquisición de radiorresistencia se encuentra asociada a niveles incrementados de glutatión en estado reducido; 2) en células tumorales resistentes se observan niveles bajos de radicales libres; 3) la reprogramación del metabolismo energético en las células tumorales con una mayor utilización de glucosa y un incremento en la producción de NADPH y de glutatión, y 4) la participación de proteínas oncogénicas como AKT, RAS o HIF1α en la respuesta molecular al estrés oxidativo apoyaría la noción de que la radiación induciría cambios globales.

Otro aspecto importante que debe tenerse en cuenta es que la supervivencia de la población de células madre cancerosas tras radioterapia es relevante para un control efectivo del cáncer ya que cuanto mayor sea el número de éstas menor será el control conseguido con la radioterapia. En nuestro trabajo se estudió la expresión del antígeno de superficie celular CD44, un presunto marcador de células madre, que se había validado como biomarcador predictivo en el control local con radioterapia del cáncer de laringe precoz. No se encontró una expresión diferencial del antígeno en las líneas celulares A431-WT y A431-R, sino que éste se expresó de forma constitutiva en las parentales y también así en las células hijas resistentes.

Para enfatizar el interés de los modelos isogénicos como el que generamos (A431-WT/A431-R), puede ser útil considerar algunas preocupaciones existentes en la clínica ante una reirradiación. A la hora de reirradiar se tiende a disminuir la dosis por fracción, con lo que se disminuye la toxicidad asociada a mayores fracciones. Esto es así porque la mayoría de carcinomas primarios tienen ratios α/ß alrededor de 10 Gy. Sin embargo, si una radioterapia previa indujo cambios en la biología del tumor y en su ratio α/ß, la respuesta frente a la radioterapia cambiaría. En el caso particular de las células A431-R

(con un α/ß de 4,6 Gy mientras que el de las A431-WT era de 12 Gy) un fraccionamiento mayor hubiera sido más eficiente en caso de una re-irradiación. Cuál sería la dosis más adecuada en estos casos es una discusión en la que los modelos isogénicos de radiorresistencia adquirida pueden contribuir.

En la segunda parte de este proyecto nos propusimos 4 objetivos para administrar radioterapia fraccionada a ratones inmunodeprimidos utilizando un acelerador lineal del hospital empleado para tratar pacientes. Primero, se minimizó la irradiación de los tejidos sanos adyacentes al tumor. En segundo lugar, se cumplió con los principios de irradiación estándar para el tratamiento humano. En tercer lugar, se incrementó la eficiencia y se redujo el tiempo necesario consiguiendo irradiar varios ratones al mismo tiempo. Y por último, el procedimiento era fácil de reproducir diariamente necesitando sólo 2 personas para llevarlo a cabo.

La mayor contribución de este trabajo fue demostrar que los efectos de la irradiación general o local no ponían en peligro la observación de la respuesta tumoral a la radiación. Asimismo, la ausencia de enfermedades infecciosas o contagiosas fue decisiva para el éxito de los experimentos y evidenciaba la eficacia de las barreras protectoras empleadas.

Dado que un número significativo de pacientes muestran resistencia al tratamiento convencional de radioterapia y cetuximab en el cáncer de cabeza y cuello localmente avanzado, en la tercera y última parte de este proyecto de tesis se exploró preclínicamente si la combinación de simvastatina con radioterapia y cetuximab merecería un mayor estudio. Se empleó la línea celular FaDu así como el modelo experimental 431-WT/A431-R. Los resultados obtenidos demostraron que la adición de simvastatina disminuía significativamente la proliferación y supervivencia clonogénica en células tratadas con radioterapia y cetuximab. La adición de simvastatina se asoció con un incremento de la apoptosis y una disminución de los niveles de oncoproteínas ERK1/2, AKT y STAT3 activadas.

El papel de las estatinas en la terapia contra el cáncer está despertando gran interés. En un estudio epidemiológico reciente se observó que la toma de estatinas reducía la mortalidad asociada al cáncer y un número de ensayos clínicos investigaron el efecto antitumoral de las estatinas.

Nuestro modelo A431-WT/A431-R es una herramienta útil a la hora de examinar nuevos tratamientos dirigidos a revertir la radiorresistencia. La adquisición de radiorresistencia basada en la explotación de una vía de señalización como la vía EGFR/MAPK hace que las células sean vulnerables al bloqueo de esa vía y/o de vías de escape alternativas. Si este estado adictivo de las células radiorresistentes se debilita con la adición de simvastatina, se podría conseguir reducir la resistencia celular. Así, los efectos del tratamiento pueden estudiarse en ambas sublíneas celulares (parental y derivada), y la comparación de ambas puede aportar información importante.

Este es, que tengamos constancia, el primer estudio *in vivo* que combina radioterapia, cetuximab y estatinas para mostrar un efecto antitumoral incrementado en carcinomas, aportando nuevos datos transnacionales que apoyan la investigación clínica con estatinas en oncología radioterápica.

5. CONCLUSIONES

Altas dosis de radiación fraccionada y una selección clonal es un método efectivo para desarrollar una línea celular isogénica radiorresistente y caracterizarla para evaluar tanto la biología de la resistencia a radiación como el tratamiento.

El nuevo par isogénico A431-WT/A431-R se caracteriza por la adquisición de un fenotipo agresivo en las células A431-R que consiste en una mayor reparación del ADN, mayor eficiencia clonogénica, crecimiento y migración más rápidos *in vitro*, notables

niveles basales de oncoproteínas relevantes, capacidades angiogénicas incrementadas y disminución significativa de la ratio α/ß.

La irradiación fraccionada de tumores xenoimplantados es viable empleando un acelerador médico lineal como alternativa a la falta de instalaciones destinadas a la investigación con radiación. El método implementado aquí permitió estudiar tanto la biología como el tratamiento de la resistencia a radiación en tumores.

La adición de simvastatina mejora la respuesta al tratamiento concomitante de radioterapia y cetuximab en células FaDu y A431-WT/A431-R tanto en cultivos como en tumores xenoimplantados. La adición de simvastatina a radioterapia y cetuximab disminuye la proliferación celular, la migración, la supervivencia clonogénica, la tasa de recrecimiento tumoral, los niveles de las oncoproteínas pAkt, pErk1/2 y pSTAT3 e incrementa la apoptosis en los tumores.

Con este trabajo preclínico aportamos evidencias que apoyan una mayor investigación básica y clínica de simvastatina en combinación con radioterapia y cetuximab para el tratamiento de los cánceres de cabeza y cuello localmente avanzados.

INTRODUCTION

1. CANCER

Normal cells in the body follow an orderly path of growth and division. Cancer is originated by the growth of the cells from a tissue due to the decontrolled and disordered multiplication of those cells. There are many different types of cancer and each one is classified by the type of cell that is initially affected, but all of them start being caused by the growth out of control of normal cells.

In a normal frame cells grow, divide, and die in an ordered way. Every cell has to follow its genetically programmed cell death, which is called apoptosis. In a person firsts years of life, normal cells rapidly divide until the individual reaches adulthood. After that, normal cells from the major part of the tissues only divide to replace cells that are already weathered or fading, and also to repair injuries. Cancer cells grow and inexorably divide instead of dying; they live longer than normal cells and produce new abnormal cells in an aberrant and permanent manner.

In cancer disease, pathological cells divide uncontrollably to form lumps or masses of tissue called tumours. Tumours can grow and lethally interfere with the normal body functions. Tumours that stay in one spot and demonstrate limited growth are generally considered to be benign. However, most tumours display a roster of cells that supply an unlimited number of cells, and have the ability to disseminate throughout the body using the blood or lymph systems (metastasis process).

1.1. Cancer today

Despite the fact that infectious diseases, including diarrhoea in children, are the most common cause of death in poor countries, cancer causes the death of one person every eight (more than malaria, AIDS and tuberculosis combined), being the leading cause of death in developed countries and the second one (after cardiovascular diseases) in developing countries. Cancer is an enormous global health burden concern, causing 12.7

millions of new cases every year from which 7.6 millions dye as a consequence of cancer disease (data from 2008) (Society 2008).

As a consequence of the growth and aging of the world population, cancer incidence gives rise. It is estimated that in 2030, about 21.4 million new cancer cases and 13.2 million cancer deaths are expected to occur (Society 2008).

1.2. Molecular basis of Cancer

Cancer cells often exhibit aberrantly structured chromosomes of various sorts: the loss of entire chromosomes, the presence of extra copies of others, and the fusion of the arm of one chromosome with part of another. These changes in overall chromosomal configuration expand the conception on how mutations can affect the genome. Alterations of overall chromosomal structure and number also constitute types of genetic change, and these changes can be considered to be the consequences of previous mutations. Aneuploidy (deviation from the euploid karyotype) is seen in many cancer cells. Often this aneuplody is consequence of the general chaos within the cancer cell. The loss of copies of one chromosome or the acquisition of extra copies can create a genetic configuration that somehow benefits the cancer cell and its runaway proliferation. DNA damage can be transmitted in germ cells as mutations alter the information content of genes, and consequently mutant alleles of a gene can be passed from parents to offspring (and therefore some types of cancer can be hereditary), however in most cases DNA is damaged as a consequence of environmental exposures of somatic cells to tobacco smoke, alcohol, chemicals derived from burning hydrocarbons or exposition to UV light (among other carcinogens).

Epigenetic events, including the repression of some genes through promoter methylation (addition of a methyl group to cytosines in CpG dinucleotides) and the de-repression of others through demethylation, also contribute importantly to tumour progression. Hypomethylation of promoters of tumour suppressor genes, homeobox genes and other sequences is also one of the most constant features of the cancer

genome. It has been described that hypomethylation (demethylation of normal methylated sequences), such as that observed in early adenomas, has a carcinogenic effect. Genome hypomethylation in tumours results in the activation of a group of germline-specific genes, which use primarily DNA methylation for repression in somatic tissues (De Smet, De Backer et al. 1996). These genes, which were discovered because their activation in tumours led to the expression of tumour-specific antigens, were named cancer-germline genes. In example, in colon carcinoma progression, half of the tumours were found to acquire mutant K-ras gene, and the genomes of most evolving, pre-neoplastic growths were found to suffer hypomethylation (loss of methylated CpGs). Although the precise contribution of hypomethylation to tumour progression remains unclear, some evidence suggests that it creates chromosomal instability. Operating through still not well known mechanisms, hypomethylation contributes to chromosomal instability, and the latter state favours acceleration of the rate of tumour progression (Weinberg 2007).

Usually when DNA is damaged, there exist mechanisms of repair and in case the damage can not be repaired, the cell is meant to dye. As we age, there is also an increase in the number of possible cancer-causing mutations in DNA. This makes age, together with the accumulation of chemicals in the body, an important risk factor for cancer. Several viruses have also been linked to cancer, as they alter gene function or contribute to carcinogenesis associated with inflammation, such as: human papillomavirus (a cause of cervical, anal canal and oropharynx cancers), hepatitis B and C (causes hepatocarcinoma), and Epstein-Barr virus (a cause of Burkitt's lymphoma and nasopharynx carcinoma). Human immunodeficiency virus (HIV) - and other factors that suppress or weaken the human immune system - inhibits the body's ability to fight infections and increases the chance of developing cancer.

Vogelstein and Kinzler suggested that cancer should be due to the alteration of multiple genes rather than to a defect in one only gene (Vogelstein and Kinzler 2004). They proposed three key types of genes responsible for the carcinogenic process:

- *Oncogenes* are responsible for controlling cell proliferation and growth. They are often mutated encoding proteins that have higher activity than wild forms of these proteins. In other instances non-aberrant proteins are expressed at high levels, e.g. by an increased number of gene copies. Activated oncogenes confer resistance to cells, decreasing cell death and giving rise to increased mitosis rates. Genes that codify for membrane receptors with tyrosine kinase activity, or for proteins that are members of the signalling pathways, or for those ones that serve as transcription factors, and genes encoding for proteins involved in the cell cycle control are potentially oncogenes. Some examples for oncogenes are *RAS*, *MYC*, *SRC* and *EGFR*.
- *Tumour suppressor genes* (or anti-oncogenes) slow down cell division. They typically represent a brake whereas oncogenes accelerate mitogenesis. When tumour suppressor genes suffer inactivating mutations, or there is a loss or reduction in their function, they permit and sometimes elicit carcinogenesis. Most of those genes codify for proteins involved in DNA repair and cell cycle control. Retinoblastoma (*RB*) and p53 (*TP53*) are classical examples of tumour suppressor genes.
- *Stabilizing genes* (or caretakers), which normal function is not related to proliferation regulation, but is related to the maintenance of the genome integrity. Inactivating mutations occurring in these genes lead to an increase of mutations accumulation in the cell. An example of stabilizing gene is *BRCA1,* associated with breast cancer, and mismatch repair mutations (mainly in the MLH1 and MSH2 genes). BRCA1 is mutated in the Lynch syndrome, and is also responsible of hereditary nonpolyposis colorectal cancer.

1.3. Cancer classification

The international standard for the classification and nomenclature of histologies is the International Classification of Diseases for Oncology, 3rd Edition (ICD-O-3). Based on

the ICD-O-3, cancers may be classified into six major categories according to their tissue type (Mandal 2004):

1. *Carcinomas* are originated from the epithelia. They account for 80 to 90 % of all cancer cases since epithelial tissues are the most abundantly found in the body from being present in the skin to the covering and lining of organs and internal passageways.
2. *Sarcomas* originate in connective and supportive tissues including muscles, bones, cartilage and fat.
3. *Leukemias* originate in leukocytes in the bone marrow. When cancerous, the bone marrow begins to produce excessive immature white blood cells that fail to perform their usual activities and the patient is often prone to infection, anaemia and coagulophaties.
4. *Myelomas* are, together with leukemias, a type of hematological cancer that specifically originates in the plasma cells of bone marrow. Plasma cells are aberrant forms of differentiated lymphocytes B.
5. *Lymphomas* are also a type of blood cancer that originates in differentiated lymphocytes associated with lymphatic system. Unlike the leukemias, which affect the blood and are called “liquid cancers”, lymphomas are “solid cancers”. These may affect lymph nodes at specific sites like stomach, brain or intestines. These lymphomas are referred to as extranodal lymphomas.
6. *Mixed types.* These tumours have two or more components of the cancer. Some of the examples include mixed mesodermal tumour, adenosquamous carcinoma and teratocarcinoma. Germinal cancers are another type that involves embryonic tissues.

1.4. Head and neck cancer

There are two types of carcinomas: adenocarcinoma and squamous cell carcinoma. Adenocarcinoma develops in an organ or gland and squamous cell carcinoma originates in the squamous epithelium. Adenocarcinomas may affect mucus membranes

and are first seen as a thickened plaque-like white mucosa. These are rapidly spreading cancers.

Cancers that are known collectively as head and neck cancers usually begin in the squamous cells that line the moist, mucosal surfaces inside the head and neck region. These squamous cell cancers are often referred to as squamous cell carcinomas of head and neck. Head and neck cancers can also begin in the salivary glands, but salivary gland cancers are relatively uncommon. Salivary glands contain many different types of cells that can become cancerous, so there are many different types of salivary gland cancer (Institute 2013).

Cancers of the head and neck are further categorized by the area of the head or neck in which they begin. These areas are described and labelled in the image of head and neck cancer regions on the next page (Figure 1).

- **Oral cavity**: Includes the lips, the front two-thirds of the tongue, the gums, the lining inside the cheeks and lips, the floor (bottom) of the mouth under the tongue, the hard palate (bony top of the mouth), and the small area of the gum behind the wisdom teeth.
- **Pharynx**: The pharynx (throat) is a hollow tube about 5 inches long that starts behind the nose and leads to the oesophagus. It has three parts: the **nasopharynx** (the upper part of the pharynx, behind the nose); the **oropharynx** (the middle part of the pharynx, including the soft palate [the back of the mouth], the base of the tongue, and the tonsils); and the **hypopharynx** (the lower part of the pharynx).
- **Larynx**: The larynx, also called the voicebox, is a short passageway formed by cartilage just below the pharynx in the neck. The larynx contains the vocal cords. It also has a small piece of tissue, called the epiglottis, which moves to cover the larynx to prevent food from entering the air passages.

- **Paranasal sinuses and nasal cavity**: The paranasal sinuses are small hollow spaces in the bones of the head surrounding the nose. The nasal cavity is the hollow space inside the nose.
- **Salivary glands**: The major salivary glands are in the floor of the mouth and near the jawbone, and they produce saliva.

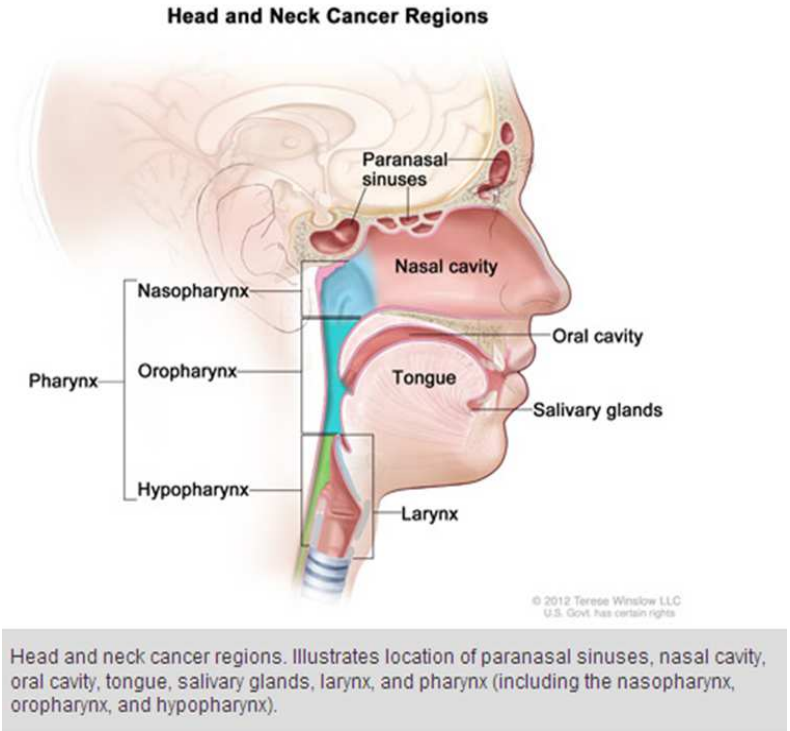

Head and neck cancer regions. Illustrates location of paranasal sinuses, nasal cavity, oral cavity, tongue, salivary glands, larynx, and pharynx (including the nasopharynx, oropharynx, and hypopharynx).

Figure 1. Head and Neck Cancer Regions (from National Cancer Institute)

At diagnosis, head and neck squamous cell carcinomas are confined to the primary site in one-third of the patients, have spread to the regional nodes in half the patients, and are metastatic to other organs in 15% of the patients. The corresponding 5-year overall survival rates are 80%, 50%, and 25% respectively, although these rates can vary substantially with the primary site, the histological type, and the efficacy or sensitivity of oncologic therapies (Thariat, Yildirim et al. 2007).

2. HER/ErbB RECEPTORS FAMILY WITH FOCUS ON EGFR

Among the mechanisms by which cancer cells acquire the capacity for autonomous proliferation there is the uncontrolled production of growth factors (specific secreted molecules that promote mitosis and cell growth) and their receptors, frequently placed on the cell membranes to which growth factors selectively bind. Both processes trigger a series of intracellular signals that ultimately lead to proliferation of cancer cells, induction of angiogenesis and metastasis. Of the many receptors and their associated signalling proteins identified, the epidermal growth factor receptor (EGFR) or HER/ErbB family has been widely acknowledged as playing a crucial role in tumourigenesis and disease progression. Most of the human epithelial cancers are characterized by functional activation of growth factors and receptors, and in head and neck cancers the epidermal growth factor receptor (EGFR) family or HER/ErbB family is commonly overexpressed (Ciardiello and Tortora 2008). Overexpression of EGFR has also been described as a mechanism of resistance to radiotherapy and chemotherapy, which add a plus of difficulty to treat cancers successfully.

EGFR/HER/ERBB family comprise four distinct transmembrane receptors: EGFR/HER1/ErbB1, HER2/ErbB-2/neu, HER3/ErbB-3, and HER4/ErbB4, and is a receptor network intimately involved in neoplastic cell growth, proliferation and survival (Contessa, Abell et al. 2006). EGFR activation initiates a signalling cascade that promote tumourigenesis via cell proliferation, survival, migration, adhesion and differentiation (Mass 2004).

The members of the EGFR/HER/ErbB family are made up of an extracellular region (ectodomain), which contains approximately 620 amino acids, a short hydrophobic transmembrane region, and a cytoplasmatic tyrosine kinase (TK) domain (endodomain). The extracellular ligand-binding domain of each family member comprises up to four subdomains, L1, CR1, L2, and CR2, where “L” signifies a leucine-rich repeat domain and “CR” is a cysteine-rich region (Lurje and Lenz 2009).

Interestingly, two ErbB/HER family members (ErbB1 and ErbB4) are autonomous; when bound to ligand growth factors, they induce receptor dimerization and generate a cascade of intracellular signals, which ultimately lead to cell proliferation, migration and differentiation. In contrast, the other two receptors of the ErbB receptor network (ErbB2 and ErbB3) are non-autonomous. As such, ErbB2 (HER2) lacks the capacity to interact with a growth factor ligand, while ErbB3 features defective TK activity. Despite this, both ErbB2 and ErbB3 form heterodimeric complexes with other members of the EGFR/HER family that are capable of generating potent downstream signalling (Lurje and Lenz 2009).

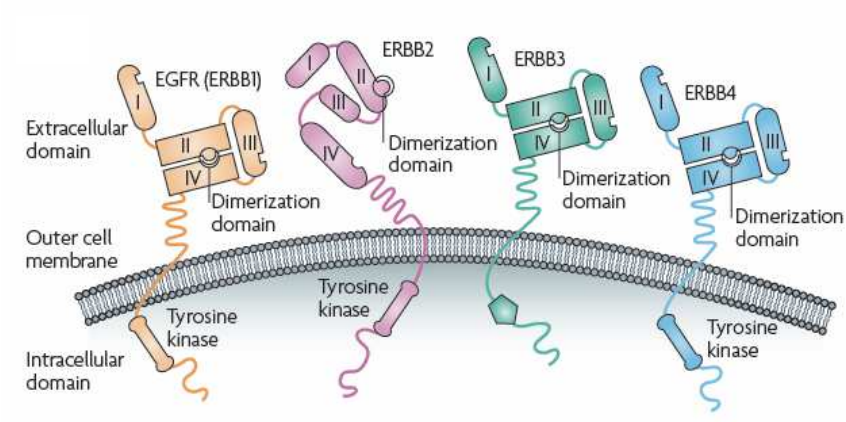

Figure 2. The four members of the ERBB family. Image from Baselga J. et al, 2009**.**

Each member of the EGFR/HER/ErbB family has its cognate ligands, whose binding induces receptor dimerization and activation of intracellular protein tyrosine kinase with subsequent initiation of numerous downstream signalling events (Lurje and Lenz 2009). Ligand growth factors such as epidermal growth factor (EGF), transforming growth factor (TGF)-α and amphiregulin (AR) bind specifically to the ectodomain of EGFR/HER1/ErbB1. While epiregulin (ER), heparin-binding EGF (HB-EGF) and betacellulin (BTC) bind to the EGFR/HER1/ErbB1 or to ERBB4, Neuroregulins (NR, heregulin and neuregulin) bind to the ectodomain of ErbB3 and ErbB4 and tomoregulin (TR) specifically binds to the ectodomain of ERBB4. However, there is no specific cognate ligand for ErbB2 (Normanno, De Luca et al. 2006).

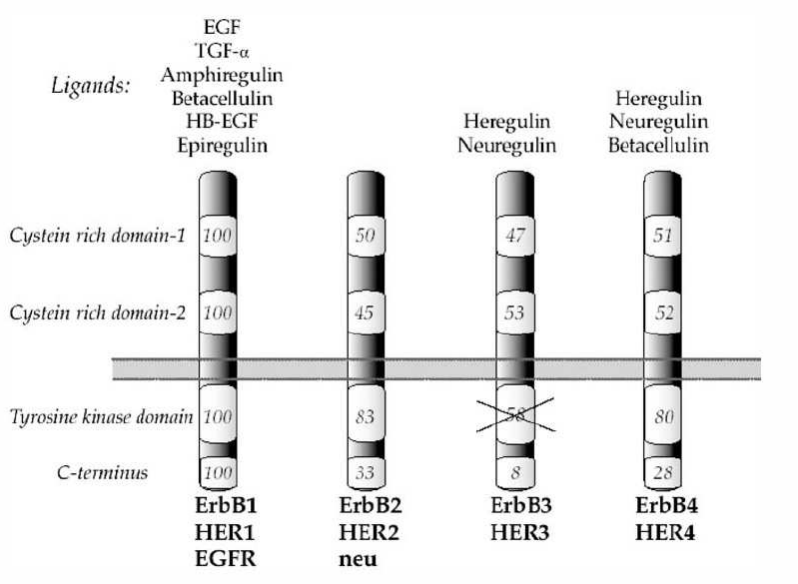

Figure 3. Schematic diagram of the four ErbB family members and their natural ligands. Image from Harari et al, 2004.

2.1. EGFR/HER1/ErbB1

The receptor tyrosine kinase EGFR (also known as HER1or ErbB1) of the ErbB (HER) family, plays pivotal roles in the etiology of cancer and is frequently aberrantly activated or overexpressed in many cancers; reason why it has been an attractive target for cancer therapy. It is a transmembrane receptor of 170 kDa which contains a single polipeptidic chain of 1186 amino acids. This transmembrane glycoprotein contains an extracellular ligand binding domain and an intracellular receptor tyrosine kinase (RTK) domain.

2.1.1. Ligands

Ten different ligands can selectively bind to each EGFR/HER/ErbB receptor. After the binding of a ligand to a single-chain receptor, the receptor forms a dimer that signals within the cells by activating receptor autophosphorylation through tyrosine kinase activity.

ErbB receptors can also be activated by ionizing radiation to produce downstream cytoprotective signalling through mitogen activated protein kinase cascade (MAPK) and phosphatidylinositol-3-kinase (PI3K) signal transduction cascades (Carter, Auer et al. 1998; Contessa, Hampton et al. 2002). This adaptive response to radiation produces radioresistance and accounts for at least part of the mechanism of accelerated repopulation during tumour regrowth (Schmidt-Ullrich, Contessa et al. 1999).

2.1.2. Binding

Binding of ligands to the extracellular domain of EGFR/HER/ErbB receptors induces the formation of receptor homo or heterodimers, and subsequent activation of the intrinsic tyrosine kinase domain. All possible homo and heterodimeric receptor complexes between members of the EGFR/HER/ErbB family have been identified in different systems. Receptor activation leads to phosphorylation of specific tyrosine residues within the cytoplasmic tail (Normanno, De Luca et al. 2006).

2.1.3. Dimerization

EGFR/HER/ErbB receptors are monomeric in the absence of ligand. Each receptor is fundamentally an inactive monomer that dimerizes in response to ligand binding. Ligand binding to Erbb receptors seems to induce a conformational change in the folder structure of the molecule that exposes the dimerization domain; this step is required for dimer formation and functional activation of EGFR, ERBB3 and ERBB4. Thus, the binding of a ligand to the extracellular domains alters the spatial configuration of the EGFR and consequently promotes homo- and heterodimerization and subsequent activation.

This process takes the form of homodimerization with a receptor of the same type or heterodimerization with another member of the EGFR/HER/ErbB family. This dimerization process results in receptor activation through tyrosine kinase mediated phosphorylation of the cytoplasmic domains that produces a biochemical “trigger” that

starts a cascade of metabolic events constituting a complex downstream signalling network, leading to various effects on specific aspects of cell function (Wells 1999).

The extracellular domain of each ErbB receptor consists of four subdomains (I–IV). Subdomains I and III (also called L1 and L2) have a beta helical fold and are important for ligand binding. Moreover, direct receptor–receptor interaction is promoted by a beta hairpin (also termed dimerization loop) in subdomain II. In the crystal structure of the extracellular domain of EGFR bound to EGF, the dimerization loop protrudes from EGFR and mediates interaction with another EGFR molecule leading to the formation of a dimer composed of two 1:1 receptor/ligand complexes (Normanno, De Luca et al. 2006). In contrast, the structure of ErbB-3 (inactive EGFR) is characterized by intramolecular interactions between domains II and IV. The structure of ErbB-2 extracellular region differs significantly from that of EGFR and ErbB-3. In the absence of a ligand, ErbB-2 has a conformation that resembles the ligand-activated state with a protruding dimerization loop. In this conformation, domains L1 and L2 are very close and this interaction makes ligand binding impossible, explaining why ErbB-2 has no ligand (Normanno, De Luca et al. 2006).

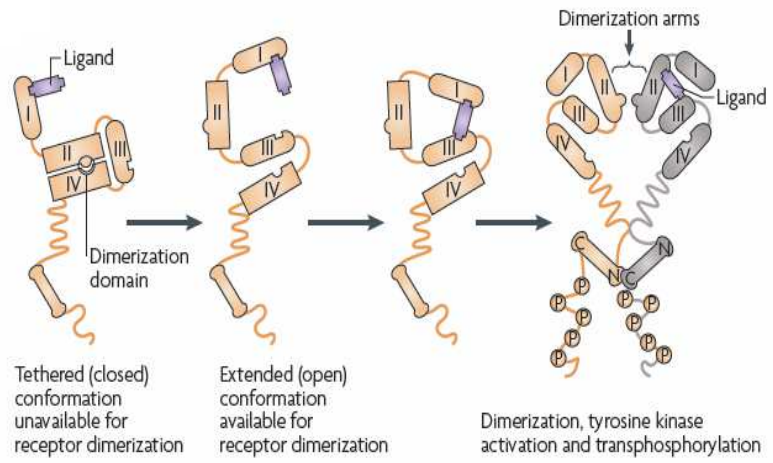

Figure 4. Conceptualization of the receptor conformational change on ligand binding. Image from Baselga J. et al, 2009.

2.1.4. Phosphorylation

After receptor dimerization, transactivation of the tyrosine kinase portion of the dimmer moiety occurs as each receptor activates its partner by phosphorylation. The phosphorylation event allows the recruitment and activation of downstream proteins and a signalling cascade is initiated, and may result in cancer cell proliferation, apoptosis blockade, invasion and metastasis activation and stimulation of tumour-induced neovascularization (Ciardiello and Tortora 2008).

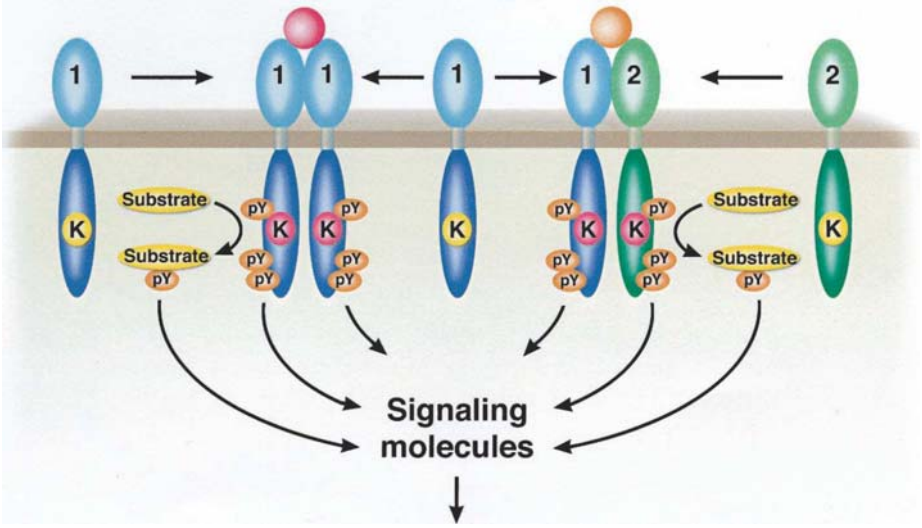

Figure 5. After EGFR dimerization, activation of the intrinsic protein kinase activity occurs, resulting in tyrosine autophosphorylation. Image from Mendelsohn et al, 2003.

2.1.5. Signalling pathways

HER/ErbB signalling system comprises a highly complex and interactive multilayered network. Signals are initiated at the cell surface, where the interaction of the ligand and the receptor takes place, and the resulting receptor dimerization and activation relays on and amplifies the signal via an intricate system of proteins, enzymes, and small-molecule secondary messengers (Yarden and Sliwkowski 2001). This process of signal transduction culminates in the nucleus, where gene control and protein transcription are modified, producing effects on key cellular regulatory processes, such as

differentiation, adhesion, cell cycle, growth, migration, and apoptosis. Dysregulated receptor function and disruptions in any or all downstream processes may result in cell transformation and malignancy.

2.1.6. Ligand independent EGFR activation

There have been described other mechanisms able to induce phosphorylation of EGFR in a ligand-independent manner, such as:

- *Transactivation*. Some proteins are able to phosphorylate tyrosine residues from the receptor intracellular region. As example, growth hormone and prolactin activate the receptor in an indirect manner through Janus tyrosine kinase 2 (JAK2) (Normanno, De Luca et al. 2006). SRC protein is also able to phosphorylate tyrosine residues 845 and 1101 of the EGFR (Biscardi, Maa et al. 1999).

- *In response to a stress situation.* The receptor can be activated in response to cytotoxic agents (Khan, Heidinger et al. 2006; Lee, Vivanco et al. 2006). However, the receptor can also be activated in response to ionizing radiation (Schmidt-Ullrich, Mikkelsen et al. 1997; Dittmann, Mayer et al. 2005). It has been reported that ionizing radiation (IR) stimulates the phosphorylation of EGFR tyrosines in MCF-7, A431 and A549 cells, causing an accelerated growth as adaptive response (Schmidt-Ullrich, Mikkelsen et al. 1997; Schmidt-Ullrich, Contessa et al. 2003; Dittmann, Mayer et al. 2005; Dittmann, Mayer et al. 2009). To date, the mechanism involved in EGFR activation in response to oxidative stress is still uncertain, but the enzyme nitric oxide synthase (NOS) is activated in response to radiation. The activation of this enzyme generates nitric oxide (NO), which induces the autophosphorylation of EGFR in Y1173 and the activation of the signalling pathways downstream EGFR. Even though the mechanism by which nitric oxide mediates tyrosine phosphorylation of EGFR remains still unknown, nitrosylation of EGFR is critical because the ionizing radiation and NO donor, S-nitroso-N-acethylpenicillamine (SNAP), increased the levels of nitrotyrosine of EGFR. In addition, inhibition of NOS/EGFR in combination with ionizing radiation decreased cell proliferation, suggesting a potential

strategy for enhancing the effectiveness of radiotherapy by targeting EGFR (Lee, An et al. 2008).

2.1.7. Internalization into the nucleus

The common outcomes following the activation of the EGFR-mediated downstream pathways in cancer cells are altered gene activities, leading to un-controlled tumour proliferation and apoptosis. High levels of EGFR were found in the nuclei of cancer cells and primary tumours including, those of skin, breast, bladder, cervix, adrenocorticoid, thyroid, and oral cavity. Some emerging evidences suggest the existence of a direct mode of the EGFR pathway that is distinct from the traditional transduction pathway. This novel route of EGFR signalling involves cellular transport of EGFR from the surface of the cell to the nucleus without apparent intermediate players, as well as the association of nuclear EGFR complex with gene promoters, and the transcriptional regulation of the target genes. Although the nature and pathological consequences of the nuclear EGFR pathway remain elusive, accumulating evidences suggest its association with increased tumour cell proliferation and poor survival rate in patients (Lo, Hsu et al. 2006).

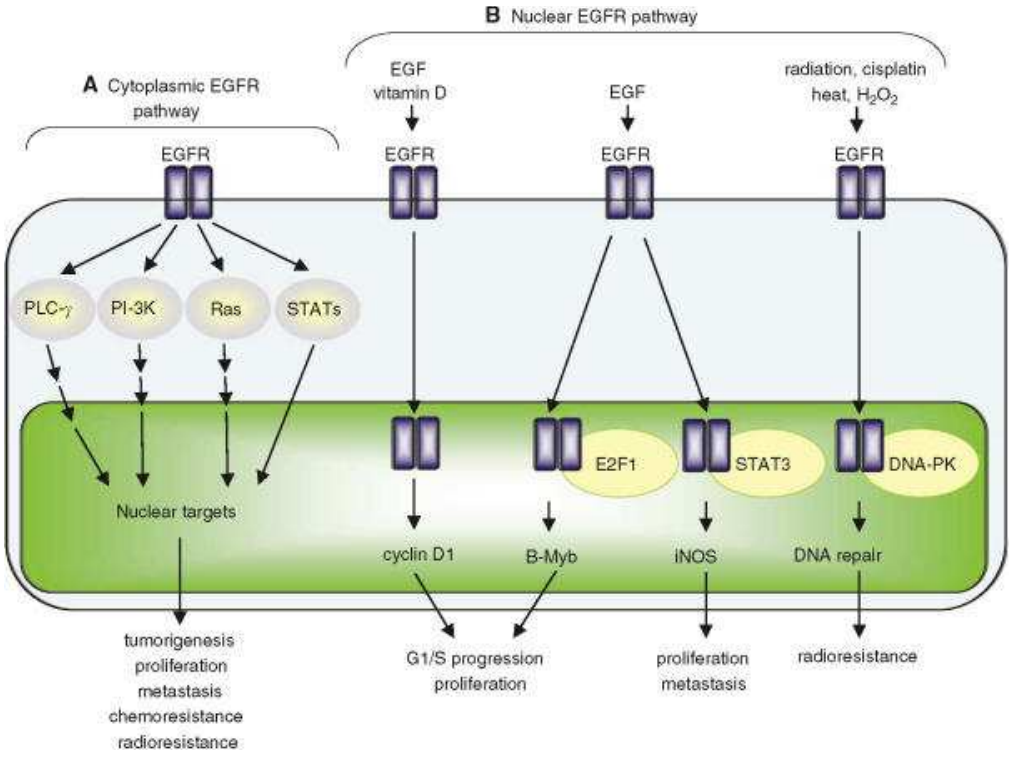

Figure 6. Cytoplasmic/traditional and nuclear modes of the EGFR signalling pathway. The EGFR signalling pathway exerts its biological effects via two major modes of actions, namely, cytoplasmic/traditional (A) and nuclear (B) modes. Image from Lo and Hung, 2006.

Receptor stimulation by growth factors binding results in a rapid endocytosis and degradation of both the receptor and the ligand. It has been observed that ligand binding induces receptor clustering in coated pits on the cell surface, followed by endocytosis, migration to multivesicular bodies and eventual degradation by lysosomal enzymes (Lo, Hsu et al. 2006), a process that is interrupted in kinase-negative receptor mutants suggesting that tyrosine kinase activity of receptors is crucial for receptor degradation/function and prevention of the recycle to the cell surface for reutilization (Ullrich and Schlessinger 1990). The rapid endocytosis and degradation of the activated EGFR and others receptors tyrosine kinase attenuates and protects cells from the signalling in response to growth factor stimulation (Lo, Hsu et al. 2006).

Some studies suggest that the oncogenic protein Cbl (Casitas B-lineage lymphoma) plays a role in the regulation of EGFR and PDGFR (Platelet-derived growth

factor receptor) degradation. Cbl protein contains several subdomains, including an SH-2 like domain that is responsible for binding to activated receptors tyrosine kinase, and a RING finger domain that functions as ubiquitin ligase. Binding of EGFR to Cbl leads to the ubiquitination of the receptor and the subsequent degradation by the proteosome (Joazeiro, Wing et al. 1999). In addition, dimerization of activated receptors results in the phosphorylation of the tyrosine kinase of Cbl that results in an attractive docking site and binding for downstream effector such as PI-3 kinase (Schlessinger 2000; Lo, Hsu et al. 2006).

EGFR localization in the nucleus has been observed in cancer cell lines, primary tumours, and also in non tumourigenic tissues under diverse physiologic conditions. This nuclear importation of the receptor from the surface can occur in a ligand dependent or independent manner. For cell surface receptors whose nuclear importation is ligand-dependent, it has been speculated that receptor internalization caused by ligand binding can serve as initial step for its transport from the cell surface to the nucleus (Lo, Hsu et al. 2006).

Even though EGFR transcriptional targets are related to proliferation, tumourigenesis and tumoural progression, the role of EGFR nuclear pathway remains still uncertain and deserves further investigation. Nonetheless, EGFR has been demonstrated to have three main roles once is in the nucleus (Dittmann, Mayer et al. 2009):

- Transcription cofactor. Through physic and functional interactions, EGFR can be associated to STAT3 and E2F1 leading to transduction of several mitogenic proteins among these cyclin D1, iNOS (inducible nitric oxide synthetase) and B-Myb oncoprotein.

- Proliferating cell nuclear antigen (PCNA) phosphorylation. EGFR induces the phosphorylation of a specific tyrosine of the PCNA in a dependent manner, stabilizing his union to the chromatin, a process that is linked to DNA repair (and cell resistance to genotoxic damage inflicted by ionizing radiation).

- Regulation of DNA repair induced by genotoxic agents. In addition, nuclear EGFR is associated through physical interactions with the phosphorylation at the residue T2609 of the DNA-dependent protein kinase (DNA-PK), which has a role during DNA non homologous end joining (NHEJ) repair. The inhibition of nuclear EGFR would reduce DNA-PK activity, decrease DNA NHEJ repair, and increase DNA residual damage lowering A549 cells survival. On the other hand, radiation increases nuclear EGFR transport and furthermore, resulted in stabilization and activation of DNA-PK (T2609).

2.2. EGFR and cancer

Aberrant expression or activity of EGFR has been strongly linked to the genesis of several human epithelial cancers. The EGFR messenger RNA and protein are overexpressed in dysplastic lesions and even in histologically normal surrounding mucosa, suggesting that EGFR hyperactivity plays an important role in cancer (Ang, Andratschke et al. 2004; Harari 2004). In general, EGFR overexpression correlates with a more aggressive clinical course and is associated to bad prognosis and resistance to cytotoxic gents, including ionizing radiation. In particular, EGFR is overexpressed in head and neck squamous cell carcinoma (HNSCC), non-small cell lung cancer (NSCLC), colorectal cancer (CRC), breast cancer, pancreatic cancer and brain cancer, although high levels of EGFR have been correlated with a decrease in the survival of other cancers such as bladder, ovarian, uterus and oesophagus (Mendelsohn and Baselga 2003; Harari 2004).

The main mechanisms by which the EGFR can be constitutively activated are the 1) autocrine production of ligands, 2) receptor overexpression and 3) several types of mutations (Thariat, Yildirim et al. 2007).

- *Increase in the production of ligands*. Autocrine production of TGF-α is frequently observed. TGF-α and EGF are usually coexpressed with the EGFR in different types of cancer, and are considered to act in an autocrine and paracrine manner,

driving to the constitutive activation of the receptor and leading to an uncontrolled tumoural growth (Thariat, Yildirim et al. 2007). Ligands can be secreted by macrophages, T cells, and keratinocytes in response to tissular damage (might be elicited by ionizing radiation), but can also be secreted by the own tumoural cells. Aberrant production of ligands is the main cause of excessive function of EGFR in cancer.

- *Increase in the levels of EGFR*. High EGFR expression is often associated with poor prognosis in several malignant tumours (breast, lung, bladder, and head and neck cancers) (Mendelsohn and Baselga 2003). The ability that cells have to transform can be due to a constitutive activation of the receptor caused by spontaneous dimerization originated by a combination of the following alterations:
    - An amplification of the EGFR gene
    - Physical proximity of the receptors (increasing dimerization chance)
    - Potentiation of the transcription of the EGFR gene

  Unfortunately, high EGFR expression is not a robust predictor of the therapy response as indicates clinical investigation with EGFR inhibitors (Harari 2004).

- *Mutations*. Apart from gene amplification, aberrant receptor activation can also be due to EGFR mutations and can confer oncogenic activity. Among the most frequent mutation of the EGFR and the best characterized, is the truncated EGFR encoding by EGFRvIII gene. EGFRvIII protein is frequently detected in glioblastomas and in HNSCCs. The deletion of exons 2 to 7 in its extracellular domain confers a constitutive activation. This mutant form of the EGFR that arise from gene rearrangement results in ligand-independent receptor activation and impaired receptor downregulation. Other activating mutations of the EGFR are observed in the kinase domain, as mainly demonstrated in non-small-cell lung cancer. Regulation of EGFR function has also been observed in cases presenting polymorphisms in intron 1. Transactivation by other ErbB receptors, mutated or not, can also lead to a gain of function (Thariat, Yildirim et al. 2007).

2.3. Anti-EGFR strategies

There are several potential strategies for targeting the EGFR, including low-molecular weight (MW) tyrosine kinase inhibitors that interfere with receptor signalling; monoclonal antibodies (MAbs) that interfere with receptor signalling; MAbs serving as carriers of radionuclides, toxins, or prodrugs; antisense oligonucleotides or ribozymes that block receptor translation (Yamazaki, Kijima et al. 1998; Ciardiello, Caputo et al. 2001); and prevention of receptor trafficking to the cell surface with intracellular single chain Fv fragments of antibodies (Jannot, Beerli et al. 1996). Of these approaches, monoclonal antibodies and the low-molecular weight tyrosine kinase inhibitors are in the most advanced stages of clinical development. As a result of their effects on the receptor and downstream signalling, anti-EGFR MAbs and the low-MW tyrosine kinase inhibitors interfere with a number of key cellular functions regulated by the receptor that explain their antitumour effects such as cell-cycle arrest, potentiation of apoptosis, inhibition of angiogenesis, inhibition of tumour-cell invasion and metastasis, and augmentation of the antitumour effects of chemotherapy and radiotherapy (Mendelsohn and Baselga 2003). Although antitumour activity is significant, responses have been seen in only a minority of the patients treated. However, in some clinical trials, anti-EGFR agents enhanced the effects of conventional chemotherapy and radiation therapy.

2.3.1. Low-MW inhibitors

The low-MW inhibitors compete with ATP for binding to the tyrosine kinase portion of the ErbB receptor family and abrogate the receptor's catalytic activity. Due to the homology (> 80%) in the kinase domain between EGFR and HER2, some of these small molecules (lapatinib) can inactive both EGFR homodimers and EGFR/HER2 heterodimers being reflected in low EGFR-mediated transactivation of the potent ErbB2 tyrosine kinase. These small molecules are also able to block the catalytic activity of EGFRvIII mutants that lack the extracellular binding domain and prevent ligand-independent activation of EGFR kinase activity (Mendelsohn and Baselga 2003).

2.3.2. Monoclonal antibodies

Monoclonal antibodies against EGFR bind to the easily accessible extracellular domain of the receptor and compete with the ligand binding to the receptor. EGFR natural ligands generally fall into two classes: high affinity or low affinity. High affinity ligands (EGF, TGF-α, HB-EGF, and BTC) bind with a dissociation constant (K_d) between 1 and 100 nM, while low affinity ligands (AR, EPR, and EPG) show a K_d greater than 100 nM (Jones, Akita et al. 1999; Ozcan, Klein et al. 2006). The murine MAb 225 and its chimeric human-murine derivative cetuximab (IMC-C225, Erbitux ImClone Systems In, New York, NY) bind to the EGFR receptor with high affinity (Kd= 0.39 nM for cetuximab), compete with ligand binding, and block the activation of receptor tyrosine kinase by EGF or TGF-α (transforming growth factor alpha) (Kawamoto, Sato et al. 1983; Sato, Kawamoto et al. 1983; Gill, Kawamoto et al. 1984). In addition, C225 induces antibody-mediated receptor dimerization, which results in receptor downregulation, and this effect may be important for its growth-inhibitory capacity (Fan, Lu et al. 1994).

2.3.2.1 Cetuximab

Cetuximab interacts exclusively with domain III of the soluble extracellular region of EGFR, partially occluding the ligand-binding region on this domain and preventing the receptor from adopting the extended conformation required for dimerization, disrupting both ligand binding and receptor dimerization.

Among the available anti-EGFR MAbs, cetuximab has been the one furthest ahead in clinical development. Cetuximab is an immunoglobulin G1 chimeric mouse- human monoclonal antibody that specifically targets the extracellular domain of EGFR, able to block EGF or TGF-α induced EGFR phosphorylation and activation. It was demonstrated to be a potent inhibitor of the proliferation and growth of cultured cancer cells that have an active autocrine EGFR loop and was capable of inducing complete regressions of well-established human tumour xenografts overexpressing EGFR (Goldstein, Prewett et al.

1995). Cetuximab has been also shown to effectively inhibit the growth of tumours expressing EGFR in cancer patients, as a result almost all EGFR-positive tumour cells can be targets for cetuximab, such as colorectal, lung, prostate, head and neck, ovarian, oesophagus, thyroid, liver and pancreatic carcinomas (Huang, Bock et al. 1999; Prewett, Hooper et al. 2002; Giaccone 2005). The downstream AKT and MAPK activation by EGF is often inhibited with cetuximab incubation. However, cetuximab treatment do not inhibit activation of HER2-HER2 homodimers (Patel, Bassi et al. 2009). To date, cetuximab has been approved for patients with colorectal and head and neck cancers (primary and also recurrent or metastatic cancers) (2006; Bonner, Harari et al. 2006).

3. RADIOTHERAPY

3.1. Mechanism of action radiotherapy

Radiotherapy consists on the medical use of ionizing radiation to directly treat cancer. It is one of the current pillars of cancer treatment as a primary therapy to definitively shrink tumours or as adjuvant modality to eradicate remaining cancer cells left by previous surgery or chemotherapy. Approximately 60% of oncologic patients undergo radiotherapy at some stage of the disease and an important part of them receive it with curative intention, including solid cancers and leukemias.

Exposure of cells to clinically relevant doses of ionizing radiation causes significant nuclear DNA damage: 1000 single-strand breaks, 40 double-strand breaks and 3000 damaged bases per gray (Gy) (Ward 1994). Ionizing radiation produces DNA damage mainly through the release of reactive oxygen and nitrogen species (ROS and RNS, respectively).

3.2. Biologic targets in radiotherapy

Ionizing radiation activates cytoplasmic signal transduction pathways involved in cell proliferation and antiapoptotic mechanisms, including growth factor receptors, changes in cytoplasmic Ca^{2+} levels and stress-response kinases (Ward 1994). The understanding of the molecular basis of cell killing and subsequent cell reactions to overcome radiation-induced cell killing (radiation resistance) has led to the implementation of new strategies broadly called bioradiotherapy. Currently, these biology-driven treatment strategies focus on: 1) radiation-induced inter and intracellular communication and signalling; 2) micro-environmental factors; 3) biological/molecular imaging; 4) DNA-damage response and repair mechanisms, and 5) tumour profiling, biomarkers and molecular targeting (Rodemann and Wouters 2011).

Nowadays, in the particular field of radiation resistance, a substantially burden of research is addressed to the development of drugs against specific biological targets responsible of the cancer cell resistance. For a successful design it is mandatory that the putative targets were:

- overexpressed in a high proportion of tumours frequently treated with radiation
- not expressed in normal tissues surrounding the tumour
- related to a low locoregional control after radiotherapy treatment
- associated to already known mechanisms of radioresistance

These substances against biological targets can act directly over tumour cells or stroma cells (as do the anti-angiogenic therapies) (Rodemann and Wouters 2011). Some clinical trials demonstrated a positive correlation between overexpression of EGFR in tumours and poor response to treatments (reviewed in (Mendelsohn and Fan 1997; Woodburn 1999; Mendelsohn 2000)). In addition, some studies have been carried out with other potential targets to combine with radiotherapy, such as HER2/neu (involved in cell growth and differentiation), TP53 (tumour suppressor gene involved in cell cycle transition, DNA repair and apoptosis), Bcl-/BAX (pro and anti-apoptotic genes), cyclin D

(kinase modulating G1-S phase expression in the cell cycle) or angiogenic factors (Huang, Wei et al. 2012 ; Toulany, Minjgee et al. 2010 ; Haffty and Glazer 2003).

3.3. Radiotherapy and EGFR

The eradication of tumour cells by the radiologic treatment can be overshadowed by the hyperactivity of the Epidermal Growth Factor Receptor (EGFR).

Despite the fact that clinical trials have demonstrated positive relationship between overexpression of EGFR in tumours and poor tumour response to treatments, the specific evidence on the correlation between tumour EGFR expression and response to radiotherapy is still scarce, likely indicating that radiation resistance is a multifaceted trait of cancer. However, several evidences support the negative role of EGFR in radiotherapy. For instance, in a preclinical study, tumours with higher EGFR protein levels were shown to be less responsive to radiation (Milas, Mason et al. 2003). In another study it was observed a positive correlation between the expression of cyclin D1, a surrogated downstream sensor of EGFR signalling and poorer tumour radioresponse (Milas, Akimoto et al. 2002). But not only in the laboratory there are evidence, EGFR was shown to be a strong predictor of tumour resistance to radiotherapy in a relatively homogenous group of patients with head and neck cancer of advanced stage (mainly stages III/IV) (Milas, Mason et al. 2003).

3.3.1. EGFR and cell radiosensitivity

Ligand binding to EGFR, such as EGF, can protect tumour cells from radiation damage and this radioprotective effect can be prevented by cells treatment with specific antibodies to the EGFR. Anti-EGFR antibodies render tumour cells more sensitive to radiation (Balaban, Moni et al. 1996; Huang, Bock et al. 1999; Huang and Harari 2000).

The radioprotective effect of EGFR ligands is attributed to the increase of mitogenesis and in the number of radioresistant S-phase cells. A rise in the level of

intracellular glutathione has been also documented (Wollman, Yahalom et al. 1994). At molecular level, EGFR is activated in response to irradiation, and can activate the Mitogen Activated Protein Kinase (MAPK) pathway to a level similar to that observed by physiologic EGF concentrations (Qiao, Yacoub et al. 2002). A short activation of the MAPK cascade has been correlated with increased proliferation, via both increased Cyclin D1 expression and an increased ability to progress through the G1-S transition. In contrast, prolonged elevation of MAPK activity has been demonstrated to inhibit DNA synthesis, via induction of the cyclin dependent kinase inhibitor proteins p16 and p21 (Park, Qiao et al. 2000). Radiosensitizing effect of the antibodies was associated with enhanced radiation-induced apoptosis (Balaban, Moni et al. 1996; Huang, Bock et al. 1999) and inhibition of cellular repair mechanisms elicited by ligand-binding/receptor activation (Huang and Harari 2000).

3.3.2. Activation of EGFR by radiation

Ionizing radiation can mimic the action of EGFR ligands and activate EGFR signalling. Ionizing radiation induces the intracellular generation of nitric oxide by endogenous nitric oxide synthase (NOS), which is required for the rapid activation of EGFR tyrosine phosphorylation (IR-mediated) (Lee, An et al. 2008). Irradiation of human breast and squamous carcinoma derived cell lines induced EGFR phosphorylation followed by activation of transduction pathways, including Raf-1 and MAPK as well as AKT protein. Activation of EGFR-mediated signals stimulated cell proliferation, which may underline acceleration of tumour clonogen repopulation during the course of fractionated radiotherapy. It has been described that in A431 cell line, following EGFR tyrosine phosphorylation induced by radiation, the increase in the production of IP_3 due to the activation of PLC represents one immediate downstream effector of the EGFR activation (Schmidt-Ullrich, Mikkelsen et al. 1997; Schmidt-Ullrich, Dent et al. 2000).

Tumour cells respond to radiation by involving protective survival mechanisms, and these mechanisms are more effective in tumours resistant to radiation therapy.

Overall, EGFR has been demonstrated to be an important molecular target for cancer therapy. Targeting EGFR as a therapeutic strategy is particularly effective when agents such as cetuximab (monoclonal antibody that blocks EGFR signalling) are combined with radiotherapy. It was described how EGFR was abnormally activated in epithelial cancers (including head and neck cancer), where the tumour cells expressed high levels of EGFR. Radiation increases the expression of EGFR in cancer cells, and blockade of EGFR signalling sensitizes cells to the effects of radiation. Bonner et al. described how cetuximab enhanced the cytotoxic effects of radiation in squamous-cell carcinoma (Harari and Huang 2001). Thus, EGFR serve as a predictor of tumour treatment outcome by radiotherapy and as a therapeutic target to enhance the efficacy of radiotherapy.

3.3.3. The linear-quadratic model

The linear quadratic model is used to fit radiation survival data to a continuously bending curve:

$$\text{Surviving Fraction} = e^{\alpha D - ßD2}$$

Where D is the dose, and α and ß are constants. The linear component, a measure of the initial slope, termed alpha, represents single-hit killing kinetics due to irreparable DNA damage, and dominates the radiation response at low doses. The quadratic component of cell killing, termed beta, represents multiple-hit killing and causes the curve to bend at higher doses. The ratio alpha/beta is the dose at which the linear and the quadratic components of cell killing are equal. The more linear the response to killing of cells at low radiation dose, the higher is the value of alpha, and the greater is the radiosensitivity of the cells.

4. STATINS

4.1. General point of view for statins

Cholesterol is a fundamental structural component of mammalian cell membranes and is essential for cellular proliferation. Statins are the most efficient and safe agents for reducing endogenous cholesterol. They are used in the prevention and treatment of arteriosclerotic vascular disease derived from hypercholesterolemia (Shepherd, Cobbe et al. 1995). They reduce the endogenous cholesterol synthesis by competitively inhibiting the principal enzyme involved: 3-hydroxy-3-methylglutaryl-coenzyme A (HMG-CoA) reductase, which converts HMG-CoA into mevalonic acid.

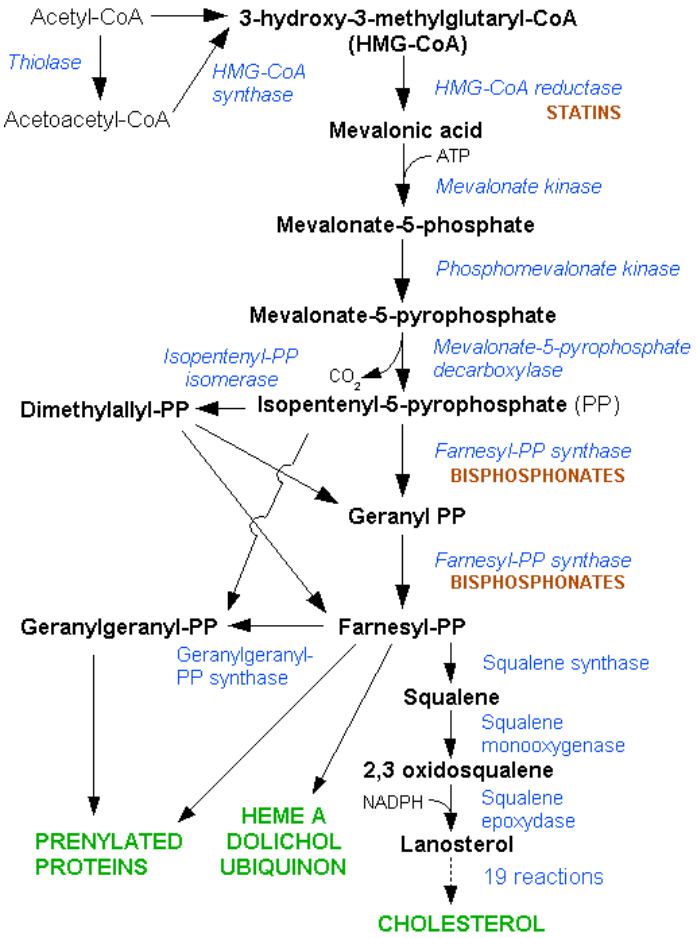

Figure 7. Cholesterol synthesis pathway. Image from International Union of Basic and Clinical Pharmacology.

Statins target cytosolic HMG-CoA reductase. They inhibit the enzyme by altering its conformation when they bind to its active site. The change in conformation at the active site makes these drugs very effective and specific. Nevertheless, even in patients with normal levels of cholesterol, statins improve cardiovascular mortality and morbidity, suggesting that other mechanisms of action distinct from the decrease of the hypercholesterolemia are involved in this benefit (Downs, Clearfield et al. 1998). Reduction of cholesterol synthesis can influence the composition of the plasma membrane, specially the regions with highest cholesterol concentration. Notably, the efficiency in the emission of cellular signalling from transmembrane receptors had been functionally associated to the fluidity of those regions (Simons and Toomre 2000).

Mevalonate, the product of HMG-CoA reductase reaction, is the precursor for cholesterol, but also for many other non-steroidal isoprenoid derivates such as farnesil and geranylgeranyl residues.

A variety of proteins have covalently attached isoprenoid groups, mainly farnesyl and geranylgeranyl residues. Many prenylated proteins are associated with intracellular membranes and mutating their prenylation sites blocks their membrane localization. Prenylation, or isoprenylation, or lipidation is the addition of hydrophobic molecules to a protein or chemical compound. The hydrophobic prenyl group (3-methyl-but-2-en-1-yl) can act to anchor its attached protein to the membrane.

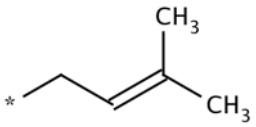

Figure 8. Prenyl group structure

Prenylation also mediates protein-protein interactions. Many intracellular signalling molecules are prenylated proteins. The trimeric G protein has a geranylgeranylated subunit (gamma), allowing this signalling protein to be inserted in the cell membrane near specific membrane receptors and to receive extracellular signals.

Another important class of prenylated molecules are the components of Ras family, which are farnesylated and intermediate the Ser/Thr/Tyr kinases activities of membrane receptors from the cell surface (Edwards and Ericsson 1999). Although statins are well tolerate, high doses can produce hepatotoxicity and miopathy due to the inhibition of ubiquinone (coenzyme Q10), a downstream product in mevalonic acid pathway. Ubiquinone supplements should be considered in these cases.

4.2. Clinical use

Statins are efficient and widely used drugs in the treatment of lipid disorders, especially hypercholesterolemia. Statins modulates a series of processes leading to:

1) Reduction of the accumulation of esterified cholesterol into macrophages.

2) Increase of endothelial NOS (which has neuroprotective effect in experimental models of cerebral infarction).

3) Reduction of the inflammatory process, and increase stability of the atherosclerotic plaques.

4) Restoration of both platelets activity and the coagulation process.

5) Inhibition of tumour cells growth and enhancement of intracellular calcium mobilization.

6) Induction of a reduction of the formation of osteoclasts in rodents (Bellosta, Ferri et al. 2000), and reduction in the number of bone fractures (Meier, Schlienger et al. 2000).

7) Finally and the most important clinical use of statins is that they have led to important progresses in the primary and secondary prevention of coronary disease. Numerous clinical studies have correlated the reduction of blood cholesterol induced by these compounds with the reduction of the number of major coronary events, as well as general mortality in coronary patients (Vaughan, Gotto et al. 2000).

4.3. Classification of statins

Statins can be classified under different classification criteria, including: how they are obtained, the way they are metabolized in the liver, the physic-chemical properties and the specific activity they have (Stancu and Sima 2001).

1). Statins classification according to their obtention:

- Some statins are obtained by synthesis: fluvastatin, atorvastatin, and cerivastatin (which was withdrawn from the world pharmaceutical market in 2001, after 31 patients died by acute renal failure caused by rhabdomyolysis).
- Others are obtained after fungal fermentation: lovastatin, pravastatin, and simvastatin.

2). Statins classification according to their liver metabolism:

All statins have the liver as target organ, which retains a percentage between 46-80% of the dose.

- Some statins follow the citocrom P450 (CYP 3A4) pathway for their liver metabolism: lovastatin, simvastatin and cerivastatin.
- Other statins follow the CYP 2C9 pathway, such as fluvastatin.
- Pravastatin is metabolized differently (Lennernas and Fager 1997).

3). Statins classification according to their physico-chemical properties:

- Some statins are hydrophobic: lovastatin, simvastatin, atorvastatin and cerivastatin
- Other statins have intermediary characteristics: fluvastatin
- Others are extremely hydrophilic, such as pravastatin.

4). Statins classification according to their specific activity:

- Some statins are administered as active compounds (acid form), such as atorvastatin, cerivastatin, fluvastatin and pravastatin.

- Other statins are administered as inactive forms (lactones), which have to be enzymatically hydrolyzed to generate the active forms. It is the case of lovastatin and simvastatin (Blumenthal 2000).

4.4. Statins and Cancer

In addition to their cholesterol-lowering effects, statins are reported to inhibit tumour cell growth (Wong, Tan et al. 2001; Paragh, Kertai et al. 2003). Statins are also known to synergistically enhance the effects of chemotherapy (Holstein and Hohl 2001; Li, Appelbaum et al. 2003), and also to overcome chemoresistance (Bogman, Peyer et al. 2001). Interestingly, survival of patients with hepatocellular carcinoma was prolonged with statin treatment (Holstein and Hohl 2001) and the risk of breast cancer (Boudreau, Gardner et al. 2004) and colorectal cancer (Poynter, Gruber et al. 2005) were reduced.

The fact that mevalonate plays a key role in cell proliferation and that many malignant cells present an increased HMG-CoA reductase activity, suggests that a selective inhibition of this enzyme could lead to a new chemotherapy for cancer disease. Reduction of cholesterol synthesis can influence the composition of the plasma membrane, having larger effects on the regions with highest cholesterol concentration (Simons and Toomre 2000) where the emission of cellular signals from transmembrane receptors is higher than in low-cholesterol membrane regions. The decrease of cholesterol and its derivatives can weaken the tumour aggressiveness associated to EGFR and it has been proposed as a possible strategy to treat cancer.

Cellular regulation can be affected by cholesterol levels, but statins also inhibit isoprene biosynthesis and its derivates, such as activated molecules as geranylpyrophosphate and farnesylpyrophosphate. Those intermediary products are essential for an efficient cellular signalling. Key proteins to execute EGFR functions, as small G proteins (RAS proteins) (Edwards and Ericsson 1999) and kinase protein B/Akt

(Partovian and Simons 2004), require isoprene residues attachments for a functional (re)localisation in the inner leaflet of the plasma membrane.

Uncontrolled cellular proliferation is one of the essential hallmarks of cancer. Consequently, a decrease in the proliferation or an increase in apoptosis, as a result of a lower activity of the signalling pathway depending on proteins such as RAS or PKB/Akt, has been thought as a possible strategy for cancer treatment. This idea remains still a working hypothesis, but some epidemiological data indicate that the taking of statins is associated with a better evolution of oncologic patients after a treatment with radiotherapy (Gutt, Tonlaar et al. 2010) or chemotherapy (Katz, Minsky et al. 2005; Tsai, Katz et al. 2006).

4.5. Simvastatin

Simvastatin is a synthetic derivative of a fermentation product of *Aspergillus terreus.* The drug is marketed generically following patent expiry.

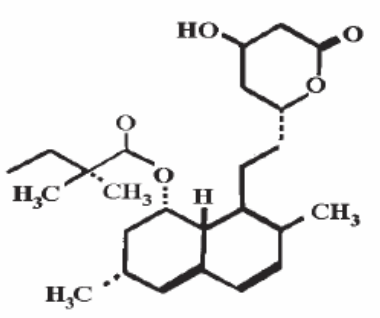

Figure 9. Simvastatin molecular structure. Image from Stancu et al, 2001.

The drug is administered in the form of an inactive lactone that is hydrolyzed after ingestion to produce the active agent. It is a white, non hygroscopic, crystalline powder that is practically insoluble in water, and freely soluble in chloroform, methanol and ethanol.

Simvastatin is a powerful lipid-lowering drug that can decrease low density lipoprotein (LDL) levels by up to 50%. In secondary prevention, 80 mg per day reduced major cardiovascular events by an absolute rate of 1.2% compared with 20 mg per day in a randomized controlled trial (Armitage, Bowman et al. 2010).

MATERIAL AND METHODS

1. GENERATION OF AN ISOGENIC CELL LINE WITH A RADIORESISTANT PHENOTYPE

1.1. Cancer cell lines and culture conditions

The human epidermoid carcinoma cell line A431 from the American Type Cell Collection (num. CRL-1555, LGC Promochem, Barcelona, Spain) was used in this study. Cells were maintained as a monolayer under standard cell culture conditions: DMEM medium (BioWhittaker) supplemented with 10 % Foetal Bovine Serum (PAA *Laboratories* GmbH), 100 U/mL penicillin (Gibco BRL Life Technologies), 100 U/mL streptomycin (Gibco BRL Life Technologies) and 15 mM HEPES (Invitrogen). Cells were maintained in an incubator at 37ºC and in an air atmosphere with a 5% CO_2 concentration. Medium was changed every 3 days and cells were trypsinized when 90% confluence was reached.

When cells reached confluence, they were washed with PBS (PAA Laboratories GMBH) and they were incubated with a solution of trypsin/EDTA with 500 mg/L trypsin 1:250 and 200 mg/L EDTA (BioWhittaker) at 37ºC for 15 minutes. After disaggregation, trypsin reaction was stopped by adding fresh medium to the dishes (3 parts of medium per 1 part of trypsin). The cell content was transferred with a pasteur plastic pipette to a 15 mL tube, and then it was centrifuged at 1000 g for 5 minutes. The cell pellet was resuspended in fresh medium to seed new subcultures.

For cell counting a Neubauer chamber was used. From an aliquot obtained from the cell monolayer disaggregation (cell suspension), a dilution 1:3 in PBS was made, in order to count around 50-100 alive cells per square subdivision of the chamber. Alive cells are seen as shinning spheres in an inverted microscope.

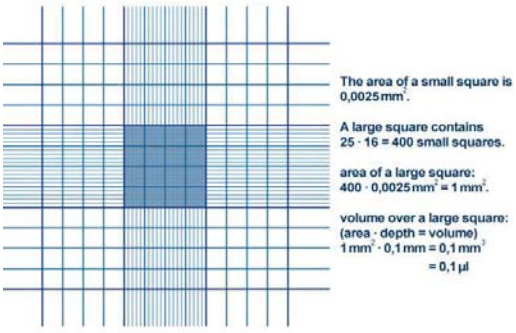

Figure 10. Neubauer chamber scheme

We apply the following formula for the calculation of the cell concentration:

Concentration (cel/mL) = (Number of cells x 10^4) / (number of square x dilution factor)

Where:

- The number of cells is the average of all the counted cells in the four squares counted.

- 10^4 is the correction factor for the Neubauer's chamber

- When a dilution was applied, as it was our case, the concentration obtained was corrected by dilution factor.

Finally, total number of cells in a cell suspension was determined by means of the following formula:

Total number of cells = Concentration (cel/mL) x mL (volume of the cell suspension from where the aliquot was obtained)

Mycoplasma sp contamination uses to escape notice and can affect the experimental results. In order to avoid this, mycoplasma detection was performed routinely. The test consists in the detection of bacterial DNA from the supernatants of confluent cell cultures

cultured in absence of antibiotics. Standard PCR technique was carried out with the primers *Mico-1* and *Mico-2*, which sequences are shown in table X below

Primers	Sequence (5'→ 3')
Mico-1	GGCGAATGGGTGAGTAACACG
Mico-2	CGGATAACGCTTGCGACTATG

Table 1. Primers sequences used for mycoplasma detection**.**

1.2. Generation of a radioresistant phenotype

A431 cells growing in 100-mm plastic dishes were irradiated at room temperature (RT) using a 6-MV X-rays lineal accelerator used for patients treatment in the *Radiotherapy Department* of the *Catalan Institut for Oncology* (Varian Clinac 600, Varian Medical Systems, Palo Alto, CA, US) at dose rate of 2.7 Gy/min in the isocentre. Dosimetry calculations were performed by the *Physic Medicine Department* of the *Catalan Institut for Oncology*.

Figure 11. Linear Accelerator Varian Clinac 600 at the Radiotherapy Department of the *Institut Catalá d'Oncologia*

Cultures were progressively treated with daily rounds of radiation over a 7-month period of time, starting with 0.75 Gy/fraction and ending with 3 Gy/fraction. Irradiation was stopped, as necessary, in order to allow for cell monolayer recovery. The procedure was continued until a total of 85 Gy had been delivered. Next, single cell suspension (1000 cells per 60-mm dishes) were plated and allowed to grow as macroscopic colonies. We next grew the cells from the colony that showed the most vigorous growth to the confluence and expanded them. These cells were used for this study and were denominated as A431-R.

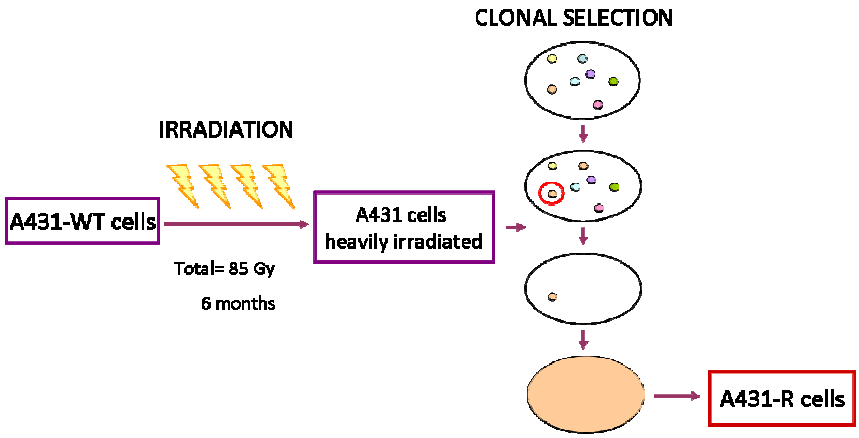

Figure 12. Radioresistant cell line generation summary

1.3. Radiosensitivity estimation and the Linear Quadratic (LQ) model

In this study of Thesis radiation sensitivity was measured by estimating cell surviving fraction, constants (α and β) of the LQ model, and mean inactivation dose. To determine the radiation sensitivity of the cells, clonogenic assays were performed. Briefly, 2000, 4000, 6000 or 8000 cells were planted in 60-mm dishes 24 h before receiving irradiation in single doses of 0, 2, 4, 6 or 8-Gy (respectively). Cells were allowed to proliferate for 14 days and then stained with crystal violet (25 % glacial acetic acid, in ethanol and 1 % crystal violet) for ten minutes. The surviving fractions (SF) were

calculated as the ratio between the number of colonies following irradiation and the number of cells plated, which were then normalized by the clonogenic efficiency (CE) of non-irradiated cells:

Cloning Efficiency (CE) = Number of colonies counted* / Number of cells seeded*

***(no treatment)**

Surviving fraction (SF) = CE treated cells / CE untreated cells

To estimate the α and β parameters of the LQ model, we used the least square regression method, from the natural logarithm of surviving fractions, of the function:

$$Y = -(\alpha D + \beta D^2)$$

Finally, the mean inactivation dose (D) between 0 and 8 Gy was calculated as described by Tucker (Tucker 1986), and which is the area under the cell survival curve we integrated by means of rectangle method .

$$D = \int_0^{\infty} S(D)dD$$

1.4. DNA repair evaluation by Pulsed field gel electrophoresis

The use of pulsed-field gel electrophoresis (PFGE) is widespread in the evaluation of DNA fragmentation caused by double-strand breaks (DSBs) following ionizing radiation. The DNA-DSBs may result in the formation of small (often acentric) chromosomal fragments. Following this initial damage, cells activate DNA repair mechanisms to prevent catastrophic mitosis and cell death due to the loss of acentric DNA fragments. The principle of PFGE methodology is that the release of DNA from cells correlates adequately with the intensity of DNA fragmentation. The estimation of DNA repair by PFGE is based

on the diminution of DNA released from cells as the length of the DNA fragments increases through the process of rejoining. Thus, a decrease in the ratio of DNA extracted from the cells over a period of time can be used as an evaluation of DNA repair.

Cell cultures were irradiated with 45 Gy (6 MV X-ray) to generate DNA double-strand breaks. To form the cell-plugs, 1% agarose type VII (Sigma) in PBS at 37ºC was used. Cell pellets obtained following monolayer harvesting were mixed with 1% agarose at 0, 1, 2, 4, 8 or 24 h after irradiation. Homogenous aliquots were pipetted into 84 µL plug moulds (Bio-Rad, Hercules, CA, US) to form cell-plugs, adjusting the number of cells per plug to 2000 cells. The cell-plugs were then transferred into ice-cold lysis buffer (pH 7.4) containing 2% sodium lauroyl-sarkosine (Fluka Chemie, Buchs, Switzerland), and 0.5 mg/mL proteinase-K (Sigma) in 0.5 M ethylenediaminetetraacetic acid (EDTA, Sigma). Lysis was performed on ice for 1 hour and then at 37ºC for 24 hours. At this point, due to the fragility of agarose plugs, the corners tended to break easily. Therefore, to ensure that the same number of cells (DNA) per lane was loaded into a gel, we cut a section of the better preserved central area. We created a specialized plug cutting device to obtain a section measuring exactly 40 µL. Gels were made of 1% low-melting point agarose, type IX (Sigma), in 0.5 x Tris-Borate-EDTA buffer (TBE, Sigma), pH 8.4. DNA fragments were resolved by PFGE (CHEF-DR-III, Bio-Rad). Electric field strength was 1.6 V/cm with a switching pulse of 3600 seconds, and a 115º reorientation field angle. PFGE was carried out in 0.5 x TBE buffer chilled at 14ºC for a total running time of 96 hours. *Saccharomyces cervisiae* and *Saccharomyces pombe* yeast chromosomes were used as DNA size markers (Bio-Rad). Gels were then stained overnight with 0.5 µg/mL ethidium bromide, washed and transilluminated at 302 nm. Fluorescence intensity of the DNA was acquired, and transformed to arbitrary units of optical density using a digital imaging analysis system (GelDoc 2000 and Quantity One software, Bio-Rad). The sum of fluorescence within DNA smears was used for calculations.

1.5. Immunofluorescence of γH2AX

To quantify the activated form of H2AX (γH2AX), conventional immunofluorescence was undertaken. Sterilized cover slips were put into 60-mm petri dishes, and then A431-WT or A431-R cells were seeded and cultured in full medium until confluence. Following irradiation (4 Gy- single dose), the culture medium was substituted by a pre-warmed and CO_2 gassed medium, and the cells were left for 30 minutes in the incubator before starting the γH2AX time-course determination. Samples were fixed with 4% neutral-buffered formaldehyde, washed (0.1% triton in PBS for 10 min) and incubated for 1 hour with protein-blocking solution. Next, the samples were incubated with primary antibodies anti-phospho-histone H2AX (Ser139) (Millipore-Upstate, Billerica, MA, US) followed by incubation with secondary antibodies Alexa Fluor 488-conjugated, both at a dilution of 1:500 for 1 h, at room temperature. Fluorescence images were captured by using a Zeiss Axioplan 2 imaging epi-fluorescence microscope equipped with a charge-coupled device camera and SPOT advanced software (Diagnostic Instruments Inc, Sterling Heights, MI, US). Five to ten randomly selected field microscopic images per slide were analyzed. Cells were counted using the ImageJ program, public domain Java image processing software (http://rsb.info.nih.gov/ij/).

1.6. Tumour xenografts generation

All experimental methods used in our studies were approved in accordance with our own institutional IDIBELL guidelines for animal care and ethics. Six to eight week old female athymic *Nude-Foxn1*^{nu} mice were purchased from Harlan (Gannat, France). Complete health reports, especially the microbiological status of the animals based on the Federation for Laboratory Science Associations (FELASA) recommendations, were certified by the vendor. The mice were housed at 20-22ºC, under pathogen free conditions at the animal facilities of the *IDIBELL-Hospital Duran i Reynals* (AAALAC accreditation number 1155). Mice were given ad libitum access to food and water.

To generate tumour xenografts, 10^6 cells were injected into subcutaneous tissues on the right thigh of athymic mice. Previously the mice were intraperitoneally anaesthetized (1 mg/kg of each solution: 50 mg/mL ketamine and 1 mg/mL medetomidine with 5 mg/mL atipamezole for the reversal of the anaesthesia effects) in order to precisely control the area in which the cells were to be injected and obtain homogenous growth of tumours. We decided to inject the cells in the right thigh of the mice, which allowed us to irradiate exclusively a limited part of the body and protect the rest of the animal body from irradiation. Tumour growth was measured twice weekly until tumours reached 1500 mm^3 in size. Tumour size was calculated using the formula:

$$\pi/6 \times (\text{large diameter}) \times (\text{small diameter})^2$$

1.7. Irradiation of xenoimplanted tumours

Radiotherapy was limited to the right thigh. Detailed explanation about animal's irradiation is explained further on in Material and Methods Section 2 (page 105). Prior to tumour irradiation, the mice were anaesthetised by an intraperitoneal injection (1 mL/kg of each solution: 50 mg/mL ketamine and 1 mg/mL medetomidine). Upon completion, 5 mg/mL atipamezole was delivered to reverse the effects of the anaesthesia. A complete mock process was performed on non-irradiated mice that served as experimental controls.

1.8. Migration studies by Wound Healing Assay

A421-WT and A431-R cells were seeded in 6-cm-diameter plates and cultured until confluent. After 12 h of culture in foetal bovine serum (FBS) free medium, the monolayers were scratched with a 200 µl pipette tip to imitate a wound (3 different locations per dish). After several washing and removal of floating cells, the distances between cell margins were measured at 0, 1, 2, 3, 6 and 24 h using specialised software (Leica, Wetzar, Germany). Three independent assays, done in duplicate, were conducted.

1.9. EGFR pathway analysis by immunoblotting

We performed a standard western blot method to determine levels of specific proteins. Cultures were maintained without FBS for 24 h before treatment with radiation, epidermal growth factor (EGF) ligand (Sigma-Aldrich, St. Louis, MO), or vehicles for the controls. Following any of these treatments, lysates were obtained. Protein concentrations in the lysates were determined by the Pierce BCA Protein Assay Kit (Thermo Scientific, Rockford, IL, US). Equal amounts of protein (35 µg) were resolved in the SDS-PAGE system (Bio-Rad, Hercules, CA, US) and blotted onto Hybond nitrocellulose membrane, which were incubated with a rabbit anti-phosphorylated (Tyr992) EGFR antibody (EGFR pY992) (Sigma-Aldrich) at a 1:1000 dilution; mouse anti-phosphorylated (Thr183 and Tyr185) MAP kinase ERK1/2 monoclonal antibody (pERK1/2) (Sigma-Aldrich) at a 1:5000 dilution, and a rabbit anti-phosphorylated (Ser473) AKT polyclonal antibody (AKT pR73) (Cell Signaling) at a 1:500 dilution in blocking solution overnight at 4ºC. The nitrocellulose-bound primary antibodies were incubated with anti–mouse IgG or anti–rabbit IgG horseradish peroxidase–linked antibody (GE Healthcare), and were detected by enhanced chemoluminescence staining ECL/ECL™ Plus (GE Healthcare). Chemoluminescence staining was transformed to arbitrary units of optical density using a digital imaging analysis system (GelDoc 2000 and Quantity One software, Bio-Rad Laboratories, Hercules, CA, USA) and the results were represented on histograms.

1.10. Levels of VEGF secretion evaluation

To measure the levels of vascular endothelial growth factor (VEGF) secretion, cells were plated in 6-mm dishes ($1x10^6$ cells per dish) and allowed to grow in a complete medium for 24 h. Next, cultures were rinsed twice with PBS buffer and incubated in FBS free medium for 24 h. The cells were then irradiated with a single 8-Gy dose. Supernatants were collected at 0, 24 and 48 h. VEGF was determined in the culture

supernatants by means of an enzyme-linked immunoabsorbent assay ELISA (R&D Systems Inc, Minneapolis, MN). Reagents, working standards, and samples were prepared as directed in the kit protocol, then excess microplate strips from the plate frame were removed then returned to the pool pouch containing the desiccant pack and then the plate was resealed. Fifty µL of Assay Diluent RD1W were added to each well, then 200 µL of Standard, control, or sample were added per well. The plate was covered with the adhesive strip provided and incubated for 2 hours at room temperature. Each well was aspirated and washed, repeating the process twice for a total of three washes. After the last wash, any remaining Wash Buffer was removed by aspirating or decanting. The plate was then inverted and blotted against clean paper towels. 200 µL of VEGF Conjugate were added to each well, the plate was then covered with a new adhesive strip, and incubated for 2 hours at room temperature. The plate was washed again as previously described. 200 µL of Substrate Solution were added to each well and the plate was protected from light, then the plate was incubated for 20 minutes at room temperature. Finally, 50 µL of Stop solution were added to each well. Optical density of each well was determined within 30 minutes, using a microplate reader set to 450 nm. If wavelength correction is available, set to 540 nm or 570 nm.

1.11. CD44 determination

The cell surface marker, CD44, was determined by a standard immunofluorescence process. Sterilized cover slips were put into 60-mm petri dishes, and then A431-WT or A431-R cells were seeded and cultured in full medium. After 48 h, the cells were fixed with 4% neutral buffered formaldehyde, washed (0.1% triton in PBS for 10 min) and incubated for 1 h with a protein-blocking solution (20% serum goat and 20% serum horse in 1X PBS). Next, the slides were incubated with a mouse anti-CD44 (156-3C11) monoclonal antibody (Cell Signaling) at 1:100 dilution overnight at 4ºC. To detect primary antibody, cover slips were incubated with Alexa Fluor 488-conjugated goat anti-mouse secondary antibody (Invitrogen) at a 1:1000 dilution for 1 h at RT. Fluorescence images were captured by using a Zeiss Axioplan 2 imaging epi-fluorescence microscope

equipped with a charge-coupled device camera and SPOT advanced software (Diagnostic Instruments Inc, Sterling Heights, MI, US). Five to ten randomly selected field microscopic images per slide were analyzed. Cells were counted using the ImageJ program, public domain Java image processing software.

Additionally, CD44 detection was measured by flow cytometry using anti CD44-APC (1:12.5; BD Biosciences Pharmingen, San Diego, CA, US) antibody in 100 µL PBS 0.5% BSA and 2 mM EDTA. After incubation for 30 minutes at 4ºC, cells were washed with 0.5% BSA 2 mM EDTA, and then the cells were re-suspended in 300 µL PBS-2% FBS- 2 mM EDTA. Flow cytometry quantification of CD44 positive-cells was performed with a BD FACSaria III cell sorter and BD FACSDiva software (BD Biosciences Pharmingen).

1.12. Cell cycle distribution analysis

A standard propidium iodine staining method was used to assess the cell cycle phase distribution of A431-WT and A431-R cells. Propidium iodine (PI) is an intercalating agent and a fluorescent molecule. PI binds to DNA by intercalating between the nucleic acids and increasing their fluorescence. As the PI also binds to RNA, treatment with nucleases is required.

Culture medium was collected and cells were washed twice with PBS then trypsinized. It is highly recommended that the number of trypsized cells plus the number of cells floating in the culture medium to be around 1-2 x 10^6 cells per mL. 1mL of the the cell suspension was centrifuged at 400 g for 5 minutes. The suspension was washed twice with 1 mL of 1% FBS in PBS and centrifuged at 500 mg for 1 minute. Cells were resuspended in 0.5 mL of 1% FBS in PBS. Suspensions of cells in PBS were well disaggregated with a pasteur pipette then gently vortexing. Cell suspensions were added drop by drop to a volume of 5 mL of 70% cold ethanol (-20ºC), then fixed at -20ºC for at least 2 hours. The samples were then centrifuged at 800 g for 5 minutes and ethanol was eliminated. Samples were washed in 1% FBS in PBS, centrifuged and the aqueous phase

was discarded. Pellets were resuspended in 50-500 µL of citrate-phosphate buffer (Na_2HPO 0.2 M: citric acid 0.1 M (192:8)) then incubate between 30 minutes and 2 hours at RT. Samples were centrifuged at 800 g for 5 minutes then eliminate citrate-phosphate buffer. Samples were resuspended in 400 µL 1% FBS in PBS then 50 µL of PI (stock 0.5 mg/mL) were added. Five µL RNAse A DNAse free (10 mg/mL) were added, then the samples were incubated at 37ºC for 30-45 minutes protected from light. Flow cytometry analysis was performed with a BD FACSCalibur cell sorter, and BD Cellquest Pro plus (BD Biosciences Pharmingen) and ModFit LT3.2 (Verity Software House, Topsham ME, US) softwares.

1.13. Epigenetic studies

1.13.1. DNA extraction

When cells growing in 10-mm dishes were confluent, 500 µL PBS were added, then the cells were scratched with a sterile scraper. The content was centrifuged for 5 minutes at 1000 rpm. The supernatant was discarded, and the pellet was homogenized with 250 µL of the solution 10-10-0.15 TEN (10 mM Tris pH 7.5, 10 mM EDTA, 0.15 M NaCl). Fifty µL of the same 10-10-0.15 TEN solution were added and the samples were homogenized. The samples were incubated with 6 µL of proteinase K (stock solution at 20 mg/mL) and 15 µL SDS 10 % for 3 hours at 55°C, then incubated for 15 minutes at 75°C to inactivate proteinase K. Two µL of RNAse A (stock solution at 10 mg/mL) were added to the samples, then incubated for 1 hour at 37ºC. Three-hundred µL of 10-10-0.65 TEN solution and 300 µL of Fenol/Sevag were added to the samples, mixed gently by inversion, and centrifuged for 10 minutes at 12000 rpm. The upper layers (aqueous phases) were recovered, gently mixed in 10 % of sodium acetate 3 M pH = 5.2 (50 µL) and 2 volumes of ethanol (1 mL), and stored at -20°C overnight. Next day, the samples were centrifuged at 12000 rpm for 10 minutes and the supernatants were discarded. Pellets (DNA) were washed twice with 1 mL of ethanol 70°C then centrifuged at 12000 rpm for 10 minutes. DNA pellets were left air dry at room temperature and resuspended in 30 µL

of TE pH 8.0. DNA purity was checked by measuring the 260/280 and the 260/230 ratios using a Nanodrop-1000.

1.13.2. DNA quality check

One-hundred µL of a 1/2500 original DNA dilution were quantified by adding 100 µL of a 1/200 dilution Quant-iT PicoGreen® dsDNA Reagent (Invitrogen), using a serial dilution of λ DNA (1000, 500, 250, 100, 50, 5, 2.5 ng/mL) as a standard. Fluorescence signal was measured with GloMax Multi+ fluorimeter (Promega Corporation) and concentrations were obtained from a linear regression of the standard points. Original DNAs were normalized to a concentration of 50 µg/µL by diluting DNAs with TE pH 8.0. Electrophoresis was performed to check for high molecular weight DNA fragments.

1.13.3. Bisulfite conversion

Bisulfite conversion of 600 ng of each sample (A431-WT and A431-R) was performed according to the manufacter's recommendations for Illumina Infinium Assay (EZ DNA methylation kit. Zymo Research). The incubation profile was 16 cycles at 95ºC for 30 seconds, 50ºC for 60 minutes and a final holding step at 4ºC. Enzymatically methylated Jurkat genomic DNA (New England Biolabs), genomic Jurkat DNA (New England Biolabs), and the whole genome amplified genomic DNA were used as total methylated, intermdiat- methylated and non- methylated controls. After bisulfite treatment, methylation-specific PCR was performed on the control samples using a set of primers to amplify a 301 bp region of the 28s ribosomal DNA (5'-AAA ATT CTT TTC AAC TTT CCC T-3' and 5'-GAG TGA ATA GGG AAG AGT TTA G-3'). PCR conditions were: 2 nM $MgCl_2$ at 95ºC for 1 minute, followed by 30 cycles at 95ºC for 30 seconds and 72ºC for 45 seconds, with a final step at 72ºC for 10 minutes.

1.13.4. DNA methylation assay

Four µL of bisulfite-converted DNA were used for hybridation on Infinium HumanMethylation450 BeadChip, following the Illumina Infinium HD Methylation protocol. This consisted of a whole genome amplification step followed by enzymatic end-point fragmentation, precipitation and resuspension. The resuspended samples were hybridized on HumanMethylation 450 BeadChips at 48ºC for 16 hours. The unhybridized and non-specifically hybridized DNAs were washed away, followed by a single nucleotide extension using the hybridized bisulfite-treated DNA as a template. The nucleotides incorporated were labeled with biotin (ddCTP and ddGTP) and 2,4-dinitrophenol (DNP) (ddATP and ddTTP). After the single-base extension, repeated rounds of staining were performed with a combination of antibodies that differentiated DNP and biotin by fixing them different fluorophores. Finally the BeadChip was washed and protected in order to scan it.

1.13.5. Scanning beadchips

The Illumina HiScan SQ scanner is a two-color laser (532 nm/660 nm) fluorescent scanner with a 0.375 µm spatial resolution capable of exciting the fluorophores generated during the staining step of the protocol. The intensities of the images were extracted using GenomeStudio (2010.3) Methylation module (1.8.5) software. The methylation score for each CpG was represented as a ß value according to the fluorescent intensity ratio. ß values may take any value between 0 (non-methylated) and 1 (completely methylated).

1.13.6. DNA methylation clustering

Genome Studio (2010.3) Methylation module (1.8.5) software was used to generate heatmaps of clustered CpGs.

2. DEVELOPMENT OF A TECHNIQUE TO IRRADIATE MICE BEARING XENOGRAFTS

2.1. Mice and animal facility

Mice were purchased as mentioned before (Material and Methods section 1.6) and the tumours were generated as explained in Material and Methods section 1.7. At a suitable tumour size, and two days before irradiation, the mice were moved from the SPF area to a quarantine room so they can adapt to the new housing conditions, and where the animals remained permanently housed in closed autoclaved plastic cages (5 mice per cage). In this room, the mice were manipulated under a laminar flow hood and using aseptic conditions. Before each radiotherapy session, they were anaesthetised, as mentioned above, and transported to the radiotherapy unit in clean autoclaved closed cages covered with a drape to conceal the animals from plain view.

2.2. Irradiation setting at the radiotherapy department

Upon arrival to the radiotherapy room, the treatment table was disinfected with alcohol and covered with sterile drapes. Surgical caps, masks and sterile gloves were worn. Figure 13 shows the scheme of how an appropriate setting for selectively irradiating tumours and reducing infections in the mice was achieved. Of note is the placement of the thigh on the edge of the radiation beam to allow sufficient coverage of the tumour, while protecting the body of the mice as much as possible.

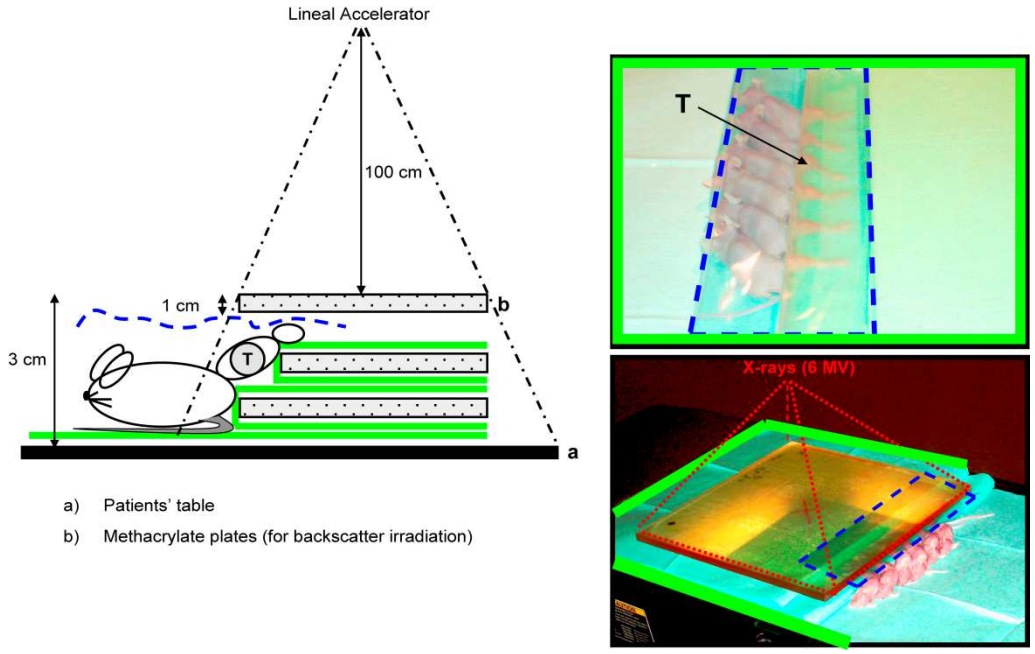

Figure 13. Scheme used for localised irradiation of xenografted tumours in multiple fractions. Tumours (T) were placed into the gap created by two poly-methyl methacrylate (PMMA) plates (b), each were 35 cm x 35 cm x 1 cm in size, separated by a smaller plate (30x30x1). The edge of beam was adjusted to cover the tumour with 1 cm margin, assuring that PMMA were included into the beam. The thighs were kept in place by using an adhesive tape, while the body of animals was maintained out of beam. Sterile drape that cover the treatment table (a) and wrapped PMMA are represented by the green lines. Dotted line illustrates the sterile transparent film we put onto the mice, protecting them from non-sterile top PMMA, as it can be also observed in the pictures on the right. The source-plate distance was set to 100 cm on the centre of the top plate. Note that dimensions in the diagram are not to scale.

2.3. Irradiation of the mice

To irradiate the animals, 6 megavolts (MV) photon beam from a Varian Clinac 2100 linear accelerator was used. A total dose of 30 Gray (Gy) in fractions of 3 Gy, separated by 24 hours, excluding Saturdays and Sundays was administrated. The dose rate was 2.7 Gy per minute at the level of tumors.

In order to verify the dose that the tumours received, as well as the precision of the setup used, an *in vivo* dosimetry was performed by means of radiochromic films (Gafchromic EBT, International Specialty Products, Wayne, NJ, USA). In total, 40 dose measurements were carried out during 4 separated days. Films were placed in contact with the tumour at the beam entrance. We found less than 3 % variation in the doses

received by the different mice on the same sessions and less than 1.5% variation between the different days. The mean deviation in absorbed dose in the tumours was 2.3 % of the prescribed dose. The aforementioned results confirmed that our experimental setup was homogeneous and reproducible. The details of tumor irradiation were published in the journal Laboratory Animals (Baro, de Llobet et al. 2012).

2.4. Endpoints criteria

Euthanasia using intraperitoneal pentobarbital solution (4.5 mL/kg dose of 200 mg/mL of Dolethal) was planned at day +90, or, before, in cases where more than one grade 2 or one grade 3 events were observed, or when the tumour size reached more than 1,500 mm3, however only the last criterion had had to be applied. We applied these criteria following the international guidelines for the welfare and use of animals in cancer research.

3. SIMVASTATIN SENSITIZES TO RADIOTHERAPY PLUS CETUXIMAB

3.1. Cancer cell lines and culture conditions

This study was carried out mostly with the human head and neck squamous cell carcinoma (HNSCC) cell line FaDu. However, to examine whether the findings with this cell line could be compatible with other cell lines that, as FaDu cells, express high to moderated levels of EGFR, which is a common molecular trait in HNSCC, we repeated some experiments using both A431 cell lines (A431-WT and A431-R). FaDu cell line was also purchased to the American Type Cell Collection (LGC Promochem, Barcelona, Spain), and was maintained under standard cell culture conditions free of mycoplasma contamination (as specified in the point 1.1. abovementioned). FaDu and A431 cells showed wild-type DNA sequence at codons 12 and 13 in the KRAS gene.

Primers	Sequence (5'→ 3')
Up	**ATGGTCCTGCACCAGTAATATGCA**
Down	**GGTGGAGTATTTGATAGTGTA**

Table 2. Primers sequences used for KRAS gene analysis (exon 2).

3.2. Radiation exposure and pharmacological treatments

Radiotherapy was administered to cell cultures at room temperature as previously described (6 megavolt X-rays at a dose rate of 2.7 Gy/min from a Varian Clinac 2100 linear accelerator). Mice received local irradiation as described elsewhere previously (Material and Methods section 1.6. abovementioned). Cetuximab (Erbitux®, Merck, Darmstadt, Germany) was directly administered to cell cultures or animals at appropriate doses ranging from 10 to 30 nM, and from 1 mg to 1.5 mg per mice a week, respectively. Simvastatin was dissolved in DMSO for cell culture experiments, and used at doses ranging from 1 to 25 μM, while it was dissolved in 1,2-propanediol in distilled water 1:1 (v/v) for animal treatments, and used at a dose of 50 mg/kg/day (simvastatin, DMSO and

propanediol were purchased from Sigma-Aldrich, St. Louis, MO). The drug doses were based on previously published works (Johnson-Anuna, Eckert et al. 2005; Wu, Jiang et al. 2009; Pueyo, Mesia et al. 2010; Lee, Lee et al. 2011; Sanli, Liu et al. 2011). Equivalent mock irradiations and treatments with appropriate vehicles were carried out as controls.

3.3. Cell proliferation assay

A total of 300 000 cells were seeded in 60 mm dishes and cultured for 3 days until semi-confluence. Then cell cultures were treated with cetuximab alone or combined with simvastatin 2 hours prior to radiotherapy and during the assays. The number of cells present in the cell cultures was counted using a Neubauer chambre at 0, 24, 48 and 72 hours.

3.4. Wound healing assay

Cells were seeded in 60 mm dishes, and cultured until confluence. Then the cell cultures were pre-treated for 48 hours with cetuximab or cetuximab and simvastatin prior to being irradiated. Immediately thereafter, monolayers were scratched as explained in previous Material and Methods section 1.8 to simulate a wound, and cultured in the presence of the drugs. Distances between the wound margins were measured at 0, 1, 2, 4, 8 and 24 hours under a Leica DMIL LED light microscope with the Leica Application Suite LAS v.2.6 software (Leica, Wetzar, Germany).

3.5. Clonogenic Assay

Two-thousand single cells were seeded in 60 mm dishes and allowed to attach for 24 hours. Then, cell cultures were pre-treated with simvastatin, cetuximab or cetuximab plus simvastatin for 24 hours. Next, cell cultures were either irradiated (2 Gy) or subjected to mock irradiation in the presence or absence of the drugs. Two different duration of treatment with drugs were performed after irradiation. Cultures were either left to grow for 24 hour more, rinsed and allowed to proliferate to form colonies up to day 14th

without drugs, or left to proliferate to form colonies in the presence of the drugs up to 14th day. Colonies were stained with crystal violet. Surviving fractions were calculated as previously explained in section 1.3. The most useful clinical marker of intrinsic radiosensitivity, the surviving fraction at 2 Gy (SF2), was used as the endpoint to preliminary assess a possible role for the addition of simvastatin to the standard therapy of radiotherapy and cetuximab.

3.6. Xenografts and in vivo treatments

Tumour xenografts were generated as explained in Material and Methods section 1.6. Cells were injected on Monday and left to growth for 7 days before the beginning of the treatments. Tumor growth was measured twice weekly. Mice were euthanized when the tumor volume reached 1,500 mm^3, or when the mice showed moderate to severe toxicities, or when significant differences between groups were observed.

The mice received fractionated radiotherapy plus either cetuximab or cetuximab and simvastatin. Moreover, mice were treated with single therapies. Radiotherapy was selectively delivered from Monday to Friday for 2 weeks using the 6 megavolt X-ray beams on the right limb hind of mice bearing xenografts. Simvastatin was administered orally on a daily basis for 12 days. Cetuximab was intraperitoneally injected two times a week for two weeks. Mice were randomly allocated to receive radiotherapy plus cetuximab or radiotherapy, cetuximab, and simvastatin as well as single treatments with radiotherapy, cetuximab or simvastatin alone. In addition, a group of mice treated in parallel was euthanized on day 4 to acquire tumor samples for immunofluorescence.

3.7. Western blot analysis

Semi-confluent cell cultures were pre-treated for 48 hours with cetuximab and simvastatin in FBS-free medium, and then irradiated with a single dose of 5 Gy. Twenty minutes after irradiation cell cultures were rinsed in ice-cold PBS and lysed in

radioimmunoprecipitation assay buffer with protease and phosphatase inhibitors. Vehicle and mock irradiation were provided for controls. Proteins (35 µg) were resolved in the SDS-PAGE system and blotted onto nitrocellulose membrane. The following primary antibodies were used: mouse anti-EGFR total at a 1:200 dilution, rabbit anti–pEGFR-Y1086 at a 1:1,000 dilution, mouse anti–pERK1/2 (phosphorylated extracellular-signal-regulated kinases 1 and 2) at a 1:5,000 dilution, and mouse anti–α-tubulin at a 1:5,000 dilution (all of the aforementioned antibodies were purchased from Sigma-Aldrich); rabbit anti-AKT total at a 1:500 dilution, rabbit anti–pAKT-S473 (phosphorylated phosphatidylinositol 3-kinase/AKT-Protein Kinase B) at a 1:500 dilution, rabbit anti-STAT3 total at a 1:1000 dilution, rabbit anti–pSTAT3-Y705 (phosphorylated signal transducer and activator of transcription number 3) at a 1:500 dilution, and anti-cleaved caspase-3 antibody at a 1:500 dilution, all from Cell Signaling (Cell Signaling Technology, Danvers, MA, US), rabbit anti ERK1/2 total (a gift from Prof. F. Viñals; refer to: J Biol Chem 1999;274:26776-2) and rabbit anti-caspase-3 (Santa Cruz Biotechnology, Inc., Santa Cruz, CA, US) at a 1:1,000 dilution. The nitrocellulose-bound primary antibodies were incubated with anti–mouse IgG or anti–rabbit IgG horseradish peroxidase–linked antibody (GE Healthcare), and were detected by enhanced chemoluminescence staining ECL/ECL™ Plus (GE Healthcare). Chemoluminescence staining was transformed to arbitrary units of optical density using a digital imaging analysis system (GelDoc 2000 and Quantity One software, Bio-Rad Laboratories, Hercules, CA, USA) and the results were represented on histograms.

3.8. Immunofluorescence for cleaved caspase-3

Cleavage of caspase-3, used as an apoptotic marker, was determined by a standard immunofluorescence process on cells cultured on sterilized cover slips, and on 3-µm cryostat sections of the xenografts scheduled on the 4th day of treatment. Regardless of the origin, the samples were fixed, permeabilized (0.1% triton in PBS for 10 min) and incubated for 1 hour with a protein-blocking solution (20% goat and 20% horse sera in PBS). Next, the samples were incubated overnight with a rabbit anti-cleaved

caspase-3 monoclonal antibody (Cell Signaling) at a 1:100 dilution at 4ºC. To detect primary antibodies, the samples were incubated with a goat anti-rabbit Alexa Fluor 594 antibody (red fluorescence) (Invitrogen, Carlsbad, CA, US) at a 1:200 dilution for 1 hour at room temperature. Then, slices were mounted using Vectashield (Vector Laboratories Inc., Burlingame, CA) mounting medium with 4'-6-diamidino-2-phenylindole DNA staining fluorochrome (blue fluorescence). Fluorescence images were captured using a Nikon Eclipse 80i epifluorescence microscope (Nikon Instruments, Kanagawa, Japan), then analyzed with Nis-Elements, Basic Research (Nikon) software. The apoptosis index was calculated as the ratio between red fluorescence (from detection of cleaved caspase-3) and blue fluorescence from nuclei.

3.9. Immunofluorescence for BrdU

5-Bromodeoxyuridine (BrdU) is an analogue of thymidine. BrdU can be introduced to live proliferating cells which in turn incorporate BrdU into the DNA during S phase, prior to cell division. BrdU administered by intraperitoneal injection (1.25 mg) one hour prior to animal sacrifice was used as a proliferation marker. BrdU was determined by a standard immunofluorescence process on 3-µm cryostat sections of the xenografts scheduled on the 4^{th} day of treatment. The samples were fixed, permeabilized (0.1% triton in PBS for 10 min) and incubated at 37ºC for 20 minutes with HCl 2N in order to denaturalise DNA. Acid was then neutralised with two washes of Borate buffer 0'1M (pH 8'5) for 5 minutes, then the samples were incubated for 1 hour with a protein-blocking solution (20% goat and 20% horse sera in PBS). Next, the samples were incubated overnight with a rat anti-BrdU antibody (AbD Serotec) at a 1:100 dilution at 4ºC. To detect primary antibodies, the samples were incubated with a rabbit anti-rat Alexa fluor 488 antibody (green fluorescence) (Molecular Probes, CA, US) at a 1:1000 dilution for 1 hour at room temperature. Then, slices were mounted using Vectashield (Vector Laboratories Inc., Burlingame, CA) mounting medium with 4'-6-diamidino-2-phenylindole DNA staining fluorochrome (blue fluorescence). Fluorescence images were captured using

a Nikon Eclipse 80i epifluorescence microscope (Nikon Instruments, Kanagawa, Japan), then analyzed with Nis-Elements, Basic Research (Nikon) software.

3.10. Immunohistochemistry for CD31/PECAM-1

Cluster of Differentiation 31 (CD31, also known as Platelet endothelial cell adhesion molecule (PECAM-1)) is frequently used to demonstrate the presence of endothelial cells in histological tissue sections, and can help to evaluate the degree of tumour angiogenesis. CD31 was determined by a standard immunohistochemistry process on 3-µm cryostat sections of the xenografts scheduled on the 4^{th} day of treatment. The samples were fixed, then endogenous peroxidises were inhibited by incubating the samples with 3% hydrogen peroxide (67 % de PBS 1x, 30 % de methanol y 3 % Hydrogen peroxide) for 10 minutes. Samples were then washed several times with distilled water, permeabilized (0.1% triton in PBS for 10 min), then incubated for 1 hour with a protein-blocking solution (20% goat and 20% horse sera in PBS). Next, the samples were incubated with a rat anti-CD31/PECAM-1 antibody (BDPharmigen) at a 1:50 dilution at RT for 30 minutes. To detect primary antibodies, the samples were incubated with a rabbit anti-rat biotilinated antibody (Dako) at a 1:200 dilution for 30 minutes at RT. The samples were then incubated with streptavidin and biotinylated peroxidase for 30 minutes at RT using the kit from Dako *StreptABComplex/HRP.* The samples were developed using a system with chromogen, diaminobenzidine (DAB) and hydrogen peroxide, which forms a final brown coloured product in the target zone for the antigen, when oxidised. Next, a common staining with hematoxiline was performed to contrast cellular stainings. The samples were then mounted using DPX synthetic resin mountant. Quantification was performed using the method described by Weidner et al (Weidner, Semple et al. 1991) with an optic microscope focusing in the tumoural regions that showed a higher number of capillaries. Images were captured using a Nikon Eclipse 80i microscope (Nikon Instruments, Kanagawa, Japan), then analyzed with Nis-Elements, Basic Research (Nikon) software.

3.11. Cholesterol measurements

For total cholesterol determination of the xenografts samples, 10 mg of protein was saponified with alcoholic KOH in a 60°C heating block for 30 min. After the mixture had cooled, 10 ml of hexane and 3 ml of distilled water were added and shaken to ensure complete mixing. Appropriate aliquots of the hexane layer were evaporated under nitrogen and used for cholesterol measurement. High performance liquid chromatography (HPLC) analysis was made using a Waters µBondapak C18 10 µm reversed-phase column (30 cm x 4 mm inner diameter), with the mobile phase being 2-propanol/acetonitrile (50:50, v/v) and the flow rate of 1 ml/min. The amount of cholesterol was calculated from standard curves and the identity of the peaks was confirmed by spiking the sample with known standards.

3.12. Statistics

All the results from the three studies of this project of Thesis were expressed as mean ± SEM. Statistically significant differences in between-group comparisons were defined by using a two-tailed significance level of $p < 0.05$ using Mann-Whitney test. The Statistical Package for Social Sciences, version 13.0 (IBM, Madrid, Spain) was used for data analysis.

OBJECTIVES

1. The first aim of this study was to develop an isogenic resistant cell line which could be used to identify molecular changes associated with acquired resistance to radiation and tumour aggressiveness in cancer.

2. The second aim of this study was to develop and describe a procedure to deliver fractionated radiotherapy to xenoimplanted tumours in immunodeficient mice using a medical linear accelerator, a method that was devised as an alternative to the lack of facilities devoted to radiation research.

3. The principal aim of the third part of this project was to test whether simvastatin may increase the therapeutic effect of radiation and cetuximab on tumor growth in xenograft models derived from human squamous cell carcinomas.

RESULTS

1. GENERATION AND CHARACTERISATION OF A RADIORESISTANT CELL LINE

Radiation resistance is a major cause of death in cancer patients. Cancer cells can react during radiotherapy by re-programming specific cell functions that may confer resistance to radiation. The understanding of this complex process is hindered due to the lack of appropriate study models. For this reason, the first objective of this project of Thesis was to describe a collection of changes that occurred through the process of development of a radioresistant isogenic cancer cell line.

1.1. A431-R cells show radiation resistance: an *in vitro* evidence

1.1.1. Based on radiation sensitivity estimation in cell cultures

The new A431-R cell line obtained after the processes of irradiation and clonal selection explained in section 1.2. of the Material and Methods, was radioresistant related to the parental A431-WT. The initial shape of survival curve for A431-R cells showed a higher shoulder than parental A431-WT cells, and the mean SF2 value significantly rose from 0.62 to 0.75 (p=0.024). The effect of successive fractions of 2 Gy is illustrated in Figure 14 A, where it was assumed that no additional repair took place between fractions in either type of cells.

A

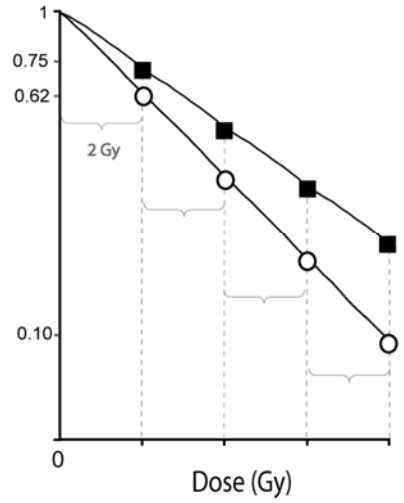

B

Radiosensitivity	A431-WT	A431-R	P-value*
SF2	0.62 ± 0.034	0.75 ± 0.036	0.024
α-component	0.24 ± 0.03(Gy^{-1})	0.14 ± 0.02 (Gy^{-1})	0.024
ß-component	0.02 ± 0.005(Gy^{-2})	0.03 ± 0.003(Gy^{-2})	0.490
D	3.00 ± 0.14 (Gy)	3.50 ± 0.10 (Gy)	0.015
α/ß ratio	12 (Gy)	4.6 (Gy)	

Abreviations: SF2=Surviving Fraction after 2Gy; α- and β-components=coefficients of the linear-quadratic equation; D=mean inactivation dose calculated as the area under clonogenic cell survival curve between 0 and 8 Gy; α/β ratio=the dose at which cell killing participation is the same for non-reparable single hit killing and cell death due to sublethal lesion saturation.

Figure 14. Radiosensitivity evaluation. The radiosensitivity of A431-R cells was lower than A431-WT. A. Representation of cell response to radiation after 4 separated doses of 2 Gy each for A431-WT cells (circles) and A431-R cells (squares). B. Radiosensitivity of A431-WT versus A431-R cell lines. (* $p < 0.05$; Mann-Whitney test).

To further evaluate variations in radiosensitivity, the α/β ratio of LQ model and the mean inactivation dose were estimated. The α/β ratio was reduced from 12 Gy for parental cells to 4.6 Gy for the resistant cells, at the expense of decreasing α-component and increasing β-component, indicating a higher ability to repair sub-lethal damage in the A431-R cells, and thus, having increased resistance to radiotherapy (Figure 14 B). The mean inactivation dose was also increased from 3 Gy to 3.5 Gy in A431 cells.

1.1.2. Based on DNA repair estimation through PFGE and H2AX foci

In light of these results, and, because DNA repair is a crucial determinant of radiosensitivity, we decided to determine whether A431-R cells acquired an increased ability to repair DNA. The ability of the cells to repair DNA damage was estimated by means of PFGE that measures rejoining of chromosome fragments, and clearance of phosphorylation on H2AX histone.

1). In A431-R cells, we found a significant diminution of residual DNA fragments, measured by PFGE, indicating that in these cells the rejoining of radiation-induced DNA fragments was more efficient than in A431-WT cells. This functional finding provides further support to radiation resistance in A431-R cells.

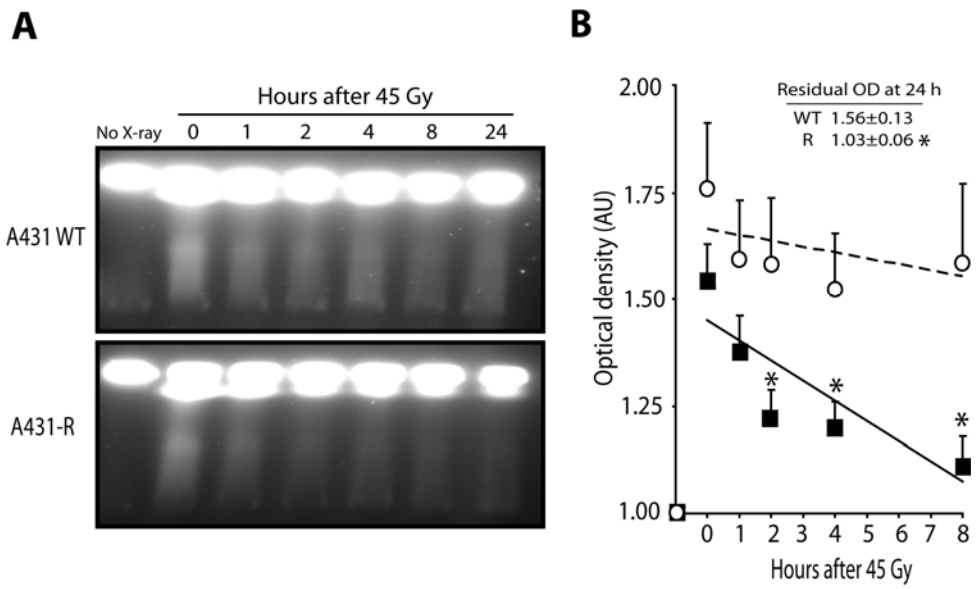

Figure 15. DNA repair evaluation. The ability of rejoining radiation-induced DNA fragments was higher in A431-R cells. A. Representative pictures from PFGE showing different degrees of DNA breakage as smears of variable intensity. To permit DNA repair, cells were cultured as adherent monolayer for 0, 1, 2, 4, 8 or 24 h after irradiation (45 Gy). B. Rejoining was normalized to untreated cells. A431-WT cells (circles) versus A431-R cells (squares). AU stands for arbitrary units. (* $p < 0.05$; Mann-Whitney test).

2). Radiation induced DNA double strand breaks are followed by the phosphorylation of H2AX histone, which can be used as a surrogate of DNA repair as it is dephosphorilated when DNA is repaired. Following a foci-induction dose of 45 Gy, foci progressively decreased during a time-course starting at 30 min and ending at 24 hours.

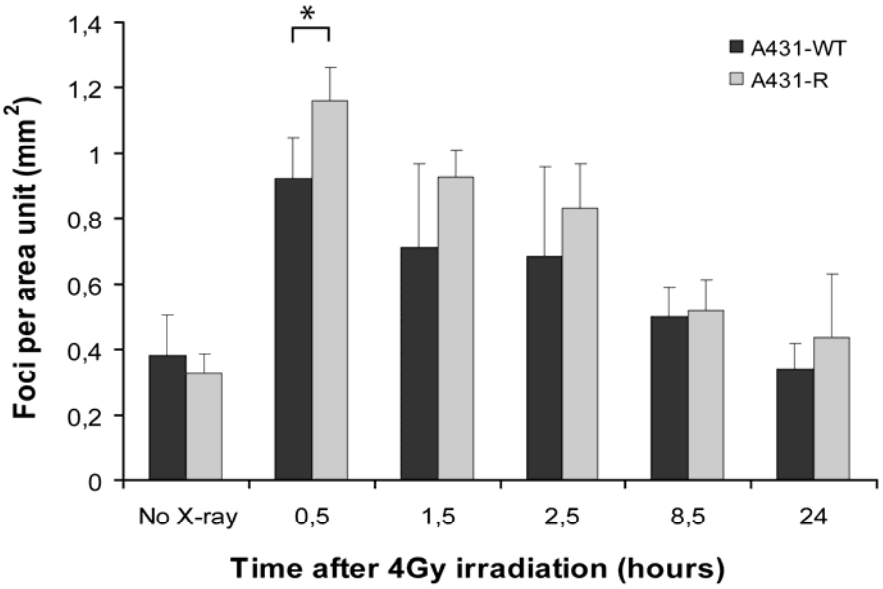

Figure 16. DNA repair after 4 Gy-induction evaluation by immunofluorecence of phosphorylated histone H2AX. (* $p < 0.05$; Mann-Whitney test).

We observed a different pattern of γ-H2AX depending on the type of cell. A significant increase in the number of foci induced 30 minutes after the irradiation was observed in the A431-R cells compared with the parental cells. However, the clearance of H2AX foci in A431-R cells seemed to be more efficient since at 24 h the number of residual foci was similar in both cell types. This observation suggests that A431-R cells could recruited more repair-complexes involving H2AX and consequently decreasing the probability of errors over damage-repair. The deep slope of H2AX-clearance indicates that repair could be more rapid in A431-R cells.

1.2. A431-R cells show radiation resistance: an *in vivo* evidence

Finally, to validate the in vitro findings and definitively establish relative radiation resistance in A431-R cells, we evaluated the effect of fractionated radiotherapy on the growth of xenografted tumours. In irradiated mice, tumour growth was inhibited by radiation in both types of cells.

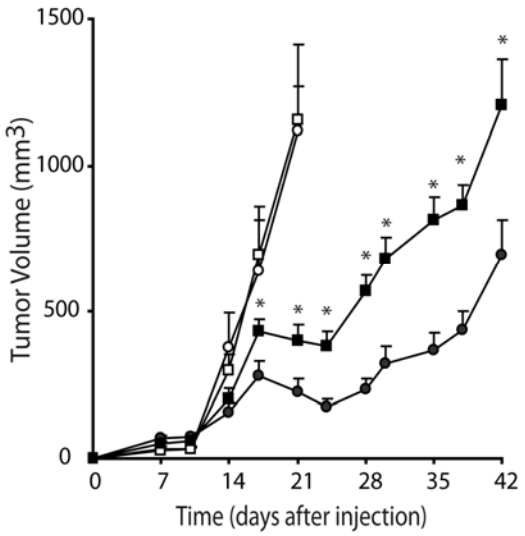

Characteristics of the growth of the tumours in mice treated with radiotherapy

	A431-WT	A431-R	P – value*
Size of tumours at the beginning of radiotherapy, at day 7 (in mm^3)	68.8 ± 10.3	50.2 ± 7.5	0.151
Size of tumours at the end of radiotherapy, at day 21 (in mm^3)	226.4 ± 43.8	401.6 ± 53.4	0.032
Growth delay(1) (in days)	7.1 ± 2.5	2.4 ± 1.5	0.222
Growth rate during the tumour re-growth(2) (in mm^3/day)	34.6 ± 6.1	45.1 ± 3.7	0.347

Explanations: (1) Growth delay was measured as time it took for tumours to reach the size they had at the end of radiotherapy.
(2) Growth rate was calculated by the least square regression method using raw data from the smallest tumour size after beginning radiotherapy to the end of follow-up (range 21 to 42 days after cell injection). Values are the mean± SE of 5 tumours per cellular type.

Figure 17. In vivo characterization of the radiroesistant phenotype. The effect of radiation therapy was lower in xenografts derived from A431-R cells. Tumour growths corresponding to A431-WT cells (circles) and A431-R cells (squares) are shown for non-irradiated (white symbols) and irradiated tumours (black symbols). 30 Gy in 2 weeks, 5 fractions of 3 Gy per week, was administered using 6 MV X-rays, from day 7 to day 21. (*p < 0.05 compared to irradiated parental tumours; Mann-Whitney test).

However, the tumours that derived from A431-R cells were significantly lesser affected by radiation, while tumours from parental cells showed higher response as tumour growth slowed sharply after radiation only to recover later. These results clearly indicate that A431-R cells were less radiosensitive than parental cells and stimulated us to investigate the emergence of a radioresistant phenotype and characterize it.

1.3. Changes involved in the radioresistant phenotype of A431-R cell line

1.3.1. Colony morphology

The baseline clonogenic efficiency of the A431-R cells was 0.19 % ± 0.01 compared to 0.12 % ± 0.02 of parental wild type cells (A431-WT) (p<0.05; Mann Whitney test) indicating that A431-R cells had slightly greater capacity of surviving as single cells. In addition to an increased ability to anchorage and succeed as a colony, the A431-R cells

formed colonies of remarkable larger size that, together with clonogenic efficiency, suggested that these cells could be potentially more aggressive than were earlier.

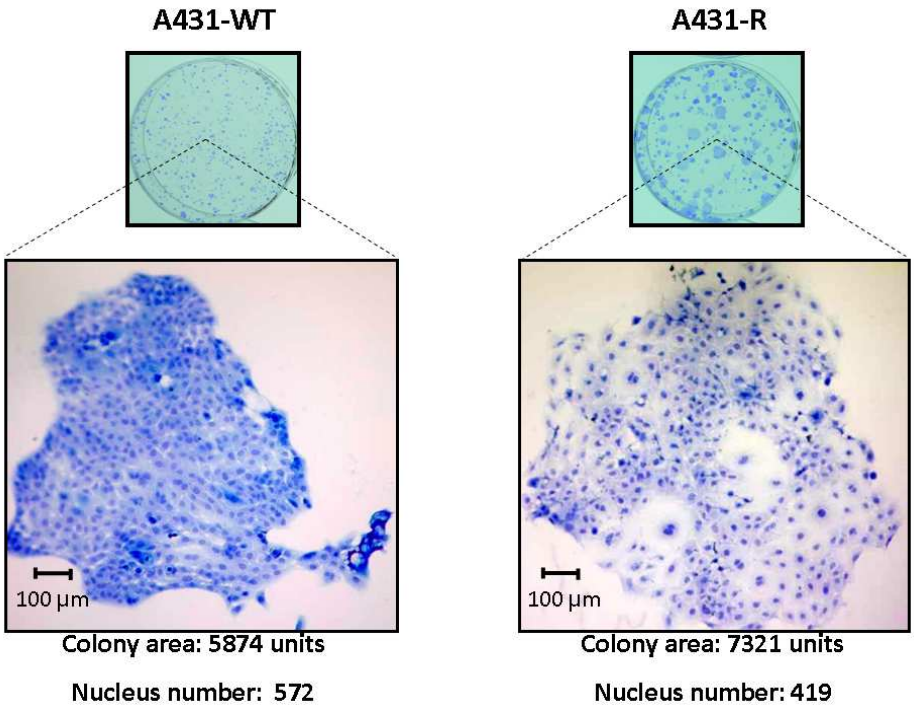

Figure 18. Radioresistant phenotype characterization. Illustrative photographs of the A431-WT and A431-R colonies. The zoom shows the size of colonies and the intensity of the staining in detail.

A431-R cells harboured a sustained ability to grow in huge colonies compared to A431-WT cells. If we take a microscopic look at the colonies, we observed that A431-WT cells were tighter within the colony forming a compacted structure, while A431-R colonies showed more intercellular spaces and more cytoplasm, sometimes taking a foam-like appearance. Despite their smaller size, A431-WT colonies present more cells per colony than A431-R ones.

1.3.2. Cell migration performance

To further explore the emergence of cellular traits that enable cells to exhibit malignant type of behaviour, we decided to determine the ability of migration of these A431-R cells. Experimental findings with the conventional wound healing assay confirmed that A431-R cells had acquired kinetic properties during selection process that allow them to migrate and heal the wound in a shorter period of time than the parental cells, a behaviour clearly consistent with the acquisition of an aggressive phenotype.

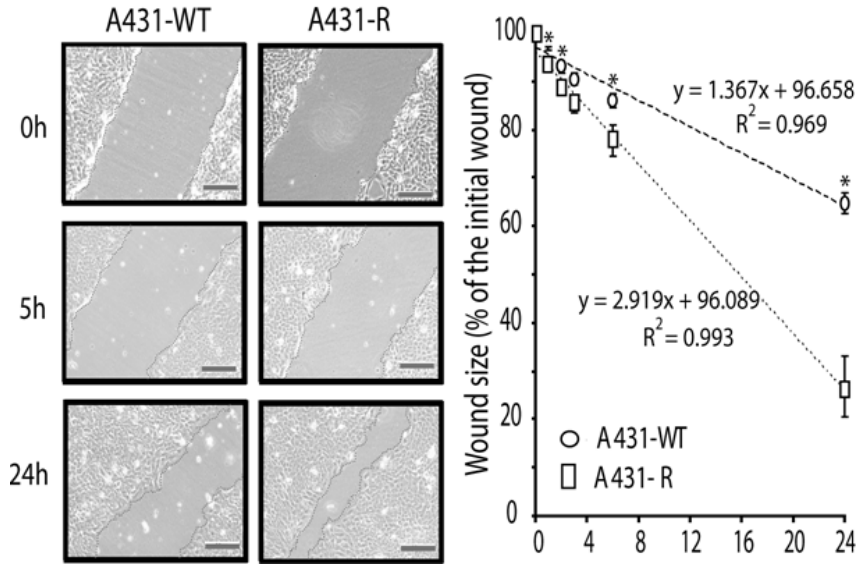

Figure 19. Radioresistant phenotype characterization. In vitro, A431-R cells showed faster migration than the parental cells. Representative microphotographs of the wound healing assay at time-points 0, 5 and 24 h (bars equal to 200 µm). Distance shortening in the wound healing was normalized to the initial distance between borders of each respective wound and was represented as the percentage of the initial wound size. (*$p < 0.05$; Mann-Whitney test).

1.3.3. Activity of the EGFR pathway

Due to the presence of cellular traits that are linked to sustained proliferative cell signalling, and, because, A431 parental cells overexpress the receptor of EGF, a major cell

signal emitter, we looked into this cellular pathway to unravel possible changes that may be involved during the development of A431-R cell line.

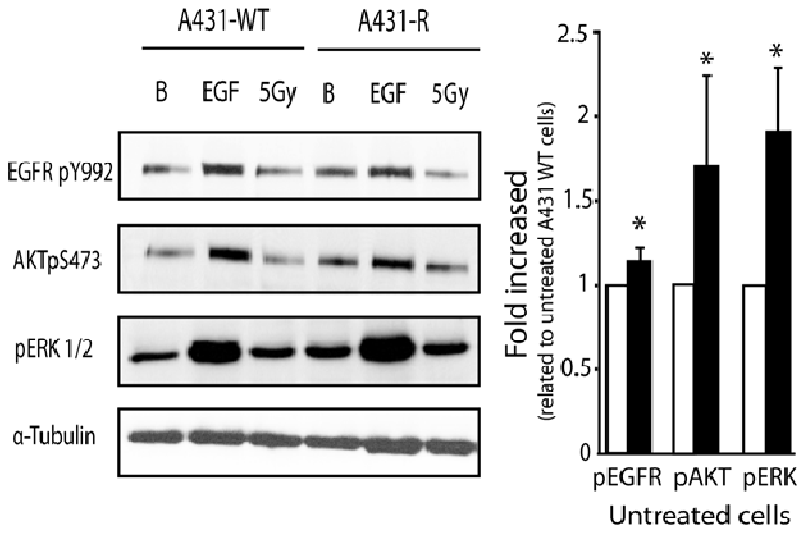

Figure 20. EGFR pathway analysis. A431-R sustained proliferative signalling through high levels of phosphorylated EGFR, AKT and ERK1/2 proteins and radiation-induced secretion of VEGF. A. Proteins were determined by Western blot in cells under baseline culture conditions (B), EGF stimulation (E) or ionising radiation (5 Gy). Before cell lysis, cells were treated with 10 ng/mL EGF for 10 min or 6 MV X-rays. α-Tubulin was used as internal control. Bar chart shows specific protein levels normalized by untreated A431-WT cells (white bars) versus A431-R cells (black bars). (* $p < 0.05$; Mann-Whitney test).

The most remarkable finding was that A431-R cells presented higher baseline levels of phosphorylated EGF receptor, and the AKT and ERK1/2 transducers, linchpin proteins that are involved in cell growth, mitogenesis, survival, DNA repair ability, and cell migration. After cell stimulation by the presence of EGF ligand, both types of cell lines reacted by increasing levels of former oncoproteins, prominently pERK1/2. When A431-WT cells were treated with ionising radiation, they reacted by increasing the levels of phosphorylated ERK1/2 proteins, a response that was seen irrespectively of EGF presence. However, in the A431-R cells, irradiation was not followed by a rise in the phosphorylated levels of EGFR, AKT or ERK1/2. In fact, a diminution relative to their baseline levels was observed, especially with respect to EGFR. We speculated whether

A431-R cells did not need to further activate these oncoproteins which were already hyperactivated at the baseline conditions.

1.3.4. Radiation-induced levels of VEGF secretion

To further evaluate distinct aspects of the radioresistant phenotype, we assessed the levels of VEGF, a crucial factor in tumour-associated angiogenesis and efficient tumour blood supply, secretion of which may also be regulated by EGFR and ionising radiation (Gorski, Beckett et al. 1999; Pueyo, Mesia et al. 2010).

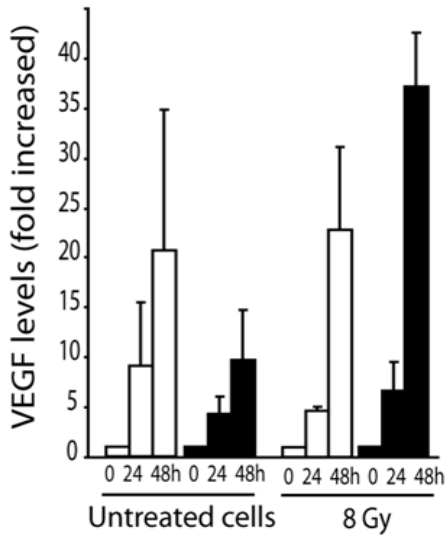

Figure 21. VEGF determination by the ELISA method at different interval times after 8 Gy. Cells were left to grow without FBS for 24 h before collecting supernatants at time 0, 24 and 48 h in A431-WT (white bars) and A431-R cells (black bars). VEGF values were normalized to the cell numbers per dish. Data were obtained from two independent experiments.

Both types of cells respond to radiation by increasing the secretion of VEGF. However, as suspected, the release of VEGF in response to radiation was more efficiently in the A431-R cells. Thus, we concluded that these cells were better adapted to resist strenuous conditions, such as the oxidative stress induced by radiotherapy, and able to promote angiogenesis to facilitate their oncogenic potential.

1.3.5. CD44 marker presence

Recently, the cell surface antigen CD44, a putative stem cell marker, has been functionally validated as a biomarker to predict local control for early laryngeal cancer treated with radiotherapy, which suggests that this antigen could be a proper surrogate indicator for radioresistant phenotypes (de Jong, Pramana et al. 2010). As intrinsic radiation resistance has been associated to cancer stem cells, we checked if there existed any difference in the proportion of putative cancer stem cells between A431-WT and A431-R cells. We analyzed by FACS the proportion of $CD44^{+}/CD31^{+/}Epcam^{+}$ cells for each cell type.

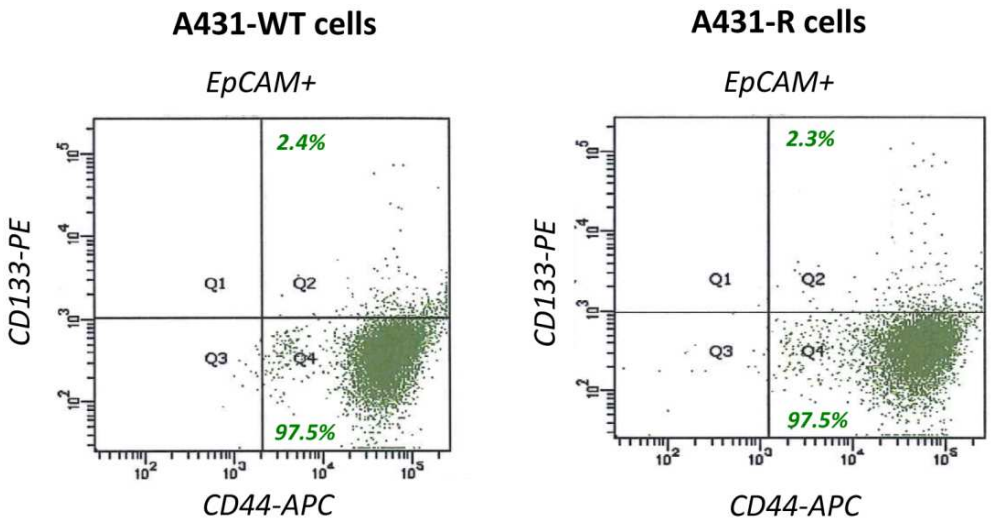

Figure 22. $CD44^{+}/CD31^{+/}Epcam^{+}$ expression determination. Flow cytometry detection of CD44, CD31, and Epcam markers for A431-WT and A431-R cell lines.

We did not found differences between both cell lines in the proportion of cancer stem cells. We found that in the parental A431-WT cell line, the proportion of $CD44^{+}/CD31^{+/}Epcam^{+}$ cells was 2.4 %, while for A431-R cells, the proportion was 2.3%.

In addition, we checked by immunofluorescence the expression of CD44 antigen in the two A431 cell lines and we did not find differential expression between both cell lines.

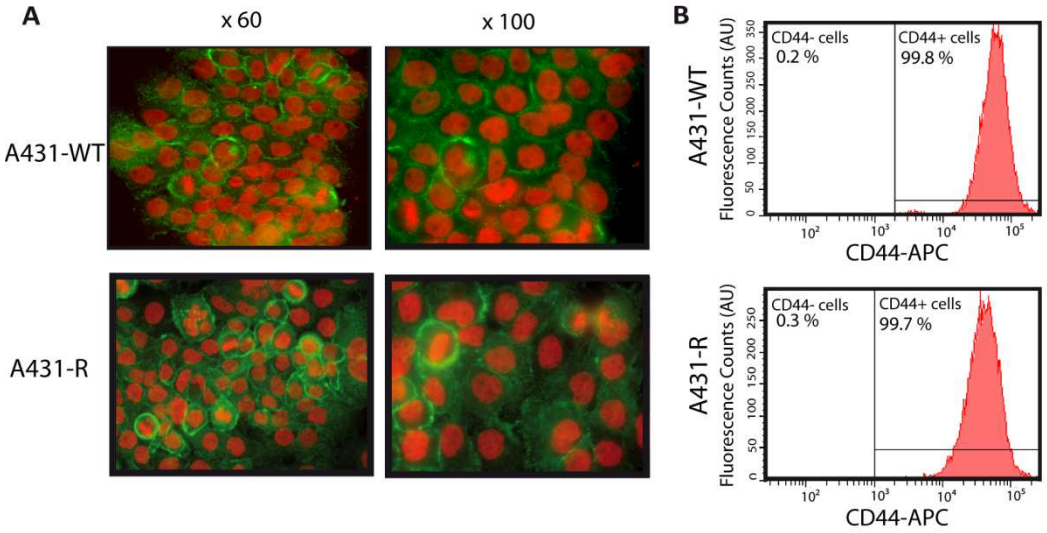

Figure 23. CD44 expression determination. CD44 antigen expression of A431-WT and A431-R cells remained unchanged. **A.** Illustrative immunofluorescence microphotographs of the surface marker CD44 under baseline culture conditions. **B.** Flow cytometry detection of CD44 marker. The x-axis shows negative and positive gates for CD44 marker in both types of cells, while the y-axis shows the number of events. AU stands for arbitrary units.

Thus, this infers that this protein was constitutively expressed in the parental and, hence, its derived resistant cell line, irrespectively of their grade of radiation sensitivity.

1.3.6. Distribution of the phases of the cell cycle

Finally, because cell cycle distribution can influence in radiation sensitivity, the distribution of cell cycle phases was examined. It is known that the cells in G2 phase are more sensitive to radiation and those cells in S phase are less sensitive or more resistant to radiation. We found that G1 phase was 63.1% versus 67.9%, S phase was 28.3% versus 19.8% and G2/M phase was 8.5% versus 12.1%, for A431-WT and A431-R cell population, respectively, suggesting a non-relevant variation in cell cycle between cell types.

1.3.7. Methylation of the genome

DNA methylation is the most studied epigenetic mark and CpG methylation is central to many biological processes. Since cancer has highlighted the contribution to disease of aberrant DNA methylation patterns, such as the presence of promoter CpG island hypermethylation-associated silencing of tumour suppressor genes and global DNA hypomethylation defects, we decided to study if there existed different methylation patterns between the radioresistant cell line generated (A431-R) and the parental cell line (A431-WT).

We obtained a list of 36 genes with a difference in the degree of methylation of more than 50 % between A431-WT and A431-R. From those 36 genes, 13 genes were hypomethylated (Delta/Beta negative values) in the A431-R cells compared to the parental ones, and the other 23 genes were hypermethylated in the radioresistant cells (Delta/Beta positive values).

Delta/Beta	TargetID	Chr	MAPINFO	Gene Name	Reference Gene
0,94	cg15365500	6	149356915	UST	Body
0,77	cg15082498	1	65421982	JAK1	5'UTR
0,76	cg22084460	19	13348050	CACNA1A	Body
0,70	cg25130590	18	77110161	ATP9B	Body
0,68	cg21073020	6	169013732	SMOC2	Body
0,68	cg11165881	3	238048	CHL1	TSS1500
0,65	cg14198450	9	78759126	PCSK5	Body
0,62	cg14350197	18	35147162	BRUNOL4	TSS1500
0,62	cg25329685	8	23315749	ENTPD4	TSS1500
0,61	cg18277764	3	239188	CHL1	5'UTR
0,61	cg19853833	18	35146668	BRUNOL4	TSS1500
0,60	cg00457019	19	2933421	ZNF77	3'UTR
0,58	cg11002851	4	37455729	C4orf19	5'UTR
0,55	cg01652721	8	10755161	XKR6	3'UTR
0,55	cg06940756	8	10927738	XKR6	Body
0,54	cg17845266	2	238769060	RAMP1	Body
0,54	cg24126618	19	39523083	FBXO27	5'UTR
0,53	cg20060108	2	102954350	IL1RL1	5'UTR
0,52	cg15779643	17	9806785	RCVRN	Body

0,51	cg27180636	3	75715783	FRG2C	3'UTR
0,51	cg21691367	6	151325642	MTHFD1L	Body
0,51	cg27453365	11	108092316	ATM, NPAT	TSS1500; Body
0,50	cg00323100	4	40059856	N4BP2	5'UTR
-0,50	cg19614454	6	139265575	REPS1	Body
-0,51	cg06228648	13	26040175	ATP8A2	Body
-0,51	cg25578781	11	128446070	ETS1	5'UTR
-0,52	cg10040196	14	100259352	EML1	TSS1500
-0,52	cg10237765	17	9863081	GAS7	Body; TSS1500
-0,53	cg14704078	13	49895592	CAB39L	Body
-0,53	cg06157924	4	942005	TMEM175	Body
-0,54	cg00405190	2	175545838	WIPF1	5'UTR
-0,55	cg14669361	6	32038747	TNXB	Body
-0,61	cg20549346	6	32297806	C6orf10	Body
-0,62	cg00101713	15	32984867	SCG5	Body
-0,62	cg05431964	11	120853286	GRIK4	Body
-0,76	cg03130248	1	245524538	KIF26B	Body

The function of proteins encoded by the 13 genes hypomethylated in the A431-R cell was as follows:

REPS1 **RALBP1 associated Eps domain containing 1**. May coordinate the cellular actions of activated EGF receptors and Ral-GTPases. (795 aa).

ATP8A2 **ATPase, aminophospholipid transporter-like, class I, type 8A, member 2**. (1188 aa).

ETS1 **Calcium binding protein 39-like**. (337 aa).

EML1 **WAS/WASL interacting protein family, member 1**. May have direct activity on the actin cytoskeleton. Induces actin polymerization and redistribution. Contributes with NCK1 and GRB2 in the recruitment and activation of WASL. May participate in regulating the subcellular localization of WASL, resulting in the disassembly of stress fibers in favour of filopodia formation (By similarity). Plays an important role in the intracellular motility of vaccinia virus by functioning as an adapter for recruiting WASL to vaccinia virus. (503 aa).

GAS7 **Echinoderm microtubule associated protein like 1**. May modify the assembly dynamics of microtubules, such that microtubules are slightly longer, but more dynamic (by similarity). (834 aa).

CAB39L **Transmembrane protein 175**. (504 aa).

TMEM175 **Glutamate receptor, ionotropic, kainate 4**. Receptor for glutamate. L-glutamate acts as an excitatory neurotransmitter at many synapses in the central nervous system. The postsynaptic actions of Glutamate are mediated by a variety of receptors that are named according to their selective agonists. (956 aa).

WIPF1 **V-ets erythroblastosis virus E26 oncogene homolog 1** (avian). Transcription factor. (485 aa).

TNXB **Tenascin XB**. (4242 aa).

C6orf10 **Putative uncharacterized protein C6orf10**. Putative uncharacterized protein ENSP00000411164. Putative uncharacterized protein ENSP00000415864. (193 aa).

SCG5 **Growth arrest-specific 7**. May play a role in promoting maturation and morphological differentiation of cerebellar neurons. (476 aa).

GRIK4 **Secretogranin V** (7B2 protein). Acts as a molecular chaperone for PCSK2/PC2, preventing its premature activation in the regulated secretory pathway. Binds to inactive PCSK2 in the endoplasmic reticulum and facilitates its transport from there to later compartments of the secretory pathway where it is proteolytically matured and activated. Also required for cleavage of PCSK2 but does not appear to be involved in its folding. Plays a role in regulating pituitary hormone secretion. The C-terminal peptide inhibits PCSK2 in vitro. (212 aa).

KIF26B **Kinesin family member 26B**. (2108 aa).

We used the online program STRING (http://string-db.org/), which present a database of known and predicted protein interactions, including direct (physical) and indirect (functional) associations. Although we expected to obtain some associations between those proteins in order to look for a specific pathway involved in one of the mechanisms underlying resistance to radiation (such as DNA repair proteins, proliferation pathways effectors...), we found no associations between the proteins whose genes were hypomethylated in the radioresistant cell line. Neither of the proteins had a role that could explain the different radiosensitivity between A431-WT and A431-R cells.

The functions of the products of the 23 genes hypermethylated in the A431-R cell line were as follows:

UST	**Uronyl-2-sulfotransferase. Sulfotransferase** that catalyzes the transfer of sulfate to the position 2 of uronyl residues. Has mainly activity toward iduronyl residues in dermatan sulfate, and weaker activity toward glucuronyl residues of chondroitin sulfate. Has no activity toward desulfated N-resulfated heparin. (406 aa).
JAK1	**Janus kinase 1**. Tyrosine kinase of the non-receptor type, involved in the IFN-alpha/beta/gamma signal pathway. Kinase partner for the interleukin (IL)-2 receptor. (1154 aa).
CACNA1A	**Calcium channel, voltage-dependent, P/Q type, alpha 1A subunit**. Voltage-sensitive calcium channels (VSCC) mediate the entry of calcium ions into excitable cells and are also involved in a variety of calcium-dependent processes, including muscle contraction, hormone or neurotransmitter release, gene expression, cell motility, cell division and cell death. The isoform alpha-1A gives rise to P and/or Q-type calcium currents. P/Q-type calcium channels belong to the 'high-voltage activated' (HVA) group and are blocked by the funnel toxin (Ftx) and by the omega-agatoxin- IVA (omega-Aga-IVA). (2506 aa).
ATP9B	**ATPase, class II, type 9B**. (1147 aa).
SMOC2	**SPARC related modular calcium binding 2**. Promotes matrix assembly and cell adhesiveness (by similarity). Can stimulate endothelial cell proliferation, migration, as well as angiogenesis. (457 aa).
CHL1	**Cell adhesion molecule with homology to L1CAM (close homolog of L1**). Extracellular matrix and cell adhesion protein that plays a role in nervous system development and in synaptic plasticity. Both soluble and membranous forms promote neurite outgrowth of cerebellar and hippocampal neurons and suppress neuronal cell death. Plays a role in neuronal positioning of pyramidal neurons and in regulation of both the number of interneurons and the efficacy of GABAnergic synapses. May play a role in regulating cell migration in nerve regeneration and cortical development. (1224 aa).

PCSK5	**Proprotein convertase subtilisin/kexin type 5**. Likely to represent a widespread endoprotease activity within the constitutive and regulated secretory pathway. Capable of cleavage at the RX(K/R)R consensus motif. (913 aa).
BRUNOL4/CELF4	**Bruno-like 4, RNA binding protein** (Drosophila). RNA-binding protein implicated in the regulation of pre-mRNA alternative splicing. Mediates exon inclusion and/or exclusion in pre-mRNA that are subject to tissue-specific and developmentally regulated alternative splicing. Specifically activates exon 5 inclusion of cardiac isoforms of TNNT2 during heart remodeling at the juvenile to adult transition. Promotes exclusion of both the smooth muscle (SM) and non-muscle (NM) exons in actinin pre-mRNAs. (486 aa).
ENTPD4	**Ectonucleoside triphosphate diphosphohydrolase 4**. Hydrolyzes preferentially nucleoside 5'-diphosphates, nucleoside 5'-triphosphates are hydrolyzed only to a minor extent. (616 aa).
ZNF77	**Zinc finger protein 77**. May be involved in transcriptional regulation. (545 aa).
C4orf19	**Uncharacterized protein C4orf19**. (314 aa).
XKR6	**XK, Kell blood group complex subunit-related family, member 6**. (641 aa).
RAMP1	**Receptor (G protein-coupled) activity modifying protein 1**. Transports the calcitonin gene-related peptide type 1 receptor (CALCRL) to the plasma membrane. Acts as a receptor for calcitonin-gene-related peptide (CGRP) together with CALCRL. (148 aa).
FBXO27	**F-box protein 27**. Substrate-recognition component of the SCF (SKP1-CUL1-F- box protein)-type E3 ubiquitin ligase complex (by similarity). (283 aa).
IL1RL1	**Interleukin 1 receptor-like 1**. Receptor for interleukin-33 (IL-33), its stimulation recruits MYD88, IRAK1, IRAK4, and TRAF6, followed by phosphorylation of MAPK3/ERK1 and/or MAPK1/ERK2, MAPK14, and MAPK8. Possibly involved in helper T-cell function. (556 aa).
RCVRN	**Recoverin**. Seems to be implicated in the pathway from retinal

	rod granulated cyclase to rhodopsin. May be involved in the inhibition of the phosphorylation of rhodopsin in a calcium-dependent manner. The calcium-bound recoverin prolongs the photoresponse. (200 aa).
FRG2C	**FSHD region gene 2 family, member C**. (282 aa).
MTHFD1L	**Methylenetetrahydrofolate dehydrogenase (NADP+ dependent) 1-like**. May provide the missing metabolic reaction required to link the mitochondria and the cytoplasm in the mammalian model of one-carbon folate metabolism in embryonic and transformed cells complementing thus the enzymatic activities of MTHFD2 (by similarity). (978 aa).
NPAT	**Nuclear protein, ataxia-telangiectasia locus**. Required for progression through the G1 and S phases of the cell cycle and for S phase entry. Activates transcription of the histone H2A, histone H2B, histone H3 and histone H4 genes in conjunction with MIZF. Also positively regulates the ATM, MIZF and PRKDC promoters. Transcriptional activation may be accomplished at least in part by the recruitment of the NuA4 histone acetyltransferase (HAT) complex to target gene promoters. (1427 aa).
ATM	**Ataxia telangiectasia mutated**. Serine/threonine protein kinase which activates checkpoint signaling upon double strand breaks (DSBs), apoptosis and genotoxic stresses such as ionizing ultraviolet A light (UVA), thereby acting as a DNA damage sensor. Recognizes the substrate consensus sequence [ST]-Q. Phosphorylates 'Ser-139' of histone variant H2AX/H2AFX at double strand breaks (DSBs), thereby regulating DNA damage response mechanism. Also involved in signal transduction and cell cycle control. May function as a tumour suppressor. Necessary for activation of ABL1 and SAPK. (3056 aa).
N4BP2	**NEDD4 binding protein 2**. Has 5'-polynucleotide kinase and nicking endonuclease activity. May play a role in DNA repair or recombination. (1770 aa).

No physical or functional associations were found between the proteins whose genes were hypermethylated in the radioresistant cell line compared to the parental cell

line, using the above mentioned program STRING, except the one between NPAT and ATM. In fact, NPAT protein positively regulates ATM promoters.

It is of note that the proteins NPAT and ATM were found to be silenciated in the radioresitant cell line. The fact that those cells have less activity of the ATM protein may imply that those cells would sense less DNA damage by this protein as they would have less activation of the checkpoint signalling upon double strand breaks (DSBs), apoptosis and genotoxic stresses (such as ionizing ultraviolet A light). However, this is not consistent with the results obtained by PFGE (Figure 15) and H2AX immunofluorescence (Figure 16) experiments, suggesting that there must be some kind of compensation afterwards: either an ulterior phosphorylation that activates ATM afterwards or either activity of other proteins, such as for example ATR, that are also involved in the detection and repair of DNA damage and compensate the downregulation of ATM. Even if ATM is the first molecule to be activated in response to DNA damage, and is the responsible for the immediate and rapid response, ATR binds to DNA in a later phase and maintain the phosphorylated states of specific substrates. However, ATR also responds to DNA damages that do not activate ATM, such as treatments with UV radiation, blockade of replication forks and hypoxia. In those cases, ATR dephosphorylates some of the substrates from ATM such as p53 and BRCA1. It could be the case for A431-R cells that ATR or other proteins compensate the silencing of ATM protein.

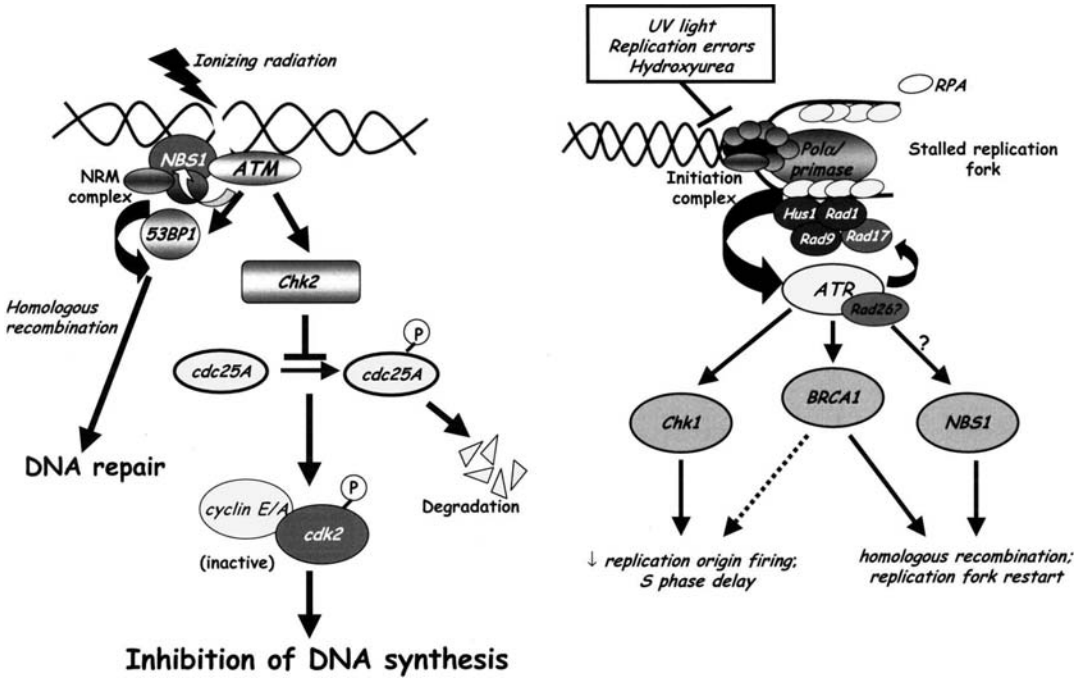

Figure 24. Roles of ATM and ATR in signaling through S-phase checkpoints (Abraham 2001)

2. DEVELOPMENT OF A TECHNIQUE TO IRRADIATE MICE BEARING XENOGRAFTS

In this section we reported as results the data obtained through the development and refinement of a method to irradiate mice bearing xenotumours. Here the focus is the validation of the method as a technique that works for experimental evaluation of radiosensitivity of human tumours in vivo. Therefore the core data refers to the health of mice from the start to the end (months later) of experiments to confirm general feasibility of the method.

2.1. Considerations

We develop and describe a procedure to deliver fractionated radiotherapy to xenoimplanted tumours in immunodeficient mice using a medical linear accelerator, a method that was devised as an alternative to the lack of facilities devoted to radiation research.

Some important considerations were taken into account:

- Mice were manipulated as mentioned in section 2.3. of Material & Methods chapter and were evaluated twice a week.
- Non-irradiated mice were subjected to the same procedures (anaesthesia, transport to the radiotherapy department, anaesthesia reversal).
- No animals were excluded or had received less than 30 Gy in 10 fractions (3 Gy per fraction).
- After radiotherapy tumours grew more slowly and took twice the time to reach a volume equivalent to non-irradiated animals.
- The most severe observation was always registered, whether it was reversible or not.

2.2. Animals global health evaluation

In table 3, we describe and summarize the animals' health during radiotherapy period and follow-up paying special attention to weight loss, physical appearance of the animals, clinical signals, alterations in the behaviour, tumour necrosis or local radiation-induced toxicity.

	Control mice (non-irradiated)								X-ray-treated mice							
	Therapy period (n = 13)				Post-therapy period (n = 12)				Therapy period (n = 32)				Post-therapy period (n = 31)			
	Grade score (%)				Grade score (%)				Grade score (%)				Grade score (%)			
Supervision parameters	0	1	2	3	0	1	2	3	0	1	2	3	0	1	2	3
Weight loss[†]	76.9	15.4	7.7	0	83.3	8.3	8.3	0	43.8	46.9	9.4	0	61.3	35.5	3.2	0
Physical aspects[‡]	100	0	0	0	100	0	0	0	100	0	0	0	100	0	0	0
Clinical signals[¶]	100	0	0	0	100	0	0	0	100	0	0	0	100	0	0	0
Behaviour alterations[#]	100	0	0	0	100	0	0	0	100	0	0	0	87.1	12.9	0	0
Infections[††]	100	0	0	–	100	0	0	–	100	0	0	–	100	0	0	–
Stools[‡‡]	100	0	0	–	100	0	0	–	100	0	0	–	100	0	0	–
Tumour necrosis[¶¶]	100	0	–	–	91.7	8.3	–	–	100	0	–	–	100	0	–	–
Local radiation toxicity[##]	100	0	0	0	100	0	0	0	100	0	0	0	100	0	0	0

Values are the proportion of an observation expressed in grades related to the total number of animals (n) within the period of follow-up
[†]*Weight loss*. Grades: 0 no weight loss; 1 less than 10%; 2 between 10 and 20%; 3 more than 20%
[‡]*Physical appearance*. Grades: 0 normal; 1 changes in skin colour; 2 paleness and cyanosis; 3 hunching and loss of muscular mass
[¶]*Clinical signals*. Grades: 0 no presence; 1 hypothermia; 2 bleeding or mucosal secretion in any orifice; 3 abdominal strain and cachexia
[#]*Behaviour alterations*. Grades: 0 no alterations; 1 unable to move normally; 2 impossible to arrive to food/drink; 3 unconsciousness and no response to stimuli
[††]*Percentage of animals with infectious disease*. Grades: 0 no infections; 1 animals infected that survived; 2 animals infected that died. Grade 3 not evaluated (NA)
[‡‡]*Stools appearance*. Grades: 0 normal; 1 soft stools; 2 visible blood. Grade 3 NA
[¶¶]*Percentage of tumour necrosis*. Grades: 0 no tumour necrosis; 1 tumour necrosis. Grades 2 and 3 NA
[##]*Local radiation-induced toxicity*. Grades: 0 no presence; 1 erythema; 2 exudative lesion; 3 necrosis

Table 3. Evaluation of the quality of life of mice during and after localized irradiation of the tumours in multiple fractions. Different criteria were analysed.

2.2.1. Mice weight as a surrogate of health

The greatest adverse effect of radiation was the diminution in the initial weight, which we ascribed to the partial exposure of the inferior right hemiabdomen, too much close of the tumour to be completely protected from the radiation beam. However, the weight loss was not remarkable and was limited to grade 1, transitory and not associated to physical or clinical signs of disease. Also, in the irradiated group, 2 animals (12.9%) moved abnormally due to tumour growth, but not to local reaction because of radiation. Interestingly, in non-irradiated mice greater weight loss was observed, which was attributable to uncontrolled tumour growth. Differences in weight loss between groups, however, were not significant (Chi-square and Mann Whitney test).

2.2.2. Infections

No infections were observed. Stools and skin/mucosa appearance were monitored showing no signs of microbiological diseases during radiotherapy period and follow-up.

The absence of infect–contagious diseases was particularly decisive for the success of experiments. This provided evidence that the barrier protections used accomplished the goal of preventing microbiological diseases in these animals. Since cancer patients are often immunosuppressed, concerns about zoonoses should not be ignored. Nevertheless, it should be emphasized that the potential risk of zoonoses is extremely low when good laboratory practices and healthy athymic mice are used. To our knowledge, there is no report in the medical literature about the incidence of opportunistic zoonoses in patients treated in such radiation oncology departments.

3. SIMVASTATIN SENSITIZES TO RADIOTHERAPY PLUS CETUXIMAB

3.1. *In vitro* effects of radiotherapy, cetuximab, and simvastatin

The principal aim of this part of the project was to test whether simvastatin may increase the therapeutic effect of radiation and cetuximab on tumor growth in xenograft models derived from human squamous cell carcinomas. Nevertheless we used cancer cell cultures before to come into *in vivo* experiments.

3.1.1. Effects on wound healing

It was first evaluated *in vitro* whether simvastatin could influence cell viability of cancer cells treated with radiation and cetuximab. We examined immediate effects of treatments by means of wound healing assay.

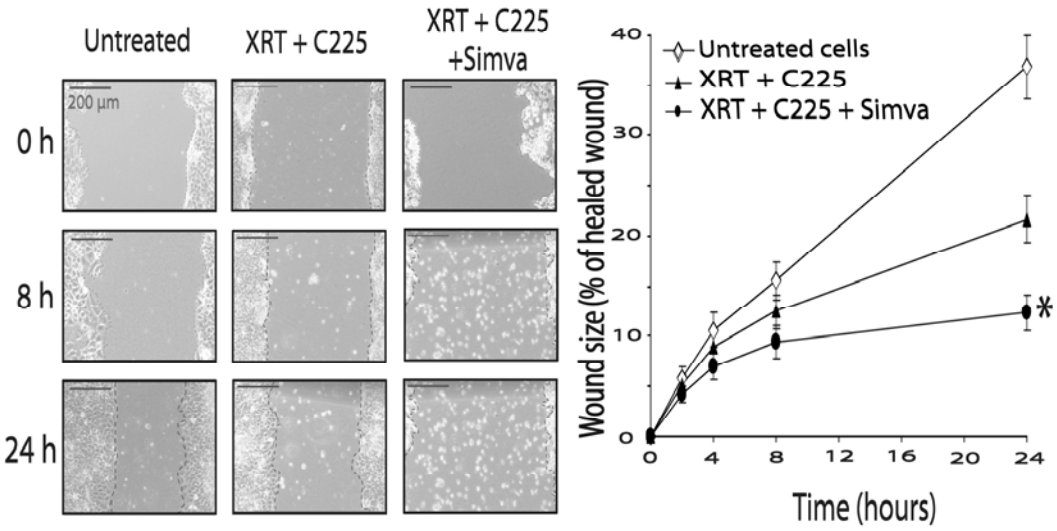

Figure 25. Addition of simvastatin to XRT and C225 treatment decreased cell migration of FaDu cells. (* $p < 0.05$; Mann-Whitney test).

	Wound Size (% of healed wound)				
	2 h	4 h	8 h	24 h	*p*-value
Non-treatment	5.80 ± 1.20	10.59 ± 1.68	15.55 ± 1.85	36.80 ± 3.23	
XRT (3 Gy)	5.61 ± 0.87	9.09 ± 1.37	13.11 ± 2.16	25.27 ± 2.19	0.077 (1)
C225 (30 nM)	5.17 ± 1.15	7.83 ± 1.47	11.07 ± 2.15	18.78 ± 3.55	0.001 (1)
Simva (15 µM)	2.04 ± 0.46	6.37 ± 1.73	9.32 ± 1.52	12.75 ± 2.37	0.001 (1)
XRT+C225	5.14 ± 1.05	8.93 ± 1.52	12.46 ± 1.73	21.66 ± 2.35	0.001 (1)
XRT+C225+Simva	4.20 ± 0.80	6.98 ± 1.36	9.43 ± 1.58	12.36 ± 1.78	0.001 (1) 0.005 (2)

Cell cultures were treated as indicated in material and methods. Values are mean ± SE of 3 independent experiments each per duplicated. Doses used in the combined treatments are the same as in the single treatments. *p*-value (Mann-Whitney test): (1) compared to non-treatment condition, (2) compared to XRT+C225 alone.

Table 4. Wound healing assays data in FaDu cell line.

Wound size decreased progressively, as wounds were repaired, over a 24-hour period. All treatments slowed down wound healing, but the rate of healing was lower in cultures that received 15 µM simvastatin. At 2, 4 and 8 hours after creating the wound, we found that the presence of simvastatin was involved in the higher inhibitory effects of the treatments, although differences were not significant. However, when the observation was extended to 24 hours, differences became more apparent and statistically significant suggesting that inhibition of cell proliferation rather than cell migration—the latter being an early event—could have been implicated in this observation. It is important to note that triple treatment with radiotherapy, cetuximab and simvastatin was more cytotoxic than radiotherapy and cetuximab without the statin which indicates a potential role for simvastatin.

We decided to evaluate whether simvastatin also influence cell migration of radioresistant A431-R cells treated with radiation and cetuximab.

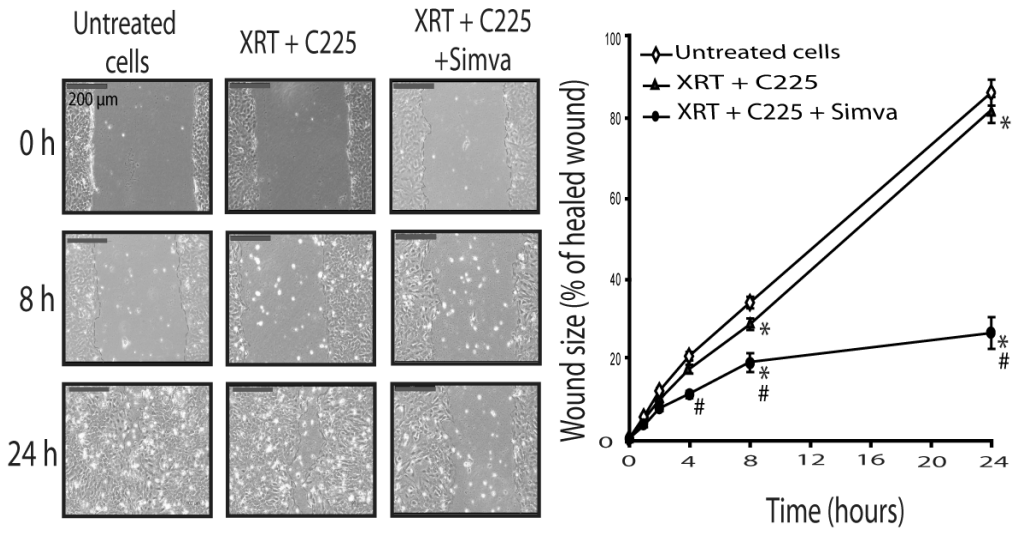

Figure 26. Addition of simvastatin to XRT and C225 treatment decreased cell migration of radioresistant A431-R cells. (* $p < 0.05$ compared to untreated condition; # $p < 0.05$ compared to XRT plus C225; Mann-Whitney test).

	Wound Size (% of healed wound)				
	2 h	4 h	8 h	24 h	*p*-value
Non-treatment	9.75 ± 0.84	17.23 ± 1.06	28.73 ± 1.48	82.25 ± 3.29	
XRT+C225	12.00 ± 1.37	20.56 ± 1.76	34.19 ± 2.80	86.73 ± 4.32	0.190 (1)
XRT+C225+Simva	7.53 ± 0.72	11.11 ± 1.00	19.08 ± 2.44	26.45 ± 4.10	0.001 (1) 0.001 (2)

Cell cultures were treated as indicated in material and methods. Values are mean ± SE of 3 independent experiments each per duplicated. Doses used in the combined treatments are the same as in the single treatments. *p*-value (Mann-Whitney test): (1) compared to non-treatment condition, (2) compared to XRT+C225 alone.

Table 5. Wound healing assays data in A431-R cell line.

For radioresistant A431-R cells, wound size decreased progressively, as wounds were repaired, over a 24-hour period. As for FaDu cells, all the treatments slowed down wound healing, but the rate of healing was lower in cultures that received 15 µM simvastatin. Both treatments had an inhibitory effect at 8 and 24 hours after creating the wound (* *p-values* < 0.05 compared to untreated condition in Figure 26). The presence of simvastatin was involved in the higher inhibitory effect of the treatment from 4 hours after creating the wound onwards, with significant differences. Statistical differences

were found between both treatments (# *p-values* < 0.05 compared to XRT+C225 in Figure 26) at 4 and 8 hours, however at 24 hours differences became more apparent. It is important to note that triple treatment with radiotherapy, cetuximab and simvastatin was more cytotoxic than radiotherapy and cetuximab without the statin in this model of radioresistant cell line, which indicates a potential role for simvastatin in reversing the resistance in this cell type.

3.1.2. Effects on cell proliferation

To investigate the effects of simvastatin on cell proliferation, we subjected FaDu and A431-WT cell cultures to the different treatments for longer periods of time of 24, 48 and 72 hours. In both cell lines, cell number increased as a function of time, but FaDu cells showed higher proliferation rates.

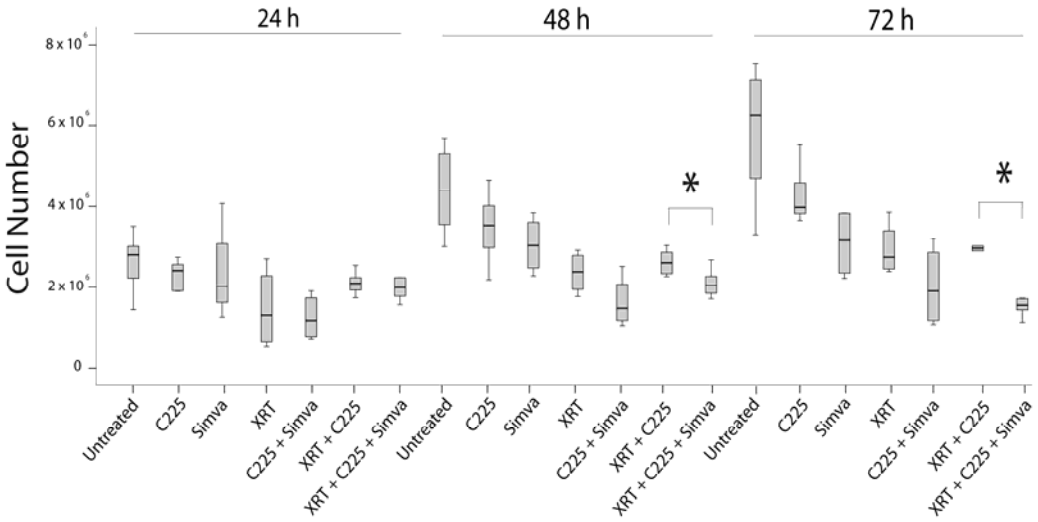

Figure 27. Effect of the different combinations of radiotherapy, simvastatin and cetuximab on FaDu cells' proliferation. (* $p < 0.05$; Mann-Whitney test).

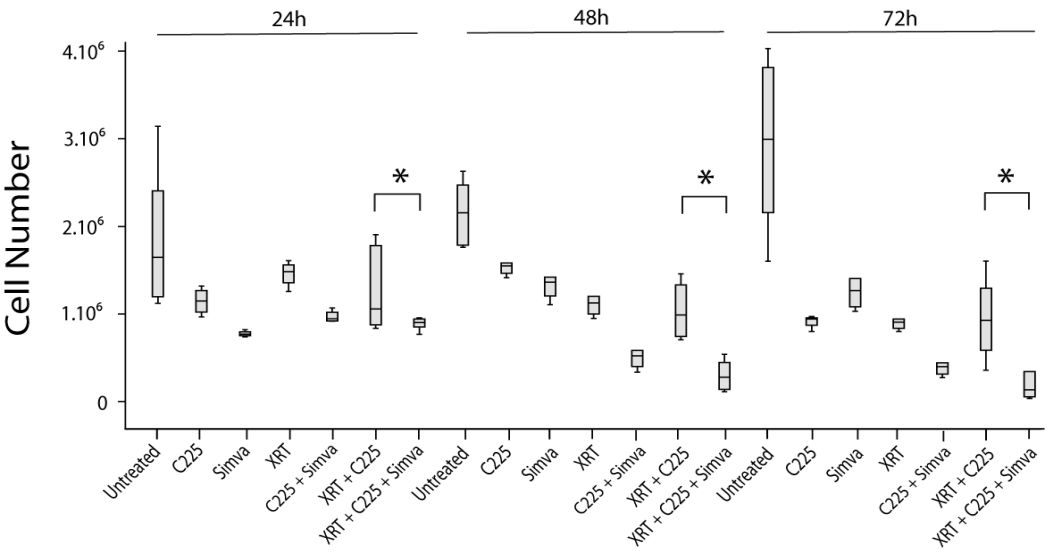

Figure 28. Effect of the different combinations of radiotherapy, simvastatin and cetuximab on A431-WT cells' proliferation. (* $p < 0.05$; Mann-Whitney test).

FaDu cell line	Cell number (10^6)					
	24 h	*p*-value	48 h	*p*-value	72 h	*p*-value
Non-treatment	2.63 ± 0.24	-	4.39 ± 0.35	-	5.88 ± 0.55	-
XRT (3 Gy)	1.46 ± 0.50	0.062 (1)	2.36 ± 0.26	0.007 (1)	2.93 ± 0.33	0.017 (1)
C225 (10 nM)	2.32 ± 0.01	0.156 (1)	3.48 ± 0.34	0.121 (1)	4.26 ± 0.28	0.071 (1)
Simva (15µM)	2.34 ± 0.60	0.497 (1)	3.05 ± 0.35	0.042 (1)	3.09 ± 0.42	0.017 (1)
XRT+C225	2.11 ± 0.11	0.093 (1) 0.286 (2)	2.62 ± 0.12	0.003 (1)	2.94 ± 0.83	0.002 (1) 0.670 (2)
XRT+C225+Simva	2.02 ± 0.16	0.071 (1) 0.631 (2)	2.10 ± 0.14	0.002 (1) 0.025 (2)	1.52 ± 0.09	0.002 (1) 0.004 (2)
C225+Simva	1.24 ± 0.29	0.027 (1)	1.63 ± 0.31	0.007 (1)	2.02 ± 0.50	0.007 (1)

A431-WT cell line	Cell number (10^6)					
	24 h	*p*-value	48 h	*p*-value	72 h	*p*-value
Non-treatment	1.89 ± 0.33	-	2.19 ± 0.15	-	2.97 ± 0.38	-
XRT (3 Gy)	1.18 ± 0.07	0.136 (1)	1.56 ± 0.04	0.010 (1)	0.95 ± 0.04	0.010 (1)
C225 (30 nM)	0.81 ± 0.02	0.011 (1)	1.35 ± 0.07	0.010 (1)	1.28 ± 0.09	0.010 (1)
Simva (15 µM)	1.49 ± 0.07	0.497 (1)	1.14 ± 0.06	0.010 (1)	0.92 ± 0.03	0.010 (1)
XRT+C225	1.29 ± 0.19	0.055 (1)	1.07 ± 0.14	0.004 (1)	0.98 ± 0.19	0.006 (1)
XRT+C225+Simva	0.92 ± 0.03	0.004 (1) 0.150 (2)	0.34 ± 0.07	0.004 (1) 0.004 (2)	0.23 ± 0.08	0.004 (1) 0.004 (2)
C225+Simva	1.01 ± 0.03	0.011 (1)	0.53 ± 0.06	0.010 (1)	0.42 ± 0.04	0.010 (1)

Cell cultures were treated as indicated in material and methods. Values are mean ± SE of 3 independent experiments each per duplicated. Doses used in the combined treatments are the same as in the single treatments.
p-value (Mann-Whitney test): (1) compared to non-treatment condition, (2) compared to XRT+C225 without simvastatin.

Table 6. Data for FaDu and A431-WT cells from the results obtained in the cell proliferation assays.

In both cell types, cell proliferation was inhibited by all the therapeutic schemes, an effect that was more obvious as time increased. For individual treatments, radiotherapy and 15 µM simvastatin alone had the highest effect. Regarding combined treatments, it is of note that the addition of cetuximab to radiation was not reflected in a significant decrease of proliferation although these cells were sensitive to cetuximab alone. On the contrary, we found that the addition of 15 µM simvastatin to radiotherapy plus cetuximab effectively resulted in a significant inhibition of proliferation, leading at 72 hours to a decrease of 2.7 fold for FaDu cells and 5.5 fold for A431-WT cells compared to radiation alone, and 1.93 fold and 4.3 fold respectively compared to radiation and cetuximab (Table 6). Interestingly, the effect of cetuximab and simvastatin on proliferation was smaller than the effect of radiotherapy, cetuximab and simvastatin together, in particular at 72 hours after the beginning of treatments. These observations suggest that cetuximab and simvastatin in collaboration may contribute to weaken cell recovery from radiation resulting in higher cell killing.

We also checked the effect of the combination of simvastatin with radiation and cetuximab on the previously generated radioresistant cell line A431-R and compared it to the conventional treatment of radiotherapy and cetuximab.

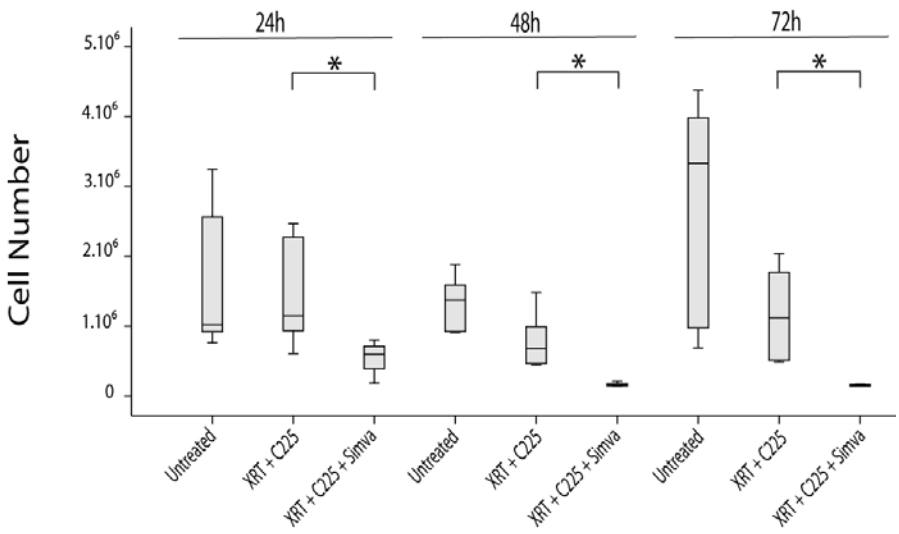

Figure 29. Effect of the different combinations of radiotherapy, simvastatin and cetuximab on A431-R cells' proliferation. (* $p < 0.05$; Mann-Whitney test).

In this third cell line analyzed, the addition of simvastatin to radiation and cetuximab dramatically also decreased cell proliferation from 24 hours of treatment, confirming the effect previously observed in FaDu and A431-WT cell lines.

3.1.3. Effects on cell survival

To further verify and extend the results of these wound healing and cell proliferation assays, the effect of treatments on clonogenic cell survival was evaluated (Table 7). The analysis was performed with two types of drug exposures in combination with the same type of irradiation and period of colony formation: drug exposure for 48 hours (24 hours pre-XRT and 24 hours post-XRT), or drug exposure maintained for 14 days. These two different strategies were aimed to discriminate a possible effect of drugs on cell proliferation during the assay rather than an early clonogenic cell killing effect, which can be properly assessed without the presence of drugs. The baseline plating efficiency for FaDu cells and A431 were comparable, 16.76% ± 2.48 % and 14.29% ± 0.63 %, respectively (Table 7). FaDu cells displayed higher radiosensitivity than A431-WT cells, and were clearly more sensitive to cetuximab, as previously was noted.

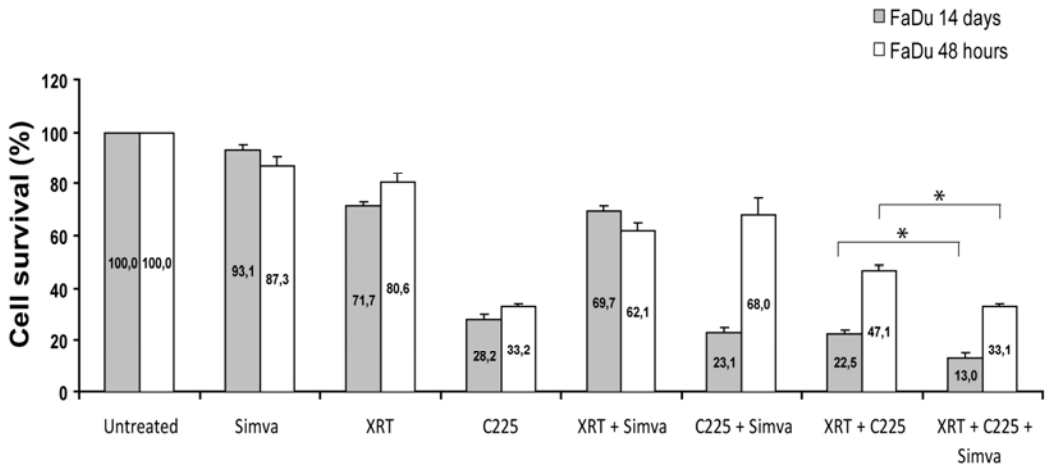

Figure 30. Effect of the different combinations of radiotherapy, simvastatin and cetuximab on FaDu cells' survival after 48 hours or 14 days of treatment. (* $p < 0.05$; Mann-Whitney test).

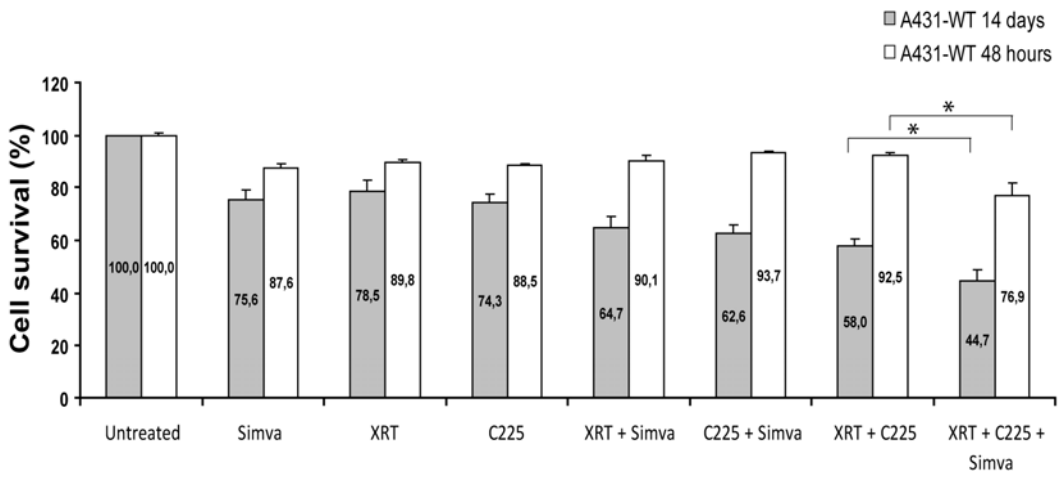

Figure 31. Effect of the different combinations of radiotherapy, simvastatin and cetuximab on A431-WT cells' survival after 48 hours or 14 days of treatment. (* $p < 0.05$; Mann-Whitney test).

One μM simvastatin was definitely less effective than the doses of simvastatin utilized in wound healing and proliferation assays. However, it is worth to mention that 1 μM simvastatin used in clonogenic assays is closer to the blood levels achieved in clinical settings rather than the dose of 15 μM simvastatin.

	Clonogenic cell survival (%)			
	Drugs for 48 h	*p*-value	Drugs for 14 days	*p*-value
Non-treatment	100 ± 0.00	-	100 ± 0.00	-
XRT (2 Gy)	80.6 ± 3.47	0.002 (1)	71.7 ± 1.37	0.001 (1)
C225 (10 nM)	33.1 ± 1.31	0.002 (1)	28.2 ± 1.92	0.001 (1)
Simva (1 µM)	87.3 ± 3.48	0.040 (1)	93.1 ± 2.01	0.026 (1)
XRT+C225	47.1 ± 1.78	0.002(1)	22.4 ± 1.76	0.002 (1)
XRT+C225+Simva	33.0 ± 1.05	0.002 (1) 0.004 (2)	13.06 ± 2.11	0.004 (1) 0.010 (2)
C225+Simva	68.0 ± 6.46	0.002 (1)	23.0 ± 2.20	0.001 (1)
A431-WT cell line	Clonogenic cell survival (%)			
	Drugs for 48 h	*p*-value	Drugs for 14 days	*p*-value
Non-treatment	100 ± 0.00	-	100 ± 0.00	-
XRT (2 Gy)	89.8 ± 0.84	0.037 (1)	78.5 ± 2.57	0.001 (1)
C225 (30 nM)	88.5 ± 1.02	0.037 (1)	74.3 ± 4.09	0.001 (1)
Simva (1 µM)	87.5 ± 1.30	0.037 (1)	75.6 ± 3.47	0.001 (1)
XRT+C225	92.5 ± 1.14	0.037 (1)	58.0 ± 3.46	0.001 (1)
XRT+C225+Simva	76.9 ± 3.63	0.037 (1) 0.050 (2)	44.7 ± 4.27	0.001 (1) 0.009 (2)
C225+Simva	93.7 ± 0.52	0.037 (1)	62.5 ± 3.50	0.001 (1)

Cell cultures were treated as indicated in material and methods. Values are mean ± SE. For FaDu and A431-WT cells 2 and 4 independent experiments each per duplicated were performed for 48 hour and 14 days schemes, respectively. Doses used in the combined treatments are the same as in the single treatments.
p-value (Mann-Whitney test): (1) compared to non-treatment condition, (2) compared to XRT+C225 without simvastatin.

Table 7. Clonogenic cell survival data for FaDu and A431-WT cells from the results obtained in the clonogenic assays.

In a 48 hours drug-exposure scheme, combination of radiotherapy, cetuximab and simvastatin yielded lesser clonogenic cell survival than combination of radiotherapy and cetuximab. However, in both cell lines, these differences were also associated to an increase of survival in cells treated with radiotherapy and cetuximab compared to the effect of cetuximab alone. An early reactive cellular response inducing a compensatory proliferation could explain this increase of colony formation, which was not seen in the triple treatment. In 14 days drug exposure experiments, it was found that for the cetuximab-sensitive FaDu cells the antibody outstandingly reduced cell survival, while the addition of radiotherapy or simvastatin almost did not increase the effect of cetuximab by itself. For cetuximab relative resistant A431-WT cells, it was observed that the addition of simvastatin or radiation to cetuximab significantly decreased colony formation. Importantly, when simvastatin was added to the long exposure of cetuximab in

combination with radiotherapy, it was caused the largest inhibitory effect in both cell lines, decreasing radiation cell killing by a factor of 5.5 fold for FaDu cells and 1.75 fold for A431-WT cells. These figures were 1.7 fold and 1.3 fold compared to radiotherapy and cetuximab alone, respectively (*p*-values <0.001).

We also analyzed the effect of the combination of simvastatin with radiation and cetuximab in 14 days drug exposure experiments on the generated radioresistant cell line A431-R.

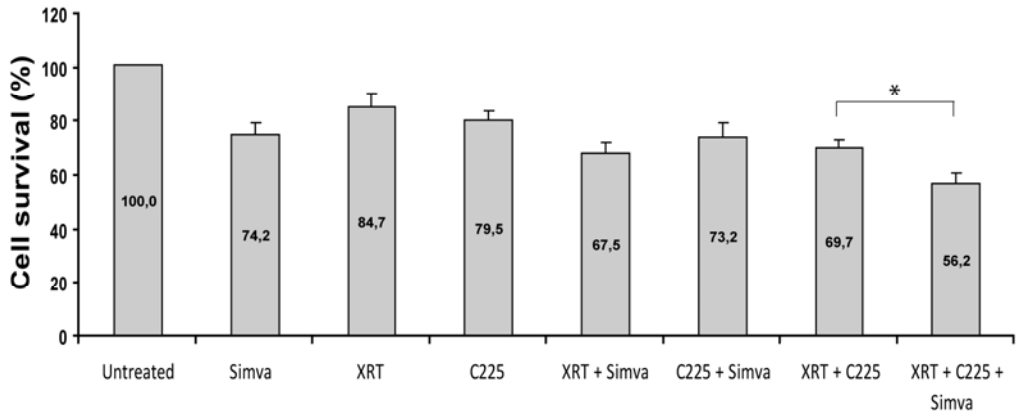

Figure 32. Effect of the different combinations of radiotherapy, simvastatin and cetuximab on A431-R cells' survival after 14 days of treatment. (* $p < 0.05$; Mann-Whitney test).

In A431-R cells, survival was also significantly decreased with the combination of radiotherapy, cetuximab, and simvastatin. For the parental cell line A431-WT we found 58% of cell survival after 14 days of treatment with radiotherapy and cetuximab. However, for the resistant A431-R cells, the survival to this same treatment was 69.7%. Addition of simvastatin to the combination of radiotherapy and cetuximab helped to revert the resistance of this phenotype, reducing the survival to 56.2%.

Taken together, the *in vitro* results suggest that simvastatin could decrease cell proliferation in combination with radiotherapy and cetuximab, being its effect potentiated in long term drug exposures.

3.2. Effects of radiotherapy, cetuximab, and simvastatin on tumour growth

Because of preliminary *in vitro* findings indicating a possible activity of simvastatin as cell proliferation inhibitor in combination with cetuximab and radiotherapy, this study was continued to investigate simvastatin role in xenografts.

We generated xenografts from FaDu and A431-WT cell lines and followed the following scheme of treatment with radiotherapy, cetuximab and simvastatin:

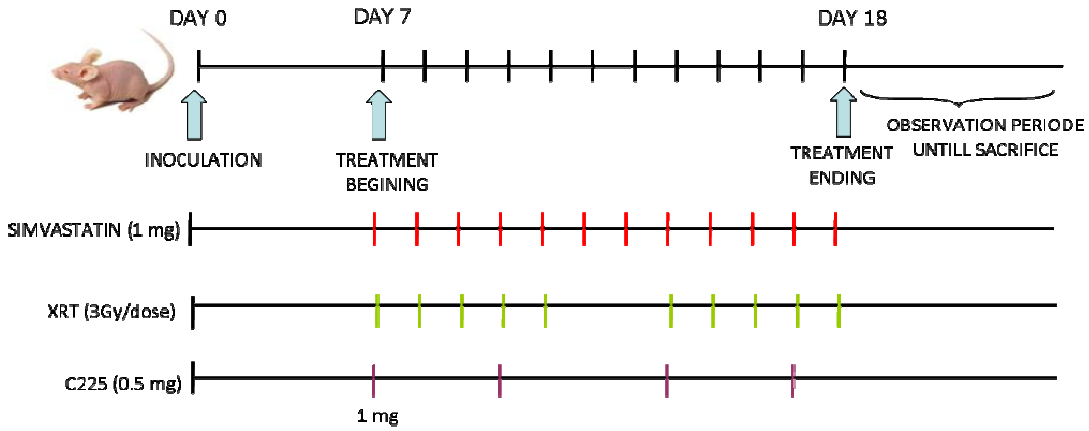

Figure 33. Treatment scheme for the generated xenografts. Treatments begin 7 days after cell inoculation.). Radiotherapy was administeres from Monday to Friday for 2 weeks. Simvastatin was administered daily (1 mg) for 12 days. C225 was administered twice a week, the first dose being double (1 mg).

Single treatment with simvastatin alone had no effect on tumor growth neither for FaDu xenografts, nor for A431-WT ones. On the contrary, treatment with cetuximab or radiotherapy significantly reduced tumor growth compared to untreated tumors, radiotherapy being the most effective treatment. FaDu-tumors were more sensitive to radiotherapy and C225 than A431-WT ones, as was also seen in the clonogenic assays.

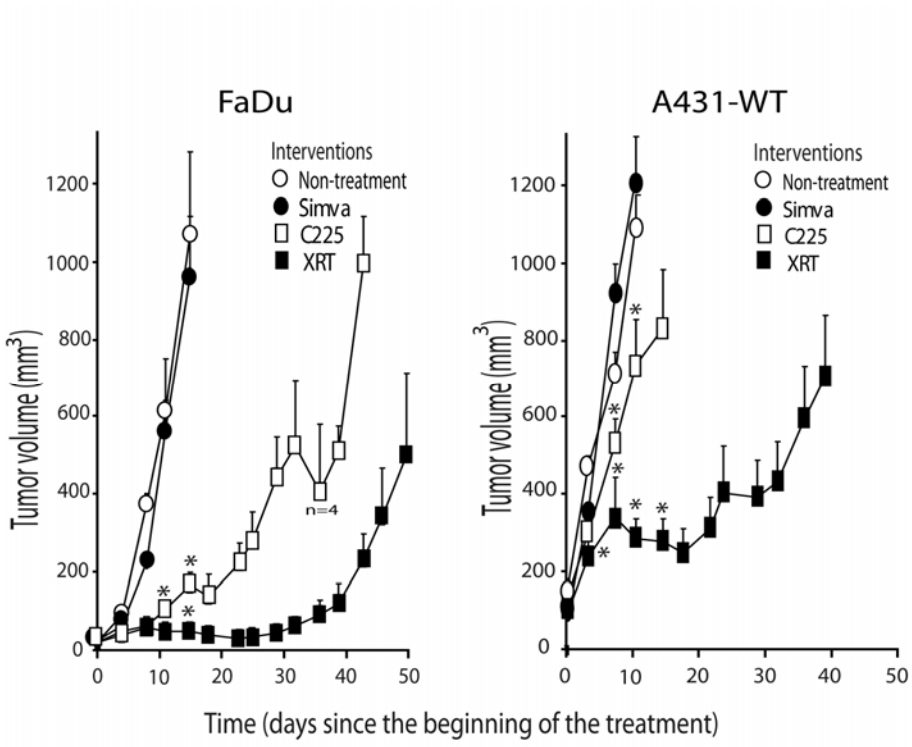

Figure 34. Effect on the growth of FaDu and A431-WT xenografts of the single treatments: radiotherapy, cetuximab and simvastatin. * $p < 0.05$ compared to untreated condition (Mann-Whitney test).

To focus on the main interest of this study we started experiments irradiating FaDu-tumors with 3 Gy a day for 10 days in combination with cetuximab in presence or absence of simvastatin.

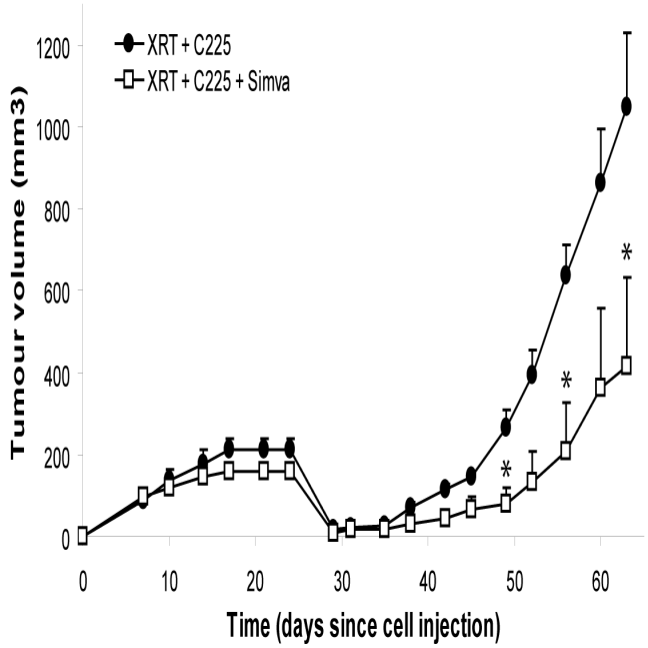

Figure 35. FaDu tumours response to radiotherapy and cetuximab treatment in presence or absence of simvastatin. (* $p < 0.05$; Mann-Whitney test).

Irrespectively of simvastatin, radiation plus cetuximab induced a transitory complete regression of tumors that lasted around 7 days. After that, tumor growth rebounded, but showed lower rates of regrowth when the animals received simvastatin.

The delay that tumors experienced to have the size the tumors had at the start of the treatment in mice that received simvastatin was 46 ± 5.8 days compared to 29 ± 3.2 days in absence of simvastatin (a difference of 17 days; *p*-value = 0.065). The time that FaDu-tumors took to triplicate their tumor volume since the start of radiotherapy was 53.7 ± 4.4 days versus 42.8 ± 1.4 days depending on the presence of simvastatin or not, respectively (a difference of 11 days; *p*-value = 0.086).

	FaDu tumours			A431-WT tumours		
	XRT+ C225	XRT+ C225+ Simva	*P-value*	XRT+ C225	XRT+ C225+ Simva	*P-value*
Size of tumors at the beginning of the treatment at day 7 (in mm^3)	89 ±15	99 ±10	0.37	97 ±15	76 ± 5	0.31
(1) Growth delay (in days)	29 ± 3.2	46 ± 5.8	0.065	0 ± 0	14.4 ± 5.9	0.081
(2) Time to triplicate tumor volume (in days)	42.8 ± 1.4	53.7 ± 4.4	0.086	47 ± 15.2	60 ± 6	0.539

Explanations:
(1) Growth delay was measured as the time after irradiation that it took the tumors to regrow to the size they had at the start of the treatment.
(2) Time the tumours took to triplicate the size they had at the time of the start of irradiation.

Table 8. Tumour growth analysis of FaDu and A431-WT xenografts

We generated tumours from A431-WT cells, but in this case, in order to prevent a complete response, radiation dose was lowered to 2 Gy a day for 10 days (total dose of 20 Gy).

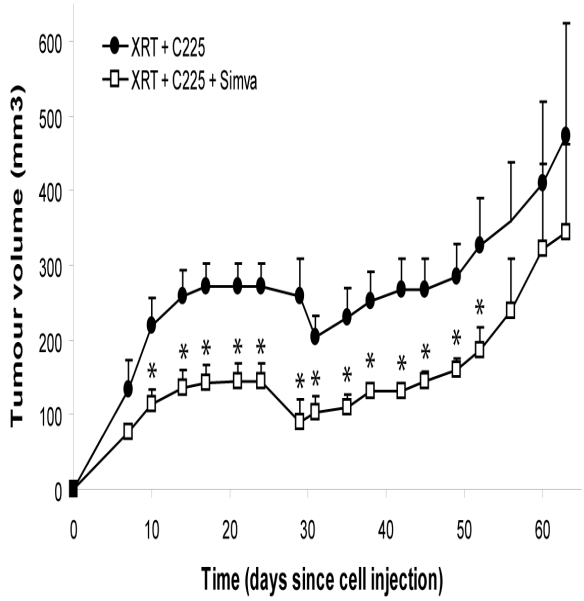

Figure 36. A431-WT tumours response to radiotherapy and cetuximab treatment in presence or absence of simvastatin. (* $p < 0.05$; Mann-Whitney test).

Contrary to the FaDu xenografts, A431-WT tumors did not achieve a complete disappearance, but similarly it was found that the mice treated with simvastatin showed A431-WT tumors with lower rates of regrowth. Consistently with a simvastatin-induced enhancement in tumor growth inhibition, the growth delay after irradiation for the tumors treated with simvastatin was 14.4 ± 5.9 days in contrast with the mice that did not receive addition of simvastatin, in which tumor size never decreased below the size the tumors had at the time of irradiation (*p*-value = 0.081). In these mice, the time to triplicate the initial tumor volume was increased if they received simvastatin from 47 ± 15.2 days to 60 ± 6 days (a difference of 13 days; *p*-value = 0.539).

We analyzed the effects of the combination of simvastatin with radiotherapy and cetuximab in tumours generated from the radioresistant cell line A431-R, and we observed a similar pattern of response.

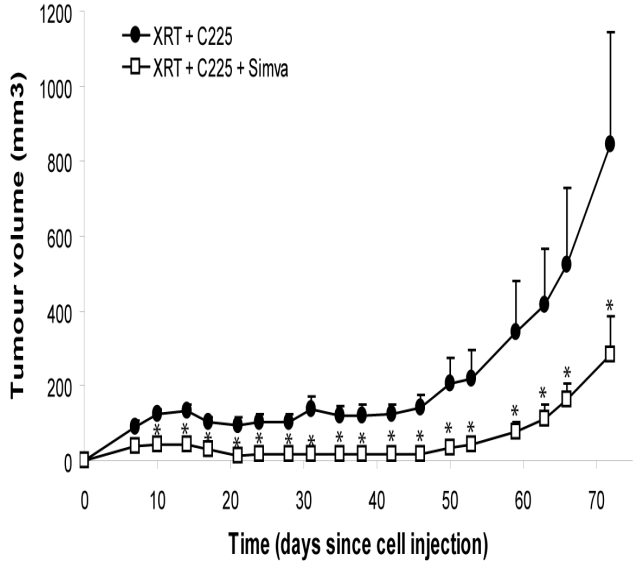

Figure 37. A431-R tumours response to radiotherapy and cetuximab treatment in presence or absence of simvastatin. (* $p < 0.05$; Mann-Whitney test).

Because *in vivo*, and *in vitro*, findings were compatible with the notion that simvastatin could enhance the antitumor effect of radiotherapy and cetuximab in FaDu

and A431 cells derived tumor, we decided to evaluate if simvastatin could negatively influence in the biology of these tumors.

3.3. Modifications induced by the therapy in the biology of xenografts

We generated new tumours and sacrifice the mice after 3 days of treatment in order to obtain short term treated tumours where to analyze the effect observed in the curves of the tumour growth for every type of cell line analyzed.

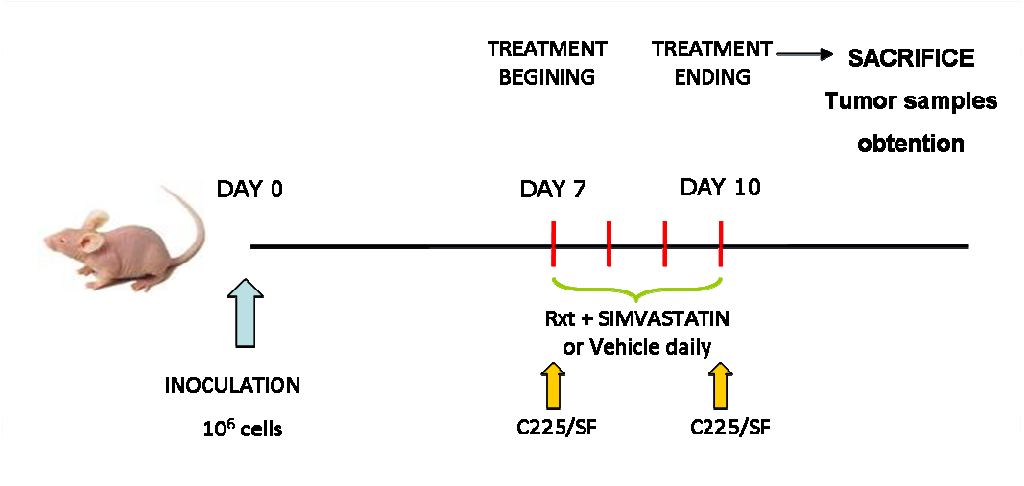

Figure 38. Treatment scheme for the generation of tumour samples for analysis. Mice were treated for 4 days, and then sacrificed to obtain tumour samples.

3.3.1. Simvastatin did not modify the tumours proliferation rate

In order to state if simvastatin influenced in the proliferation rate of the different xenografted tumours, we evaluated the incorporation of bromodeoxyuridine (BrdU), which is a synthetic analogue of thymidine. BrdU is incorporated into the newly synthesized DNA of replicating cells (during the S phase of the cell cycle), substituting for thymidine during DNA replication. This is why the detection of BrdU is commonly used in measuring proliferating cells in living tissues.

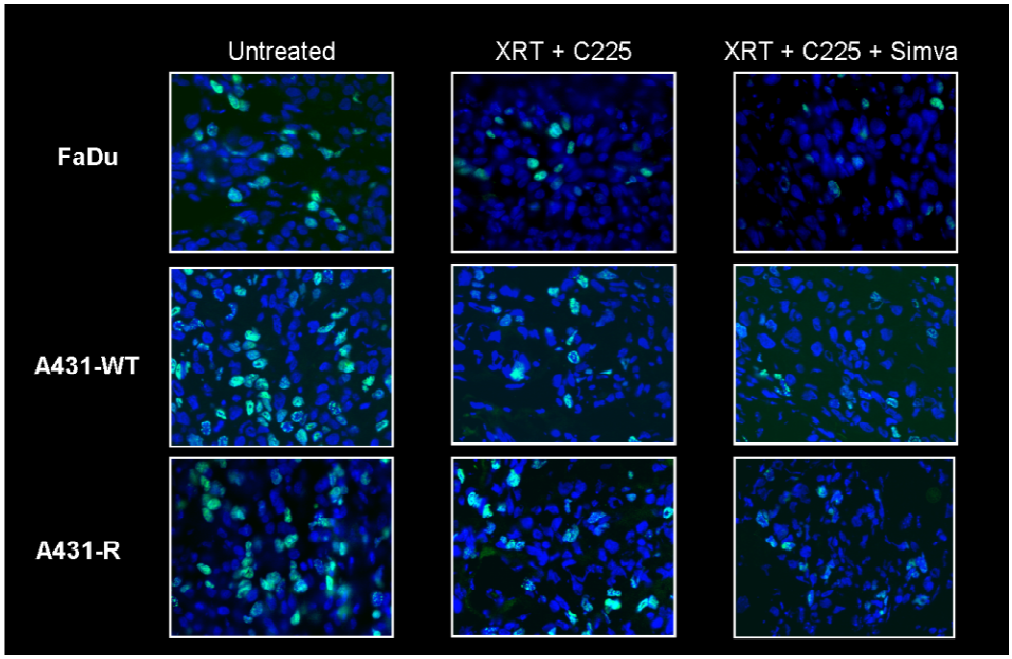

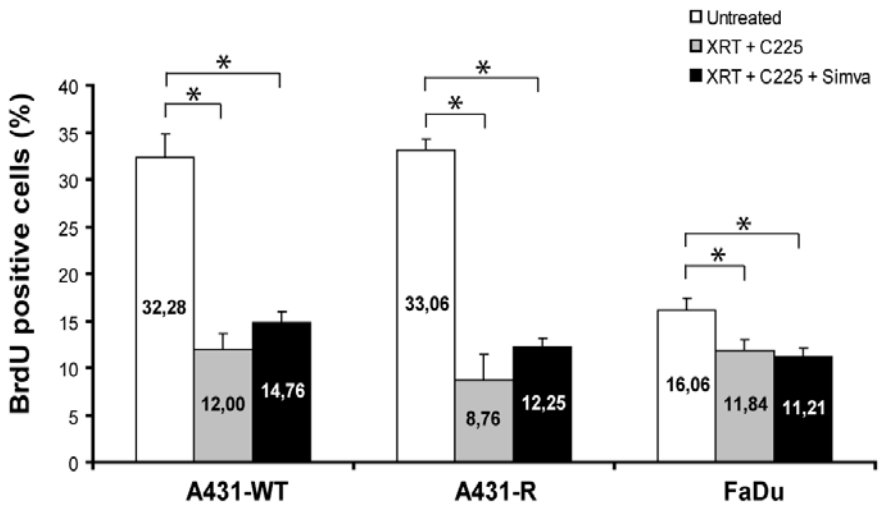

Figure 39. BrdU incorporation analysis in the tumours derived from FaDu, A431-WT and A4341-R cells. BrdU immunostaining with DAPI microphotographs (x60) and BrdU positive cells percentage quantification (* $p < 0.05$; Mann-Whitney test).

We observed, for the three different cell lines studied, statistically reduction in the proliferation rate of tumors treated with radiotherapy and cetuximab disregard of simvastatin. Although at first sight of the pictures it seemed that addition of simvastatin

to XRT+C225 reduced BrdU rate in A431-WT and A431-R cells, when quantification was completed no significant differences were found.

3.3.2. Simvastatin increased the apoptosis rate of tumours treated with radiotherapy and cetuximab

We hypothesized that the observed effect of simvastatin might be related to apoptosis activation, rather than proliferation. In order to establish whether apoptosis was increased by simvastatin in FaDu and A431-WT tumors, xenografted tumors were sampled as previously described. We determined the cleaved caspase-3, a surrogate marker that indicates irreversible cell death through apoptosis.

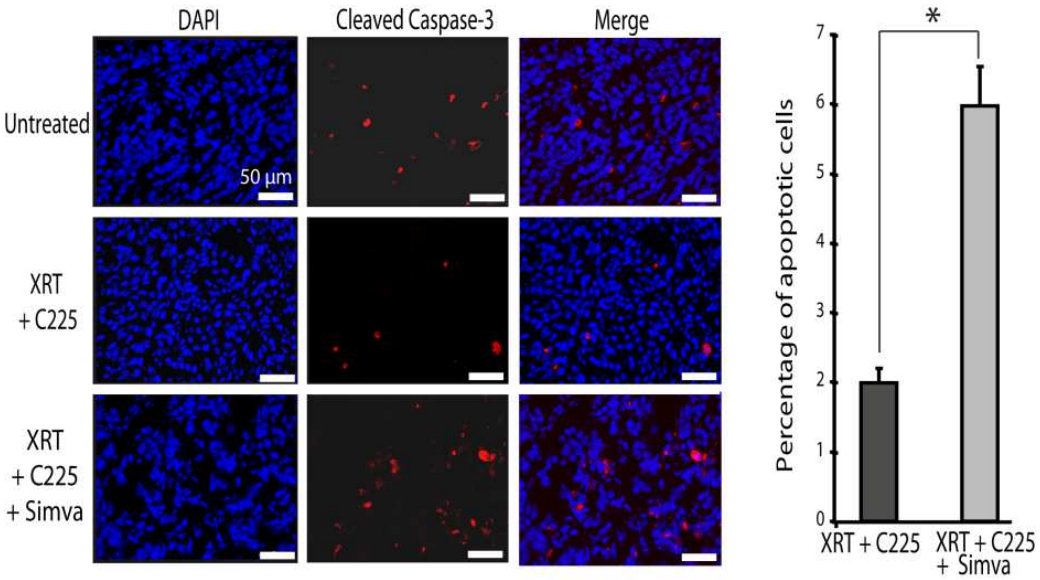

Figure 40. Cleaved caspase-3 determination in FaDu xenografts. Caspase-3 with DAPI microphotographs and Caspase-3 positive cells percentage quantification. (* $p < 0.05$; Mann-Whitney test).

Although the tumors received only 3 days of treatment and the percentages of apoptotic cells were relatively low, we already found that the number of cleaved caspase-3 positive cells was significantly higher in FaDu-derived tumors treated with triple treatment at this time-point (1.99% ± 0.20% vs 5.96% ± 0.56%; $p = 0.0001$).

The same observation was made in A431-WT derived tumors (4.40% ± 0.62% vs 8.83% ± 1.46%; $p = 0.005$) and for A431-R derived ones (2.89% ± 0.30% vs 4.28% ± 0.37%; $p = 0.019$). In the three cases, the addition of simvastatin to the treatment of radiotherapy and cetuximab, increased the apoptosis in the tumours.

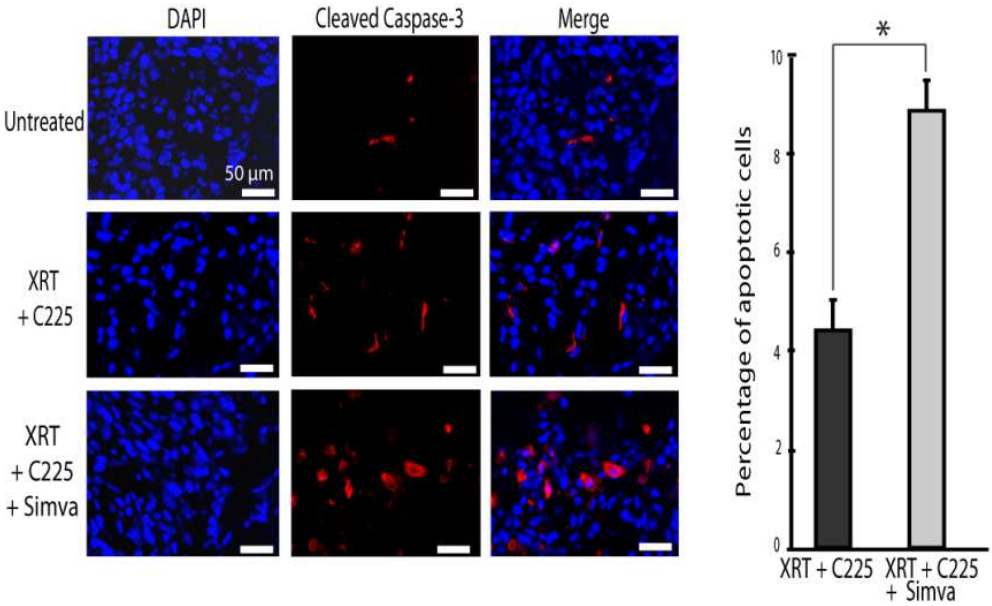

Figure 41. Cleaved caspase-3 determination in A431-WT xenografts. Caspase-3 with DAPI microphotographs and Caspase-3 positive cells percentage quantification (* $p < 0.05$; Mann-Whitney test).

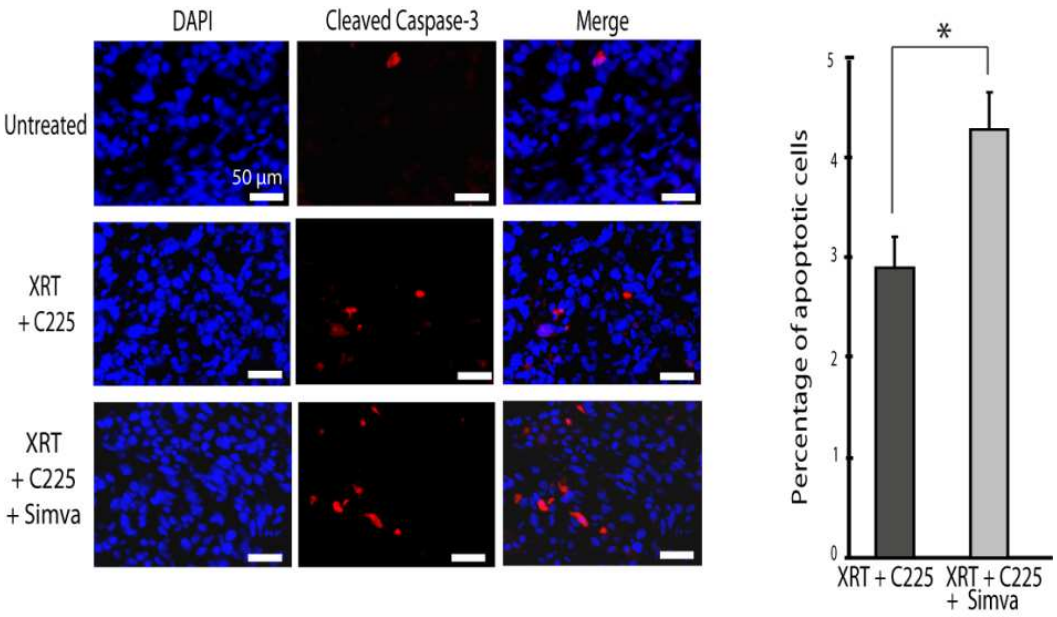

Figure 42. Cleaved caspase-3 determination in A431-R xenografts. Caspase-3 with DAPI microphotographs and Caspase-3 positive cells percentage quantification (* $p < 0.05$; Mann-Whitney test).

3.3.3. Simvastatin had no clear effect on neoangiogenesis

We wonder if the addition of simvastatin to the conventional treatment of radiotherapy plus cetuximab has any effect on the number of blood vessels, so we stained the tumours for Cluster of Differentiation 31 (CD31, also known as Platelet endothelial cell adhesion molecule (PECAM-1)). CD31 is used to demonstrate the presence of endothelial cells in histological tissue sections, and can help to evaluate the degree of tumour angiogenesis.

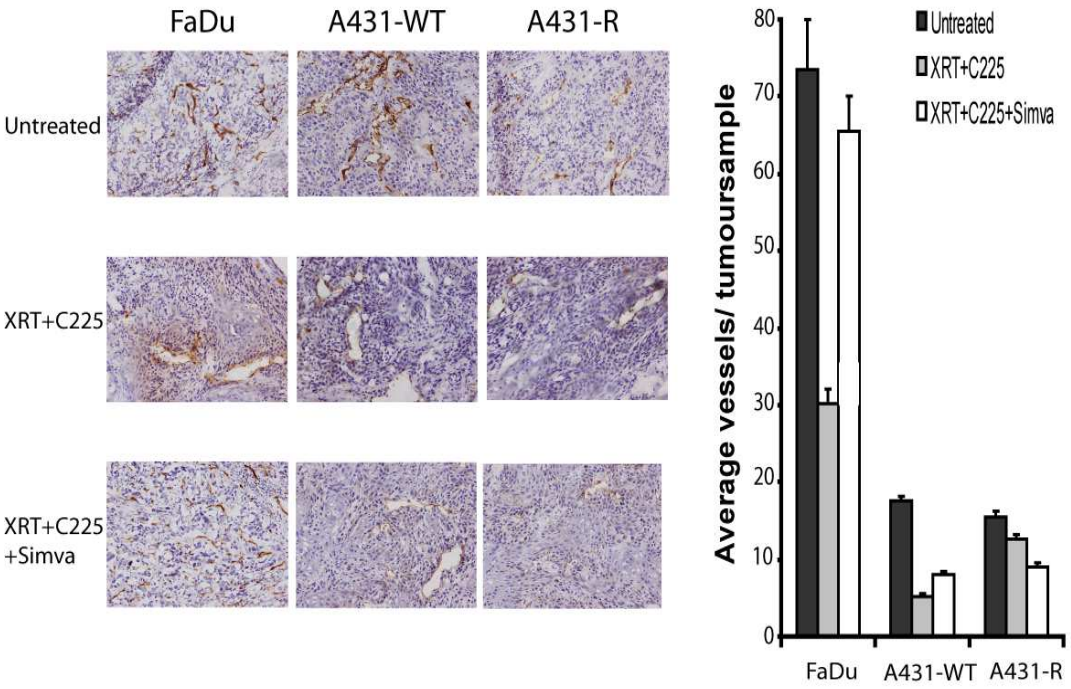

Figure 43. CD31 staining and analysis for FaDu, A431-WT and A431-R derived tumours. Microphotographs of the immunostaining for CD31 of the samples from the tumours treated for 4 days (20x). Quantification of the average number of vessels per sample of the three different types of tumours untreated and treated with the two different treatments.

We observed that FaDu and A431-WT presented different responses to the treatment of radiotherapy, cetuximab and simvastatin, regarding angiogenesis.

For FaDu cell type we observed that the tumours that received radiotherapy and cetuximab presented lower number of vessels than the tumours that received this treatment plus simvastatin, indicating that the inhibitory effect of cetuximab on neoangiogenesis was shadowed by simvastatin. However, the vessels from the tumours treated with simvastatin in addition to radiotherapy and cetuximab presented lower vessel lumen, compared to those tumours treated only with radiotherapy and cetuximab.

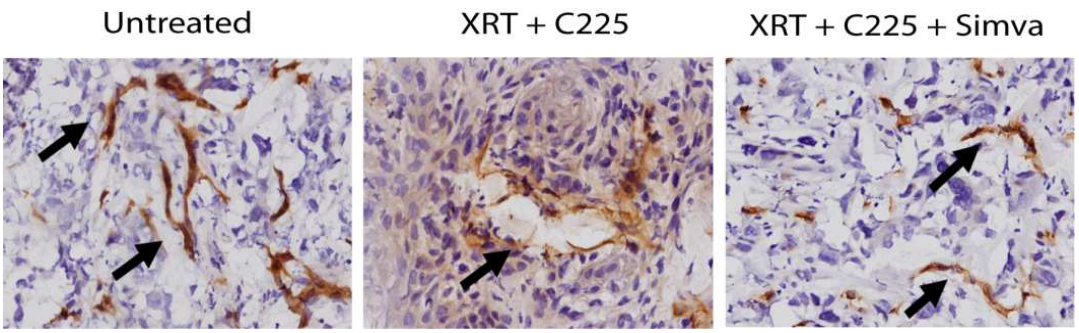

Figure 44. Zoom of the microphotographs of the immunostaining for CD31 for FaDu derived treated for 4 days (20x).

During the past ten years, the classical concept of primary tumours initiating avascularly then inducing angiogenesis has been challenged by some studies that suggested that microtumours may initiate growth by exploiting pre-existent vessels, a process known as vascular co-option. Some authors had described that some tumour cells can take benefit from already existing big and well structured vessels, instead of creating new ones de novo. Those vessels are called co-opted and they already exist in normal tissues. Tumour cells grow around those existing vessels, which they use as their owns to from a perivascular cuff (Holash, Maisonpierre et al. 1999; Carmeliet and Jain 2000; Zhao, Yang et al. 2011). This could be the case for FaDu cells. However, when simvastatin is added to the treatment of radiotherapy and cetuximab, we no longer observed that effect. Instead, we observed smaller vessels that could be less functional and less efficient in the conduction of nutrients and oxygen. This could explain why tumours treated with simvastatin added to the treatment of radiotherapy and cetuximab had a slower tumour growth.

For A431-WT derived tumours, we observed the same tendency as for FaDu tumours, to have the inhibitory effect of cetuximab on neoangiogenesis shadowed by simvastatin, as the number of vessels increased in the tumours that received the triple treatment. In the case of A431-WT, the size of lumen of the vessels in the tumours treated with addition of simvastatin, compared to the ones that only received radiotherapy and cetuximab was similar.

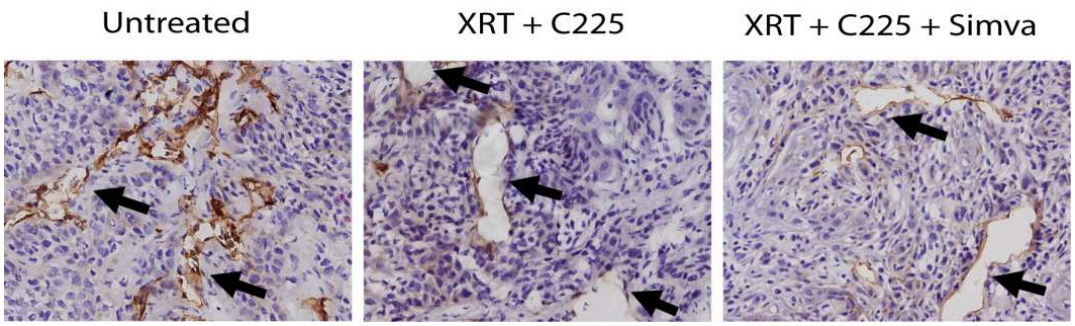

Figure 45. Zoom of the microphotographs of the immunostaining for CD31 for A431-WT derived treated for 4 days (20x).

When tumours derived from A431-WT and A431-R were not treated, there were no differences between both cell lines in the number of vessels, however, when radiotherapy combined with cetuximab was administered to the tumours, we appreciated higher number of vessels in the A431-R xenografts than in the A431-WT ones (Figure 42). The treatment of radiotherapy and cetuximab for A431-R tumours did not inhibit neoangiogenesis as much as in A431-WT ones. This observation is consistent with previous results that indicate that radiotherapy elicits a higher VEGF levels in supernatants of A431-R cultures compared to the A431-WT ones (Figure 21), and that A431-R cells overexpress pEGFR, pAkt and pErk 1/2 (Figure 20), which means that there are more competence for cetuximab to inhibit EGFR. However, addition of simvastatin helped cetuximab to compete for EGFR and reduce the number of vessels.

3.4. Analysis of the EGFR pathway

3.4.1. FaDu cell line molecular analysis

We also investigated whether simvastatin could affect crucial cellular signaling pathways involved in the malignant phenotype of cancers. We found that the ionizing radiation elicited the phosphorylation of EGFR on 1086-tyrosine. However, the addition of simvastatin to XRT did not modify phosphorylated levels of EGFR (Figure 46). In contrast,

C225 had an inhibitory effect on the radiation-induced phosphorylation of EGFR, which was neither changed in presence of simvastatin, indicating that simvastatin had little effect on EGFR (at least on phosphorylated tyrosine 1086). Although simvastatin was inactive on EGFR, we observed a noticeable reduction of the phosphorylation of ERK1/2. Simvastatin also decrease the activation of pAKT and pSTAT3 but in lesser degree than on ERK1/2 protein. No effect on the levels of total EGFR, ERK1/2, AKT and STAT3 were found.

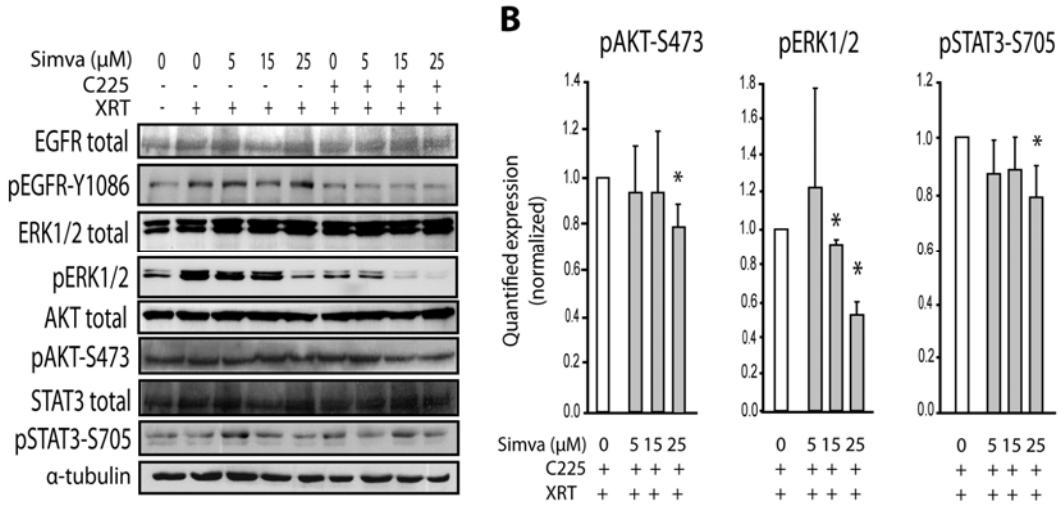

Figure 46. Analysis of the EGFR pathway for FaDu cell line. (*p < 0.05; Mann-Whitney test).

We also determined the cleaved caspase-3 in cultured cells, and we found that levels of cleaved caspase-3 increased in simvastatin-treated cells in a dose dependent manner while the levels of pro-caspase-3 remained unchanged. These findings were consistent with immunohistochemical results in xenografts.

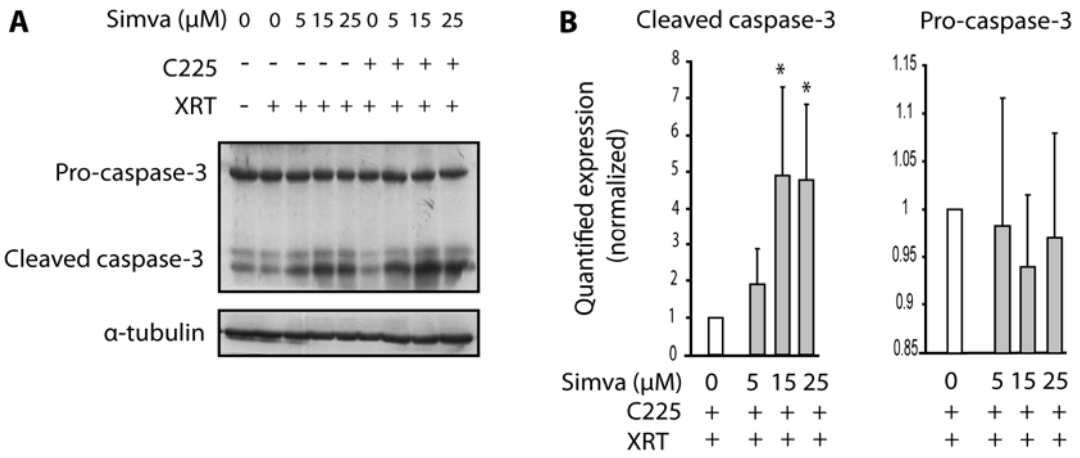

Figure 47. Caspase-3 determination in FaDu cells. (*p<0.05; Mann-Whitney test).

3.4.2. A431-WT and A431-R cell lines molecular analysis

We investigated whether the EGFR proliferative signaling pathway was also affected by simvastatin in A431-WT and A431-R cell lines. We corroborate that ionizing radiation elicited the phosphorylation of EGFR on 1086-tyrosine residue, and that C225 had an inhibitory effect on the radiation-induced phosphorylation of EGFR in both cell types, as it happened in FaDu cell line.

We observed that simvastatin alone had little effect on EGFR (at least on phosphorylated tyrosine 1086 residue). However, when simvastatin was combined with XRT and C225, we observed a decrease in the phosphorylation of EGFR (tyrosine 1086), compared to the levels of the protein for XRT and C225 condition, and this diminution reached significance in the case of A431-R cell line (Figures 48 and 49).

The most remarkable observation was the decrease in the phosphorylation of STAT3 in presence of simvastatin, which was statistically significant for both cell types, but has a higher impact on A431-R cells. In parallel, we observed that when levels of phosphorylated STAT3 decreased, the phosphorylation of ERK1/2 increased.

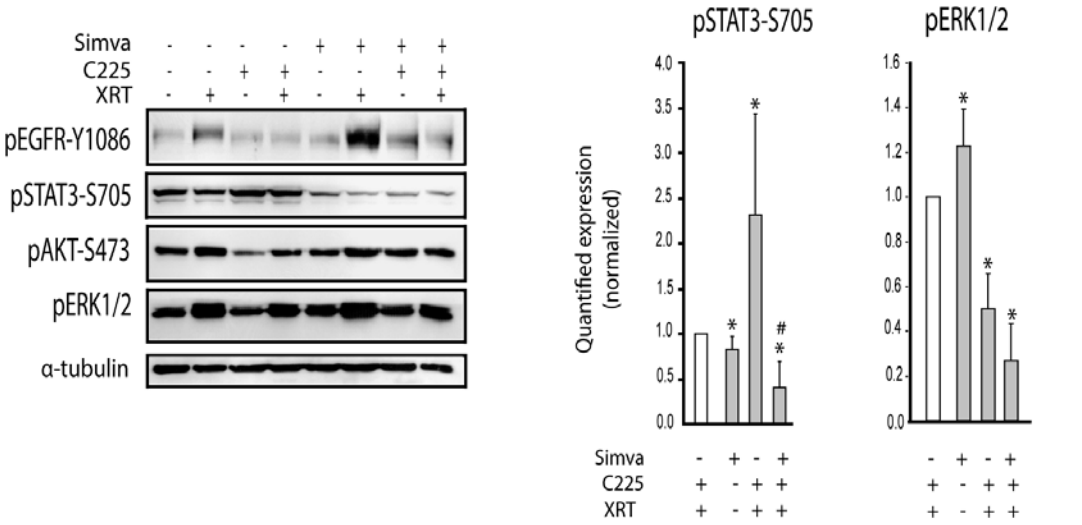

Figure 48. Analysis of the EGFR pathway for A431-WT cell line. Optical densitometry quantifications (in arbitrary units) of the protein levels are indicated as fold relative to the untreated condition, bars show SEM. **p* < 0.05 compared to untreated condition, and # p<0.05 compared to XRT plus C225 (Mann Whitney test).

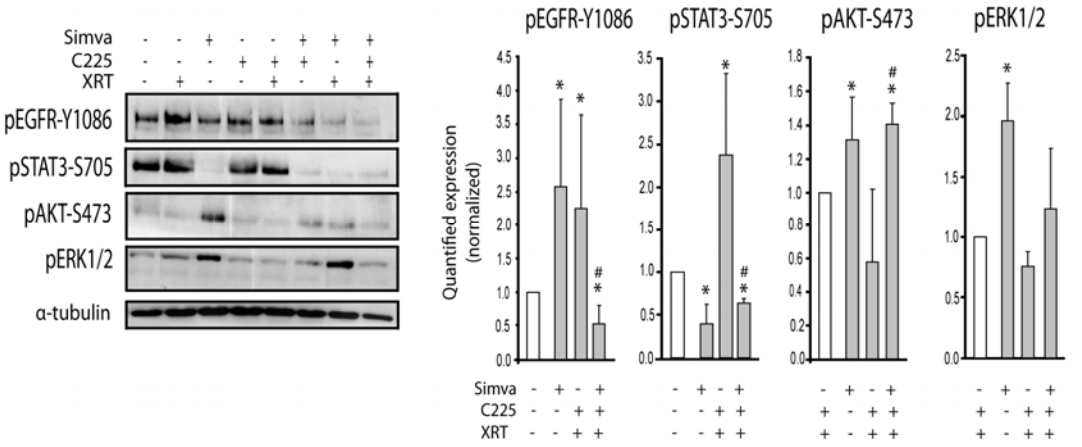

Figure 49. Analysis of the EGFR pathway for A431-R cell line. Optical densitometry quantifications (in arbitrary units) of the protein levels are indicated as fold relative to the untreated condition, bars show SEM. **p* < 0.05 compared to untreated condition, and # p<0.05 compared to XRT plus C225 (Mann Whitney test).

3.5. Cholesterol levels analysis

Simvastatin reduces the rates of endogenous cholesterol synthesis by inhibiting the 3-HMG-CoA reductase. We wanted to check if the statin simvastatin has successfully

inhibited the synthesis of endogenous cholesterol in the mice treated with simvastatin combined with radiotherapy and cetuximab.

With the help of the group from Dr Albert Morales, from the Hospital Clinic, cholesterol levels were measured in the tumours derived from FaDu cell line (obtained as explained in the section 3.3.).

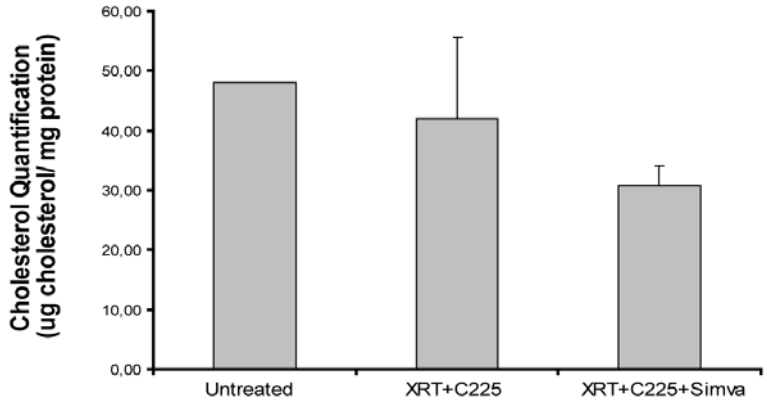

Figure 50. Cholesterol quantification in FaDu xenografts.

Even if we could appreciate a tendency to have reduced levels of cholesterol in the tumours that were treated with simvastatin, no conclusion can be made as the number of samples jeopardized to achieve a statistical analysis robust enough.

DISCUSSION

The work presented here has been divided in three parts. In the first part of this project of Thesis, it has been demonstrated that, by subjecting culture cells to fractionated radiation and clonal selection, we were able to obtain a modified cohort of cells. The ultimate aim of this part was to develop an isogenic resistant cell line which could be used to identify molecular changes associated with acquired resistance to radiation and tumour aggressiveness in cancer. The identification and understanding of such mechanisms is of valuable interest, not only in overcoming radiation resistance, but also, underpinning the biology of recurrent cancer after radiotherapy. Hence, based on this knowledge, specific therapies for cancer could be devised. Although a comprehensive mechanistic study was not undertaken, our study showed that, indeed, relevant mechanisms associated with resistance to radiation were activated.

It was developed a stable isogenic resistant cell line, called A431-R, derived from parental A431 cells. The diminution of radiosensitivity in A431-R cells was found to be comparable to other published studies. Similar decreases in SF2 and α-component of LQ model were reported in radioresistant isogenic cells derived from OE33 esophagal adenocarcinoma cells. These changes were also associated with an increased efficiency in DNA repair (Lynam-Lennon, Reynolds et al. 2010). Equivalent levels of acquired tolerance to radiation were c found in the resistant version of the human lung adenocarcinoma cell line, Anip973 (Xu, Gao et al. 2008).

In these already published studies, as well as in our own (de Llobet, Baro et al. 2013), the generated radioresistant cells showed moderate levels of radiation desensitization, a fact that could raise concers about the clinical impact of theses change.

Classification of human tumours according to clinical radioresponsiveness. Variation in SF2

Group	Representative cancers	SF2-Ratio
A	Neuroblastoma, lymphoma, myeloma	0.42
B	Medulloblastoma, small-cell lung carcinoma	0.5
C + D	Breast, bladder, cervix, pancreas, colo-rectal, non-small cell lung cancer	1
E	Melanoma, osteosarcoma, glioblastoma, renal carcinoma	1.2
A431 WT		1
A431 R		1.2

Table 9. Classification of human tumours according to their SF2 as a measure of their clinical radioresponsiveness. Modified from Deacon et al. Taking as SF2 unit the SF2 of groups C+D (Deacon, Peckham et al. 1984).

Table 9 shows gradient-related radiation sensitivities with clinical relevance. It indicates that an apparent low increase in SF2-Ratio shifts radiocurability from the breast cancer to the resistant melanoma cancer. It should be taken into account that in fractionated radiotherapy a small variation in radiosensitivity could have a greater effect on the utterly response than the simple difference in a single fraction, as shown in Figure 14.

Besides radiation resistance, it was evidenced that A431-R cells acquired higher cloning efficiency and faster growth and migration ability; these properties were observed to be associated with remarkable baseline levels of relevant oncoproteins and elevated angiogenic capabilities. The establishement of an estable cell population with augmented malignat profil such as that described in this part of the Thesis is consistent with prior researchs. Earlier, our group showed that radiation was found to induce the emergence of aggressive phenotypes in A431-WT cells (including higher rates of tumor growth and elevated tumor-associated angiogenesis), changes that were associated to radioation-induced overexpression of EGFR/MAPK (Pueyo, Mesia et al. 2010). Recently, similar phenotype was elicited by radiation-induced cell signalling involving the protein

encoded by the receptor *c-Met* (De Bacco, Luraghi et al. 2011). These findings strongly suggest that cancer cells may develop adaptive responses to damaging agents, such as ionising radiation, leading to the gain of molecular mechanisms to protect themselves from the lethal effects of these agents. Cellular stress regulates distinct genetic and epigenetic programs that may determine the acquisition of tolerance to radiation and the biology of cancer cells, as consequence, re-programming cellular machinery.

This notion is supported by new discoveries in radiation resistance:

1. The acquisition of resistance to radiation was found to be associated with increased levels of reduced state of glutathione, pointing at a better expression of genes encoding enzymes that maintain glutathione operative (Lynam-Lennon, Reynolds et al. 2010).
2. Similar meaning would be ascribed to the low levels of intracellular free radicals observed in isogenic resistant human non-small cell lung cancer cells (Lee, Oh et al. 2010).
3. In these adjustments, glutathione levels may be a mirror of the re-programming energy metabolism associated to cancer cells that impinge higher utilization of glucose and enhancing NADPH production, ready to be used in protronate glutathione synthesis (Pena-Rico, Calvo-Vidal et al. 2011).
4. The participation of oncogenic proteins such as AKT (through mTOR), RAS or HIF1α in glycolytic fuelling as a response to oxidative stress (Semenza 2010; DeBerardinis, Lum et al. 2008) gives additional support to the notion that global changes are induced by radiation, and they together go beyond the idea of an isolated phenomenon of resistance.

Radiation-induced resistant cells have also revealed changes attributed to radiation in transciptome. Upregulation or downregulation of different roster of genes encoding proteins that are involved in DNA repair and anti-apoptosis, as well as in motility, invasion and angiogenesis have been reported. However, the representation of

the genes involved in resistance varies, depending on the authors (Fukuda, Sakakura et al. 2004; Xu, Gao et al. 2008; Lee, Oh et al. 2010). Variations in the genetic origin of cells, methods used to generate the experimental model and the technical differences to analyze gene expression may all have influenced the diversity of findings. Interestingly, an experimental design based on isogenic cells, such as the A431-WT and A431-R pair, could make it more suitable to directly attribute changes in gene regulation to ionising radiation because isogenic cells were born with the same genetic background.

Keeping in mind the former notion, an epigenetic research was undergone using A431-R and A431-WT cell populations. A series of genes that were silenced or induced (up-methylated) in the radioresistant cell subline A431-R were compared to the parental ones. Few physical or functional associations were found between the proteins whose genes were hypo or hypermethylated in the radioresistant cell line compared to the parental cell line. Discussion for the findings related to NPAT and ATM involved in DNA repair has been provided in the corresponding section of results.

Besides comparisons between genes that resulted in methylation changes induced by radiation, we wanted to discuss possible associations between the proteins encoded by genes that suffered epigenetic modifications and proteins involved in the most common pathways of carcionogenesis (TNF, EGFR, HIF1α, STAT3, ERK, TGFβ, p53, Rb, k-RAS, RAF and Myc). The findings are showed in Figure 51:

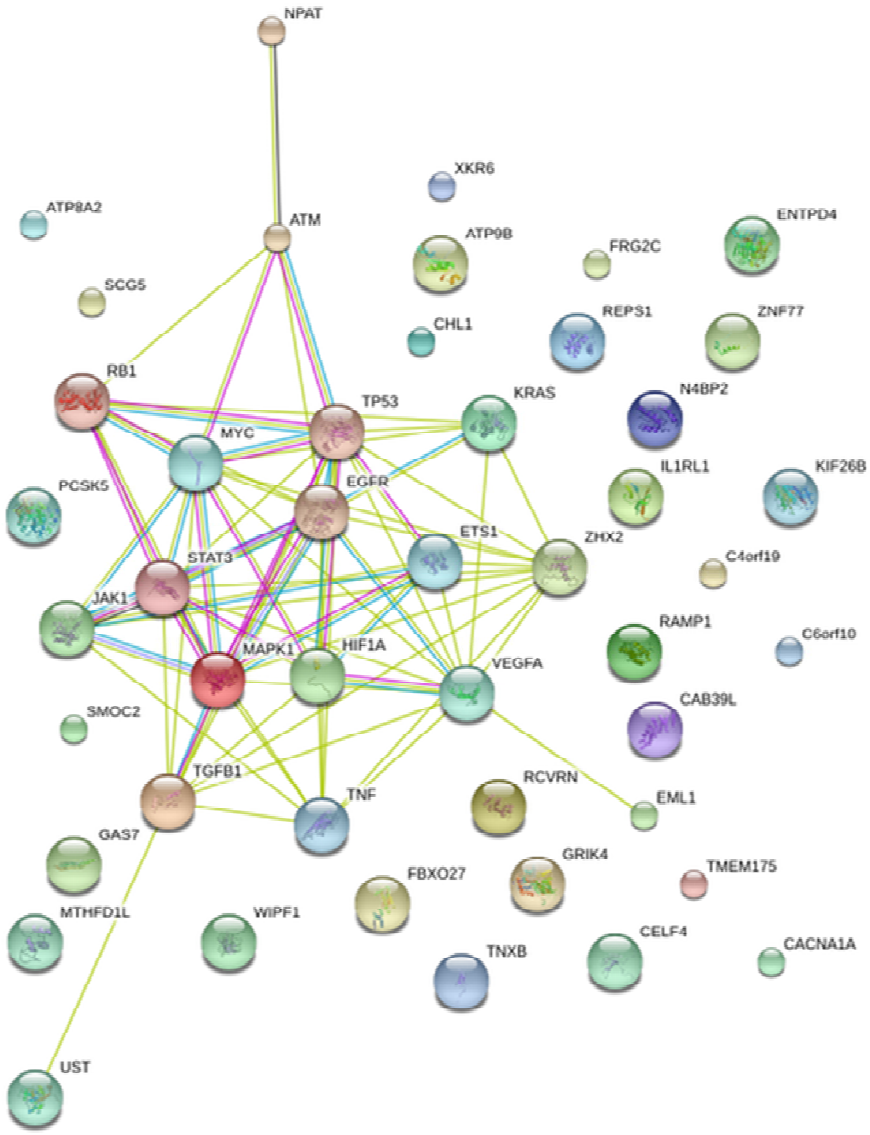

Figure 51. Evidence for the associations between the proteins resulting from the genes that were found hyper or hypomethylated in the A431-R cell line and the main proteins involved in carcinogenesis using STRING programme (ZHX2 = RAF protein).

The map of potential interactions (Figure 51) considering hypomethylated promoters indicates that:

1. The transcription factor ETS1, which was found silenced in the radioresistant A431-R cell subline, was associated with HIF1α, VEGFA (evidence for activation), MAPK1, ZHX2, and p53 (evidence for binding).

2. Factor EML1, which was also found hypomethylated in A431-R cells, was associated with VEGFA with evidence of post-translational modification.

For those promoters found hypermethylated, the map indicates that:

1. JAK interacted with EGFR, MAPK1 (evidence for binding), RAF, MYC, TNF, ETS1, and STAT3 (evidence for binding and for translational modification).
2. ATM was associated with Rb, Myc (evidence for binding), EGFR, and p53 (evidence for binding, for catalysis and for post-translational modification).
3. UST interacted in turn with TGF.
4. RAF acted as a transcriptional repressor form k-RAS, ETS1, STAT3, MAPK1, Myc, VEGFA (evidence for activation), p53 (evidence for post-translational modification), TNF, EGFR and JAK1.

However, it is necessary to recognize that the interpretation of these results is elusive, and complicate to conclude its biological rellevance. Epigenetic studies from different parental/radioresistant generated pairs would be useful to elucidate which epigenetic modifications are involved in the acquisition of a more resistant and aggressive phenotype after a process where a high radiation dose was administered, making the cells more radioresistant, and provide information of putative targets for acquired radioresistance.

To further difficult the interpretation of the data derived from transcriptome and/or methylation pattern, it should be mentioned that the findings using cultured cells are not influenced by factors such as tumour hypoxia, microenvironment (including tumour-stroma heterotypic interaction) and angiogenesis that occur in real oncogenesis. To improve these limitations, further efforts are needed using in vivo experimental models.

Another important aspect that should be addressed is that the survival of cancer stem cell population following radiation therapy is rellevant for control of cancer by radiotherapy (Krause, Yaromina et al. 2011; Nguyen, Murph et al. 2011): the higher number of cancer stem cells per tumour is, the lower tumour control is achieved in models of experimental radiotherapy (Baumann, Krause et al. 2009). Consistently, radioresistance of cancer stem cells compared to non-tumorogenic cells has been evidenced (Lagadec, Vlashi et al. 2010; Pajonk, Vlashi et al. 2010; Printz 2011; Vlashi, McBride et al. 2009). Following each dose fraction, it has been proposed, that non-stem cancer cells die and cancer stem cells potentially increase in number, participating to accelerated repopulation (Gao, McDonald et al. 2013). In irradiated prostate cancer lines, long term recovery resulted in increased cancer stem cells properties of the recovered cell population (Cho, Kim et al. 2012). The progressive selection of well-adapted sublines during fractionated irradiation may thus be a consequence of the higher survival of the cancer stem cell population.

In the experimental model used in the present work, it was investigated the expression of the cell surface antigen CD44, a putative stem cell marker functionally validated as a predictive biomarker of local control for early laryngeal cancer treated with radiotherapy (de Jong, Pramana et al. 2010). It was not find any differential expression of CD44 antigen in A431 isogenic cell lines (A431-WT/A431-R), a condition that can be attributed to the fact that CD44 in this pair of cells was not a variable that participated in the selective process, being an endorsed skill from the beginning of the creation of the parental cell line. Similarly, others researchers have analyzed protein expression of the stem cell markers Oct4, Sox2, and ALDH1 in two isogenic models of cancer cells (A549-R/ A549-p; SK-BR-3-R /SK-BR-3-p). While Oct4 expression appeared approximately 2-fold increased in SK-BR-3-R compared to SK-BR-3p cells, expression was similar in A549-R/A549-p cells, and differences in expression were not observed for Sox2 and ALDH1 in either models. Yet the radiosensitivity of

ALDH1+ cells isolated from the radioresistant subline was significantly reduced when compared to that of ALDH1+ cells isolated from the patient line (Mihatsch, Toulany et al. 2011). These cells were also more sensitive to ALDH1 inhibition. These results suggest that the relevance of ALDH1 for radioresistance needs to be further investigated. In oesophageal isogenic models, the expression of the stem cells markers β-catenin, Oct3/4, and β_1 integrin gene and protein levels were elevated in the radioresistant, when compared to the parent line (Zhang, Komaki et al. 2008).

To emphazise the outstanding relevance of isogenic radioresistant cell lines for the determination of the molecular radiation response several comments should be addressed. The current laboratory procedures for analyzing these biological events may however not be readily transferable to a clinical setting. The need for the discovery of novel prognostic and predictive biomarkers of radioresponse is widely recognised. A number of possible candidates for markers have been investigated including changes in DNA damage response and cell cycle checkpoints, the development of micronuclei, apoptotic events and clonal cell survival. The potential of these models may however be under-utilised and data to date suggests selection of a stem-cell like cell population. Future studies using isogenic radioresistant models should thus explore their stemness properties. These studies may lead to the identification of novel drug targets and the development of therapeutic agents that will increase tumour cell sensitivity to radiation therapy.

To further emphasize the utility of isogenic models it should be discussed several concerns about reirradiation. When cancer recurrences occur, treatment options must provide the patient with the longest possible interval of good-quality survival. A consideration of the potential morbidity associated with additional therapy in relation to the potential survival benefit that might be achieved is required. For patients who present locally recurrent disease in a previously irradiated field, therapeutic options

are limited, being surgery, the preferred option for those with limited-volume disease. Although historically, radiation oncologists have been cautious about re-irradiation of tumour recurrences because of concerns about the risk of late toxicity, particularly radionecrosis, which can actually occur within the first months after the end of the re-irradiation, re-irradiation is being revisited as a therapeutic alternative for selected patients, and a renewed clinical interest can be found (Joseph, Tai et al.). The current technological advancements in imaging and high-precision radiation delivery, and available clinical data are changing the nihilistic perception about re-irradiation (Deantonio, Gambaro et al. 2010; Fogh et al. 2010, Andrews et al. ; Lengyel, Baricza et al. 2003; Grosu, Weber et al. 2005).

Regarding re-irradiation, a major concern is the dose per fraction because of the severity of the biological effects positively correlates with the size of fraction, both in tumours and healthy tissues (Joseph, Tai et al.). When the indication for re-irradiation is not palliative, radiation oncologists prefer daily fractionations around 1.8 or 2 Gy, or even lower such is the case for hyperfractionation. This general practice is aimed to decrease toxicity associated to large fractions as anticipated by the linear-quadratic (LQ) model (Cornforth and Bedford 1987). With respect to LQ, the majority of primary carcinomas, including lung, rectal and head and neck cancers, have large α/β ratios ($\approx$ 10 Gy). Large α/β values, and thefore highly responsive tumours, are associated with tumours characterized by elevated cell proliferation, single-hit high radioresponsiveness (high α-component), and little ability to accumulate and repair sublethal damage (low β-component) (Deacon, Peckham et al. 1984; Fowler 1989; Fowler 2010). Under these circumstances, multifractionated radiotherapy delivering 2-Gy per day inactivates cancer cells and allows repairing sublethal damage in non-proliferative tissues leading to well-established therapeutic indexes. However, in the case of cancers harbouring low α/β ratio ($\leq$ 2 Gy), the 2-Gy conventional fractionation may not be an ideal scheme. For these tumours, the LQ model predicts an improved therapeutic ratio with hypofractionation when α/β of both tumour and normal tissues are similar (Ritter 2008). What can be

inferred and deserved some discussion is if the adaptative radiation changes in α/β occurring in cells like A431-R would be translatable to the re-irradiation setting, and if it could be a concern.

In the second part of this project of Thesis, we dealed with four objectives to administer fractionated radiotherapy to immunodeficient mice in the Radiotherapy Department of the Duran Reynals' Hospital. First, the irradiation of healthy tissues around the tumour was minimized. Second, the standard irradiation principles for human treatments were fulfilled. Third, the time-consuming and increased efficiency was reduced by irradiating several mice at a time. Finally, it was easy to reproduce and repeat on a daily basis by only two people.

This type of work was found necessary to implement experiments using in vivo models to reduce the gap between in vitro models and clinical setting. It was demonstrated the feasibility of fractionated irradiation using immunodeficient mice to evaluate the role of radiotherapy on experimental tumours simulating a clinical setting. The major contribution of this study, however, was to demonstrate that general or local effects of irradiation did not jeopardize the tumour radiation-response observation over a long follow-up. In addition, the absence of infect-contagious diseases was particularly decisive for the success of experiments. This provided evidence that the barrier protections used accomplished the goal of preventing microbiological diseases in these animals. Since cancer patients are often immunosuppressed, concerns about zoonoses should not be ignored. Nevertheless, it should be emphasised that the potential risk of zoonoses is extremely low when good laboratory practices and healthy athymic mice are used.

In the third part of this project of Thesis, we pre-clinically explored whether a treatment regime involving the addition of simvastatin to XRT and C225 merits further research. Given the fact that XRT and concurrent C225 is a common treatment for locally

advanced head and neck squamous cell carcinomas, and a significant number of failures are still a cause of death from cancer, this is a relevant question.

We have shown that the addition of simvastatin significantly decreased proliferation and clonogenic survival of cells treated with XRT and C225. Moreover, we used an experimental model with tumor cells derived from squamous cell carcinoma of the hypopharynx that suggests that simvastatin may increase the antitumor effect of XRT plus C225— at doses and fractions of XRT that mimic doses administered in the clinical setting. FaDu cell line from HNSCC overexpresses the EGFR, and the cell line A431 from squamous carcinoma also overexpresses EGFR, even in higher degree than FaDu cells. For this reason, A431 cell line seemed to us a good model for cetuximab modelling and the effects of simvastatin were recapitulated using this cell line validating the notion that simvastatin may have a role in combination with XRT and C225.

The addition of simvastatin was associated with an increase in apoptosis and a decrease in the levels of activated ERK1/2, AKT, and STAT3 oncoproteins, a set of observations that provide support to the higher anti-tumor effects produced by the triple treatment.

The role of statins in cancer therapy has been reviewed previously elsewhere (Chan, Oza et al. 2003; Sleijfer, van der Gaast et al. 2005; Hindler, Cleeland et al. 2006; Gauthaman, Fong et al. 2009). In non-cancerous tissues, statins reduce the proliferation of the atherosclerotic plaque and the chronic inflammatory process associated with atheromatosis (Schartl, Bocksch et al. 2001). Similarly, simvastatin represses the proliferation of glomerular mesangial cells, suggesting a preventive role in diabetic nephropathy, an effect mediated by its interference with isoprenylation of small GTP-binding proteins (Danesh, Sadeghi et al. 2002). In addition to the anti-proliferative and anti-inflammatory properties of statins in non-neoplastic tissues, increasing evidence supports a role for statins in cancer through the inhibition of cancer cell proliferation,

angiogenesis, and metastatic potential. These effects have been proved in numerous different cell lines derived from myeloid and lymphoblastic leukaemia, neuroblastoma, rhabdomyosarcoma, meduloblastoma squamous cell carcinoma of the cervix, melanoma, high-grade glioma, and cancer of the kidney, testis, breast, stomach, prostate and small-cell lung cancer (Soma, Pagliarini et al. 1992; Dimitroulakos, Ye et al. 2001; Khanzada, Pardo et al. 2006; Wu, Jiang et al. 2009). Published data indicate that statins can sensitize cancer cells to chemical drugs such as doxorrubicine, nitrosureas, cis-platin, and 5-fluorouracil (Wang, Collie-Duguid et al. 2002; Werner, Sacher et al. 2004). Recently, it was reported that the combination of simvastatin and C225 sensitize colon cancer cells bearing *RAS* mutations (Lee, Lee et al. 2011). In combination with XRT, the statin lovastatin has also been found to have a radiosensitising effect in lung cancer and osteosarcoma cell lines that express mutated RAS (Sanli, Liu et al. 2011; Miller, Kariko et al. 1993). Interestingly, several randomized-controlled trials and case-control studies have found that statins used to lower cholesterol levels may exert a protective effect against cancer (Gutt, Tonlaar et al. ; Boudreau, Gardner et al. 2004; Graaf, Beiderbeck et al. 2004). In addition, a recent epidemiological study found evidence suggesting that statin use can reduce cancer-related mortality (Nielsen, Nordestgaard et al. 2012). A number of clinical trials have investigated the antitumor effect of statins. In one trial, the combination of 5-fluorouracil and the statin pravastatin was associated with a higher tumor response and better survival than chemotherapy alone in patients with unresectable hepatocarcinoma (Kawata, Yamasaki et al. 2001). Similarly, a review carried out by Hindler et al. described the promising results for statin use in HNSCC and other types of cancer (Hindler, Cleeland et al. 2006).

An important consideration is that the work done in preparing A431-R and experimental fractionated radiotherapy was crucial to undertake the third part of this research. We were able to combined simvastatin with XRT + C225 in the treatment of the radioresistant generated A431-R, we observed that the initial resistance of these cells to the treatment is in part reverted. In fact, cell migration, cell proliferation and cell survival were decreased when simvastatin was combined to the treatment with XRT+C225. In

addition, tumour growth was slowed down when simvastatin was added to XRT+C225 treatment. The model A431-WT/A431-R we have generated can be a useful tool to examine new treatments directed to revert radioresistance produced from a prior treatment with radiotherapy. Indeed, the acquisition of radiation resistance based on the explotation of EGFR/MAPK pathway poses cells vulnerable to C225. The addictive status of radioresistant cells evidences the existence of an achilles' heel for further tumour control with the addition of simvastatin. Treatment effects can be studied in both cell sublines and comparison with the parental cells could give important information.

To our knowledge, our is the first *in vivo* study of combined XRT, C225, and statins to show increased antitumor effects in HNSCC, providing new translational data to support clinical investigation of statins in radiation oncology. The findings we report are consistent with the mechanism of anti-cancer action of simvastatin described previously as monotherapy or in combination with radiation or classical chemotherapies. However, this is the first report in which simvastatin has been successfully assessed in combination with an anti-EGFR therapy using xenoimplanted tumors. We have observed that statins have antiproliferative effects (Chan, Oza et al. 2003; Gauthaman, Fong et al. 2009), and that they can contribute to cancer cell killing by apoptosis (Khanzada, Pardo et al. 2006; Wu, Jiang et al. 2009; Lee, Lee et al. 2011; Sanli, Liu et al. 2011). We have also observed that the levels of ERK1/2, AKT and STAT3 proteins that promote cancer progression were reduced by simvastatin, a finding that correlated with a loss of cell viability and with apoptosis. In addition to increasing apoptosis, this decrease in activated ERK1/2, AKT and STAT3 levels—oncoproteins known to have a role in repairing radiation-induced damage and, in promoting the development of aggressive malignant phenotypes (Liang, Ang et al. 2003; Pueyo, Mesia et al. 2010; de Llobet, Baro et al. 2013)—could impair the ability of cancer cells to recover from XRT and C225.

The evidence in the present report warrants further clinical investigation, although we have to add some comments that deserve a particular mention. We and others have found significant anti-tumor activity at concentration levels ranging from 1

μM to 25 μM. However, the typical plasma levels to treat hypercholesterolemia are approximately 10 times lower (Thibault, Samid et al. 1996). This observation raises additional concerns about statin-induced liver and muscle toxicity, especially given that only a few clinical trials have been carried out to address this issue. One phase I trial in patients with HNSCC established that 7.5 mg/kg/day of lovastatin for 2 weeks (the dose for dyslipidemia is 1 mg/kg/day) followed by a 1-week break was a well-tolerated scheme (provided that creatinine clearance > 70 mL/min) (Knox, Siu et al. 2005). Nevertheless, lovastatin doses can be safely escalated (35 mg/kg/day) as long as ubiquinone (co-enzyme Q) is given concomitantly (Thibault, Samid et al. 1996; Kim, Kim et al. 2001; Knox, Siu et al. 2005). The existing uncertainties about the effective dose of statins in cancer therapy are aggravated by the fact that lovastatin and simvastatin are administered as inactive prodrugs, and need to be enzymatically activated to β-hydroxy acid by esterases and paraoxonases-mediated hydrolysis (Billecke, Draganov et al. 2000). To our knowledge, no published studies have measured the actual active acid form of simvastatin or lovastatin in cell cultures and/or in mice—in which liver statins undergo active transformation—to properly infer the statin dose that should be used in clinical cancer trials. Although clinical and epidemiological data suggest that relative low plasma concentrations of statins could be sufficient to achieve an anti-tumor effect, reasonably, new phase I trials with pharmacokinetic and pharmacodynamic studies are warranted.

CONCLUSIONS

1. Heavy fractionated doses of radiation and clonal selection is a method to effectively develop an isogenic radioresistant cell lines, and thereafter characterize them to evaluate both the biology of radiation resistance and treatment.

2. The new isogenic pair A431-WT/A431-R is characterized by the acquisition of an aggressive phenotype in A431-R cells consisting in greater DNA repair, higher cloning efficiency, *in vitro* faster growth and migration ability, remarkable baseline levels of relevant oncoproteins, elevated angiogenesis capabilities, and a significant decrease in the α/ß ratio.

3. Fractionated irradiation of xenoimplanted tumours is feasibility using a medical linear accelerator in absence of specific facilities. The method implemented here allowed studding both the biology and treatment of radiation resistance in tumours.

4. The addition of simvastatin enhances the anti-tumor response of concomitant XRT and C225 in FaDu cells and A431-WT/A431-R both in culture and in xenoimplanted tumors. The addition of simvastatin to XRT + C225 decreases cell proliferation, wound healing, clonogenic survival, regrowth rate of tumours, pAkt, pErk1/2, and STAT3 oncoprotein levels, and increased apoptosis in the tumours.

5. In this preclinical work, we have provided evidence that supports further basic and clinical investigation of simvastatin in combination with XRT and C225 for HNSCC disease.

REFERENCES

(2006). "Cetuximab approved by FDA for treatment of head and neck squamous cell cancer." Cancer Biol Ther **5**(4): 340-2.

Abraham, R. T. (2001). "Cell cycle checkpoint signaling through the ATM and ATR kinases." Genes Dev **15**(17): 2177-96.

Ang, K. K., N. H. Andratschke, et al. (2004). "Epidermal growth factor receptor and response of head-and-neck carcinoma to therapy." Int J Radiat Oncol Biol Phys **58**(3): 959-65.

Armitage, J., L. Bowman, et al. (2010). "Intensive lowering of LDL cholesterol with 80 mg versus 20 mg simvastatin daily in 12,064 survivors of myocardial infarction: a double-blind randomised trial." Lancet **376**(9753): 1658-69.

Balaban, N., J. Moni, et al. (1996). "The effect of ionizing radiation on signal transduction: antibodies to EGF receptor sensitize A431 cells to radiation." Biochim Biophys Acta **1314**(1-2): 147-56.

Baro, M., L. I. de Llobet, et al. (2012). "Development and refinement of a technique using a medical radiation therapy facility to irradiate immunodeficient mice bearing xenografted human tumours." Lab Anim **46**(4): 345-8.

Baselga, J. and S. M. Swain (2009). "Novel anticancer targets: revisiting ERBB2 and discovering ERBB3." Nat Rev Cancer **9**(7): 463-75.

Baumann, M., M. Krause, et al. (2009). "Cancer stem cells and radiotherapy." Int J Radiat Biol **85**(5): 391-402.

Bellosta, S., N. Ferri, et al. (2000). "Non-lipid-related effects of statins." Ann Med **32**(3): 164-76.

Billecke, S., D. Draganov, et al. (2000). "Human serum paraoxonase (PON1) isozymes Q and R hydrolyze lactones and cyclic carbonate esters." Drug Metab Dispos **28**(11): 1335-42.

Biscardi, J. S., M. C. Maa, et al. (1999). "c-Src-mediated phosphorylation of the epidermal growth factor receptor on Tyr845 and Tyr1101 is associated with modulation of receptor function." J Biol Chem **274**(12): 8335-43.

Blumenthal, R. S. (2000). "Statins: effective antiatherosclerotic therapy." Am Heart J **139**(4): 577-83.

Bogman, K., A. K. Peyer, et al. (2001). "HMG-CoA reductase inhibitors and P-glycoprotein modulation." Br J Pharmacol **132**(6): 1183-92.

Bonner, J. A., P. M. Harari, et al. (2006). "Radiotherapy plus cetuximab for squamous-cell carcinoma of the head and neck." N Engl J Med **354**(6): 567-78.

Boudreau, D. M., J. S. Gardner, et al. (2004). "The association between 3-hydroxy-3-methylglutaryl conenzyme A inhibitor use and breast carcinoma risk among postmenopausal women: a case-control study." Cancer **100**(11): 2308-16.

Carmeliet, P. and R. K. Jain (2000). "Angiogenesis in cancer and other diseases." Nature **407**(6801): 249-57.

Carter, S., K. L. Auer, et al. (1998). "Inhibition of the mitogen activated protein (MAP) kinase cascade potentiates cell killing by low dose ionizing radiation in A431 human squamous carcinoma cells." Oncogene **16**(21): 2787-96.

Ciardiello, F., R. Caputo, et al. (2001). "Antisense oligonucleotides targeting the epidermal growth factor receptor inhibit proliferation, induce apoptosis, and cooperate with cytotoxic drugs in human cancer cell lines." Int J Cancer **93**(2): 172-8.

Ciardiello, F. and G. Tortora (2008). "EGFR antagonists in cancer treatment." N Engl J Med **358**(11): 1160-74.

Contessa, J. N., A. Abell, et al. (2006). "ErbB receptor tyrosine kinase network inhibition radiosensitizes carcinoma cells." Int J Radiat Oncol Biol Phys **65**(3): 851-8.

Contessa, J. N., J. Hampton, et al. (2002). "Ionizing radiation activates Erb-B receptor dependent Akt and p70 S6 kinase signaling in carcinoma cells." Oncogene **21**(25): 4032-41.

Cornforth, M. N. and J. S. Bedford (1987). "A quantitative comparison of potentially lethal damage repair and the rejoining of interphase chromosome breaks in low passage normal human fibroblasts." Radiat Res **111**(3): 385-405.

Chan, K. K., A. M. Oza, et al. (2003). "The statins as anticancer agents." Clin Cancer Res **9**(1): 10-9.

Cho, Y. M., Y. S. Kim, et al. (2012). "Long-term recovery of irradiated prostate cancer increases cancer stem cells." Prostate **72**(16): 1746-56.

Danesh, F. R., M. M. Sadeghi, et al. (2002). "3-Hydroxy-3-methylglutaryl CoA reductase inhibitors prevent high glucose-induced proliferation of mesangial cells via modulation of Rho GTPase/ p21 signaling pathway: Implications for diabetic nephropathy." Proc Natl Acad Sci U S A **99**(12): 8301-5.

De Bacco, F., P. Luraghi, et al. (2011). "Induction of MET by ionizing radiation and its role in radioresistance and invasive growth of cancer." J Natl Cancer Inst **103**(8): 645-61.

de Jong, M. C., J. Pramana, et al. (2010). "CD44 expression predicts local recurrence after radiotherapy in larynx cancer." Clin Cancer Res **16**(21): 5329-38.

de Llobet, L. I., M. Baro, et al. (2013). "Development and characterization of an isogenic cell line with a radioresistant phenotype." Clin Transl Oncol **15**(3): 189-97.

De Smet, C., O. De Backer, et al. (1996). "The activation of human gene MAGE-1 in tumor cells is correlated with genome-wide demethylation." Proc Natl Acad Sci U S A **93**(14): 7149-53.

Deacon, J., M. J. Peckham, et al. (1984). "The radioresponsiveness of human tumours and the initial slope of the cell survival curve." Radiother Oncol **2**(4): 317-23.

Deantonio, L., G. Gambaro, et al. (2010). "Hypofractionated radiotherapy after conservative surgery for breast cancer: analysis of acute and late toxicity." Radiat Oncol **5**: 112.

DeBerardinis, R. J., J. J. Lum, et al. (2008). "The biology of cancer: metabolic reprogramming fuels cell growth and proliferation." Cell Metab **7**(1): 11-20.

Dimitroulakos, J., L. Y. Ye, et al. (2001). "Differential sensitivity of various pediatric cancers and squamous cell carcinomas to lovastatin-induced apoptosis: therapeutic implications." Clin Cancer Res **7**(1): 158-67.

Dittmann, K., C. Mayer, et al. (2005). "Radiation-induced epidermal growth factor receptor nuclear import is linked to activation of DNA-dependent protein kinase." J Biol Chem **280**(35): 31182-9.

Dittmann, K., C. Mayer, et al. (2009). "Radiation-induced lipid peroxidation activates src kinase and triggers nuclear EGFR transport." Radiother Oncol **92**(3): 379-82.

Downs, J. R., M. Clearfield, et al. (1998). "Primary prevention of acute coronary events with lovastatin in men and women with average cholesterol levels: results of AFCAPS/TexCAPS. Air Force/Texas Coronary Atherosclerosis Prevention Study." Jama **279**(20): 1615-22.

Edwards, P. A. and J. Ericsson (1999). "Sterols and isoprenoids: signaling molecules derived from the cholesterol biosynthetic pathway." Annu Rev Biochem **68**: 157-85.

Fan, Z., Y. Lu, et al. (1994). "Antibody-induced epidermal growth factor receptor dimerization mediates inhibition of autocrine proliferation of A431 squamous carcinoma cells." J Biol Chem **269**(44): 27595-602.

Fogh, S. E., D. W. Andrews, et al. (2010). "Hypofractionated stereotactic radiation therapy: an effective therapy for recurrent high-grade gliomas." J Clin Oncol **28**(18): 3048-53.

Fowler, J. F. (1989). "The linear-quadratic formula and progress in fractionated radiotherapy." Br J Radiol **62**(740): 679-94.

Fowler, J. F. (2010). "21 years of biologically effective dose." Br J Radiol **83**(991): 554-68.

Fukuda, K., C. Sakakura, et al. (2004). "Differential gene expression profiles of radioresistant oesophageal cancer cell lines established by continuous fractionated irradiation." Br J Cancer **91**(8): 1543-50.

Gao, X., J. T. McDonald, et al. (2013). "Acute and fractionated irradiation differentially modulate glioma stem cell division kinetics." Cancer Res **73**(5): 1481-90.

Gauthaman, K., C. Y. Fong, et al. (2009). "Statins, stem cells, and cancer." J Cell Biochem **106**(6): 975-83.

Giaccone, G. (2005). "Epidermal growth factor receptor inhibitors in the treatment of non-small-cell lung cancer." J Clin Oncol **23**(14): 3235-42.

Gill, G. N., T. Kawamoto, et al. (1984). "Monoclonal anti-epidermal growth factor receptor antibodies which are inhibitors of epidermal growth factor binding and antagonists of epidermal growth factor binding and antagonists of epidermal growth factor-stimulated tyrosine protein kinase activity." J Biol Chem **259**(12): 7755-60.

Goldstein, N. I., M. Prewett, et al. (1995). "Biological efficacy of a chimeric antibody to the epidermal growth factor receptor in a human tumor xenograft model." Clin Cancer Res **1**(11): 1311-8.

Gorski, D. H., M. A. Beckett, et al. (1999). "Blockage of the vascular endothelial growth factor stress response increases the antitumor effects of ionizing radiation." Cancer Res **59**(14): 3374-8.

Graaf, M. R., A. B. Beiderbeck, et al. (2004). "The risk of cancer in users of statins." J Clin Oncol **22**(12): 2388-94.

Grosu, A. L., W. A. Weber, et al. (2005). "Reirradiation of recurrent high-grade gliomas using amino acid PET (SPECT)/CT/MRI image fusion to determine gross tumor volume for stereotactic fractionated radiotherapy." Int J Radiat Oncol Biol Phys **63**(2): 511-9.

Gutt, R., N. Tonlaar, et al. (2010). "Statin use and risk of prostate cancer recurrence in men treated with radiation therapy." J Clin Oncol **28**(16): 2653-9.

Haffty, B. G. and P. M. Glazer (2003). "Molecular markers in clinical radiation oncology." Oncogene **22**(37): 5915-25.

Harari, P. M. (2004). "Epidermal growth factor receptor inhibition strategies in oncology." Endocr Relat Cancer **11**(4): 689-708.

Harari, P. M. and S. M. Huang (2001). "Head and neck cancer as a clinical model for molecular targeting of therapy: combining EGFR blockade with radiation." Int J Radiat Oncol Biol Phys **49**(2): 427-33.

Hindler, K., C. S. Cleeland, et al. (2006). "The role of statins in cancer therapy." Oncologist **11**(3): 306-15.

Holash, J., P. C. Maisonpierre, et al. (1999). "Vessel cooption, regression, and growth in tumors mediated by angiopoietins and VEGF." Science **284**(5422): 1994-8.

Holstein, S. A. and R. J. Hohl (2001). "Synergistic interaction of lovastatin and paclitaxel in human cancer cells." Mol Cancer Ther **1**(2): 141-9.

Huang, C. Y., C. C. Wei, et al. (2012). "Bortezomib enhances radiation-induced apoptosis in solid tumors by inhibiting CIP2A." Cancer Lett **317**(1): 9-15.

Huang, S. M., J. M. Bock, et al. (1999). "Epidermal growth factor receptor blockade with C225 modulates proliferation, apoptosis, and radiosensitivity in squamous cell carcinomas of the head and neck." Cancer Res **59**(8): 1935-40.

Huang, S. M. and P. M. Harari (2000). "Modulation of radiation response after epidermal growth factor receptor blockade in squamous cell carcinomas: inhibition of damage repair, cell cycle kinetics, and tumor angiogenesis." Clin Cancer Res **6**(6): 2166-74.

Institute, N. C. (2013). "Head and Neck Cancers." from http://www.cancer.gov/cancertopics/factsheet/Sites-Types/head-and-neck.

Jannot, C. B., R. R. Beerli, et al. (1996). "Intracellular expression of a single-chain antibody directed to the EGFR leads to growth inhibition of tumor cells." Oncogene **13**(2): 275-82.

Joazeiro, C. A., S. S. Wing, et al. (1999). "The tyrosine kinase negative regulator c-Cbl as a RING-type, E2-dependent ubiquitin-protein ligase." Science **286**(5438): 309-12.

Johnson-Anuna, L. N., G. P. Eckert, et al. (2005). "Chronic administration of statins alters multiple gene expression patterns in mouse cerebral cortex." J Pharmacol Exp Ther **312**(2): 786-93.

Jones, J. T., R. W. Akita, et al. (1999). "Binding specificities and affinities of egf domains for ErbB receptors." FEBS Lett **447**(2-3): 227-31.

Joseph, K., P. Tai, et al. "Workshop report: A practical approach and general principles of re-irradiation for in-field cancer recurrence." Clin Oncol (R Coll Radiol) **22**(10): 885-9.

Katz, M. S., B. D. Minsky, et al. (2005). "Association of statin use with a pathologic complete response to neoadjuvant chemoradiation for rectal cancer." Int J Radiat Oncol Biol Phys **62**(5): 1363-70.

Kawamoto, T., J. D. Sato, et al. (1983). "Growth stimulation of A431 cells by epidermal growth factor: identification of high-affinity receptors for epidermal growth

factor by an anti-receptor monoclonal antibody." Proc Natl Acad Sci U S A **80**(5): 1337-41.

Kawata, S., E. Yamasaki, et al. (2001). "Effect of pravastatin on survival in patients with advanced hepatocellular carcinoma. A randomized controlled trial." Br J Cancer **84**(7): 886-91.

Khan, E. M., J. M. Heidinger, et al. (2006). "Epidermal growth factor receptor exposed to oxidative stress undergoes Src- and caveolin-1-dependent perinuclear trafficking." J Biol Chem **281**(20): 14486-93.

Khanzada, U. K., O. E. Pardo, et al. (2006). "Potent inhibition of small-cell lung cancer cell growth by simvastatin reveals selective functions of Ras isoforms in growth factor signalling." Oncogene **25**(6): 877-87.

Kim, W. S., M. M. Kim, et al. (2001). "Phase II study of high-dose lovastatin in patients with advanced gastric adenocarcinoma." Invest New Drugs **19**(1): 81-3.

Knox, J. J., L. L. Siu, et al. (2005). "A Phase I trial of prolonged administration of lovastatin in patients with recurrent or metastatic squamous cell carcinoma of the head and neck or of the cervix." Eur J Cancer **41**(4): 523-30.

Krause, M., A. Yaromina, et al. (2011). "Cancer stem cells: targets and potential biomarkers for radiotherapy." Clin Cancer Res **17**(23): 7224-9.

Lagadec, C., E. Vlashi, et al. (2010). "Survival and self-renewing capacity of breast cancer initiating cells during fractionated radiation treatment." Breast Cancer Res **12**(1): R13.

Lee, H. C., S. An, et al. (2008). "Activation of epidermal growth factor receptor and its downstream signaling pathway by nitric oxide in response to ionizing radiation." Mol Cancer Res **6**(6): 996-1002.

Lee, J., I. Lee, et al. (2011). "Effect of simvastatin on cetuximab resistance in human colorectal cancer with KRAS mutations." J Natl Cancer Inst **103**(8): 674-88.

Lee, J. C., I. Vivanco, et al. (2006). "Epidermal growth factor receptor activation in glioblastoma through novel missense mutations in the extracellular domain." PLoS Med **3**(12): e485.

Lee, Y. S., J. H. Oh, et al. (2010). "Differential gene expression profiles of radioresistant non-small-cell lung cancer cell lines established by fractionated irradiation: tumor protein p53-inducible protein 3 confers sensitivity to ionizing radiation." Int J Radiat Oncol Biol Phys **77**(3): 858-66.

Lengyel, E., K. Baricza, et al. (2003). "Reirradiation of locally recurrent nasopharyngeal carcinoma." Strahlenther Onkol **179**(5): 298-305.

Lennernas, H. and G. Fager (1997). "Pharmacodynamics and pharmacokinetics of the HMG-CoA reductase inhibitors. Similarities and differences." Clin Pharmacokinet **32**(5): 403-25.

Li, H. Y., F. R. Appelbaum, et al. (2003). "Cholesterol-modulating agents kill acute myeloid leukemia cells and sensitize them to therapeutics by blocking adaptive cholesterol responses." Blood **101**(9): 3628-34.

Liang, K., K. K. Ang, et al. (2003). "The epidermal growth factor receptor mediates radioresistance." Int J Radiat Oncol Biol Phys **57**(1): 246-54.

Lo, H. W., S. C. Hsu, et al. (2006). "EGFR signaling pathway in breast cancers: from traditional signal transduction to direct nuclear translocalization." Breast Cancer Res Treat **95**(3): 211-8.

Lo, H. W. and M. C. Hung (2006). "Nuclear EGFR signalling network in cancers: linking EGFR pathway to cell cycle progression, nitric oxide pathway and patient survival." Br J Cancer **94**(2): 184-8.

Lurje, G. and H. J. Lenz (2009). "EGFR signaling and drug discovery." Oncology **77**(6): 400-10.

Lynam-Lennon, N., J. V. Reynolds, et al. (2010). "Alterations in DNA repair efficiency are involved in the radioresistance of esophageal adenocarcinoma." Radiat Res **174**(6): 703-11.

Mandal, A. (2004). "Cancer Classification." from http://www.news-medical.net/health/Cancer-Classification.aspx.

Mass, R. D. (2004). "The HER receptor family: a rich target for therapeutic development." Int J Radiat Oncol Biol Phys **58**(3): 932-40.

Meier, C. R., R. G. Schlienger, et al. (2000). "HMG-CoA reductase inhibitors and the risk of fractures." Jama **283**(24): 3205-10.

Mendelsohn, J. (2000). "Blockade of receptors for growth factors: an anticancer therapy--the fourth annual Joseph H Burchenal American Association of Cancer Research Clinical Research Award Lecture." Clin Cancer Res **6**(3): 747-53.

Mendelsohn, J. and J. Baselga (2003). "Status of epidermal growth factor receptor antagonists in the biology and treatment of cancer." J Clin Oncol **21**(14): 2787-99.

Mendelsohn, J. and Z. Fan (1997). "Epidermal growth factor receptor family and chemosensitization." J Natl Cancer Inst **89**(5): 341-3.

Mihatsch, J., M. Toulany, et al. (2011). "Selection of radioresistant tumor cells and presence of ALDH1 activity in vitro." Radiother Oncol **99**(3): 300-6.

Milas, L., T. Akimoto, et al. (2002). "Relationship between cyclin D1 expression and poor radioresponse of murine carcinomas." Int J Radiat Oncol Biol Phys **52**(2): 514-21.

Milas, L., K. A. Mason, et al. (2003). "Epidermal growth factor receptor and its inhibition in radiotherapy: in vivo findings." Int J Radiat Biol **79**(7): 539-45.

Miller, A. C., K. Kariko, et al. (1993). "Increased radioresistance of EJras-transformed human osteosarcoma cells and its modulation by lovastatin, an inhibitor of p21ras isoprenylation." Int J Cancer **53**(2): 302-7.

Nguyen, G. H., M. M. Murph, et al. (2011). "Cancer Stem Cell Radioresistance and Enrichment: Where Frontline Radiation Therapy May Fail in Lung and Esophageal Cancers." Cancers (Basel) **3**(1): 1232-1252.

Nielsen, S. F., B. G. Nordestgaard, et al. (2012). "Statin use and reduced cancer-related mortality." N Engl J Med **367**(19): 1792-802.

Normanno, N., A. De Luca, et al. (2006). "Epidermal growth factor receptor (EGFR) signaling in cancer." Gene **366**(1): 2-16.

Ozcan, F., P. Klein, et al. (2006). "On the nature of low- and high-affinity EGF receptors on living cells." Proc Natl Acad Sci U S A **103**(15): 5735-40.

Pajonk, F., E. Vlashi, et al. (2010). "Radiation resistance of cancer stem cells: the 4 R's of radiobiology revisited." Stem Cells **28**(4): 639-48.

Paragh, G., P. Kertai, et al. (2003). "HMG CoA reductase inhibitor fluvastatin arrests the development of implanted hepatocarcinoma in rats." Anticancer Res **23**(5A): 3949-54.

Park, J. S., L. Qiao, et al. (2000). "A role for both Ets and C/EBP transcription factors and mRNA stabilization in the MAPK-dependent increase in p21 (Cip-1/WAF1/mda6) protein levels in primary hepatocytes." Mol Biol Cell **11**(9): 2915-32.

Partovian, C. and M. Simons (2004). "Regulation of protein kinase B/Akt activity and Ser473 phosphorylation by protein kinase Calpha in endothelial cells." Cell Signal **16**(8): 951-7.

Patel, D., R. Bassi, et al. (2009). "Anti-epidermal growth factor receptor monoclonal antibody cetuximab inhibits EGFR/HER-2 heterodimerization and activation." Int J Oncol **34**(1): 25-32.

Pena-Rico, M. A., M. N. Calvo-Vidal, et al. (2011). "TP53 induced glycolysis and apoptosis regulator (TIGAR) knockdown results in radiosensitization of glioma cells." Radiother Oncol **101**(1): 132-9.

Poynter, J. N., S. B. Gruber, et al. (2005). "Statins and the risk of colorectal cancer." N Engl J Med **352**(21): 2184-92.

Prewett, M. C., A. T. Hooper, et al. (2002). "Enhanced antitumor activity of anti-epidermal growth factor receptor monoclonal antibody IMC-C225 in combination with irinotecan (CPT-11) against human colorectal tumor xenografts." Clin Cancer Res **8**(5): 994-1003.

Printz, C. (2011). "Radiation treatment generates therapy-resistant cancer stem cells from less aggressive breast cancer cells." Cancer **118**(13): 3225.

Pueyo, G., R. Mesia, et al. (2010). "Cetuximab may inhibit tumor growth and angiogenesis induced by ionizing radiation: a preclinical rationale for maintenance treatment after radiotherapy." Oncologist **15**(9): 976-86.

Qiao, L., A. Yacoub, et al. (2002). "Pharmacologic inhibitors of the mitogen activated protein kinase cascade have the potential to interact with ionizing radiation exposure to induce cell death in carcinoma cells by multiple mechanisms." Cancer Biol Ther **1**(2): 168-76.

Ritter, M. (2008). "Rationale, conduct, and outcome using hypofractionated radiotherapy in prostate cancer." Semin Radiat Oncol **18**(4): 249-56.

Rodemann, H. P. and B. G. Wouters (2011). "Frontiers in molecular radiation biology/oncology." Radiother Oncol **101**(1): 1-6.

Sanli, T., C. Liu, et al. (2011). "Lovastatin sensitizes lung cancer cells to ionizing radiation: modulation of molecular pathways of radioresistance and tumor suppression." J Thorac Oncol **6**(3): 439-50.

Sato, J. D., T. Kawamoto, et al. (1983). "Biological effects in vitro of monoclonal antibodies to human epidermal growth factor receptors." Mol Biol Med **1**(5): 511-29.

Schartl, M., W. Bocksch, et al. (2001). "Use of intravascular ultrasound to compare effects of different strategies of lipid-lowering therapy on plaque volume and composition in patients with coronary artery disease." Circulation **104**(4): 387-92.

Schlessinger, J. (2000). "Cell signaling by receptor tyrosine kinases." Cell **103**(2): 211-25.

Schmidt-Ullrich, R. K., J. N. Contessa, et al. (1999). "Molecular mechanisms of radiation-induced accelerated repopulation." Radiat Oncol Investig **7**(6): 321-30.

Schmidt-Ullrich, R. K., J. N. Contessa, et al. (2003). "ERBB receptor tyrosine kinases and cellular radiation responses." Oncogene **22**(37): 5855-65.

Schmidt-Ullrich, R. K., P. Dent, et al. (2000). "Signal transduction and cellular radiation responses." Radiat Res **153**(3): 245-57.

Schmidt-Ullrich, R. K., R. B. Mikkelsen, et al. (1997). "Radiation-induced proliferation of the human A431 squamous carcinoma cells is dependent on EGFR tyrosine phosphorylation." Oncogene **15**(10): 1191-7.

Semenza, G. L. (2010). "Defining the role of hypoxia-inducible factor 1 in cancer biology and therapeutics." Oncogene **29**(5): 625-34.

Shepherd, J., S. M. Cobbe, et al. (1995). "Prevention of coronary heart disease with pravastatin in men with hypercholesterolemia. West of Scotland Coronary Prevention Study Group." N Engl J Med **333**(20): 1301-7.

Simons, K. and D. Toomre (2000). "Lipid rafts and signal transduction." Nat Rev Mol Cell Biol **1**(1): 31-9.

Sleijfer, S., A. van der Gaast, et al. (2005). "The potential of statins as part of anti-cancer treatment." Eur J Cancer **41**(4): 516-22.

Society, A. C. (2008). "Cancer Facts and Figures (2nd edition)". www.cancer.org, from http://www.cancer.org/acs/groups/content/@epidemiologysurveilance/documents/document/acspc-027766.pdf.

Soma, M. R., P. Pagliarini, et al. (1992). "Simvastatin, an inhibitor of cholesterol biosynthesis, shows a synergistic effect with N,N'-bis(2-chloroethyl)-N-nitrosourea and beta-interferon on human glioma cells." Cancer Res **52**(16): 4348-55.

Stancu, C. and A. Sima (2001). "Statins: mechanism of action and effects." J Cell Mol Med **5**(4): 378-87.

Thariat, J., G. Yildirim, et al. (2007). "Combination of radiotherapy with EGFR antagonists for head and neck carcinoma." Int J Clin Oncol **12**(2): 99-110.

Thibault, A., D. Samid, et al. (1996). "Phase I study of lovastatin, an inhibitor of the mevalonate pathway, in patients with cancer." Clin Cancer Res **2**(3): 483-91.

Toulany, M., M. Minjgee, et al. (2010). "ErbB2 expression through heterodimerization with erbB1 is necessary for ionizing radiation- but not EGF-induced activation of Akt survival pathway." Radiother Oncol **97**(2): 338-45.

Tsai, H. K., M. S. Katz, et al. (2006). "Association of statin use with improved local control in patients treated with selective bladder preservation for muscle-invasive bladder cancer." Urology **68**(6): 1188-92.

Tucker, S. L. (1986). "Is the mean inactivation dose a good measure of cell radiosensitivity?" Radiat Res **105**(1): 18-26.

Ullrich, A. and J. Schlessinger (1990). "Signal transduction by receptors with tyrosine kinase activity." Cell **61**(2): 203-12.

Vaughan, C. J., A. M. Gotto, Jr., et al. (2000). "The evolving role of statins in the management of atherosclerosis." J Am Coll Cardiol **35**(1): 1-10.

Vlashi, E., W. H. McBride, et al. (2009). "Radiation responses of cancer stem cells." J Cell Biochem **108**(2): 339-42.

Vogelstein, B. and K. W. Kinzler (2004). "Cancer genes and the pathways they control." Nat Med **10**(8): 789-99.

Wang, W., E. Collie-Duguid, et al. (2002). "Cerivastatin enhances the cytotoxicity of 5-fluorouracil on chemosensitive and resistant colorectal cancer cell lines." FEBS Lett **531**(3): 415-20.

Ward, J. F. (1994). "DNA damage as the cause of ionizing radiation-induced gene activation." Radiat Res **138**(1 Suppl): S85-8.

Weidner, N., J. P. Semple, et al. (1991). "Tumor angiogenesis and metastasis--correlation in invasive breast carcinoma." N Engl J Med **324**(1): 1-8.

Weinberg, R. A. (2007). The biology of cancer.

Wells, A. (1999). "EGF receptor." Int J Biochem Cell Biol **31**(6): 637-43.

Werner, M., J. Sacher, et al. (2004). "Mutual amplification of apoptosis by statin-induced mitochondrial stress and doxorubicin toxicity in human rhabdomyosarcoma cells." Br J Pharmacol **143**(6): 715-24.

Wollman, R., J. Yahalom, et al. (1994). "Effect of epidermal growth factor on the growth and radiation sensitivity of human breast cancer cells in vitro." Int J Radiat Oncol Biol Phys **30**(1): 91-8.

Wong, W. W., M. M. Tan, et al. (2001). "Cerivastatin triggers tumor-specific apoptosis with higher efficacy than lovastatin." Clin Cancer Res **7**(7): 2067-75.

Woodburn, J. R. (1999). "The epidermal growth factor receptor and its inhibition in cancer therapy." Pharmacol Ther **82**(2-3): 241-50.

Wu, H., H. Jiang, et al. (2009). "Effect of simvastatin on glioma cell proliferation, migration, and apoptosis." Neurosurgery **65**(6): 1087-96; discussion 1096-7.

Xu, Q. Y., Y. Gao, et al. (2008). "Identification of differential gene expression profiles of radioresistant lung cancer cell line established by fractionated ionizing radiation in vitro." Chin Med J (Engl) **121**(18): 1830-7.

Yamazaki, H., H. Kijima, et al. (1998). "Inhibition of tumor growth by ribozyme-mediated suppression of aberrant epidermal growth factor receptor gene expression." J Natl Cancer Inst **90**(8): 581-7.

Yarden, Y. and M. X. Sliwkowski (2001). "Untangling the ErbB signalling network." Nat Rev Mol Cell Biol **2**(2): 127-37.

Zhang, X., R. Komaki, et al. (2008). "Treatment of radioresistant stem-like esophageal cancer cells by an apoptotic gene-armed, telomerase-specific oncolytic adenovirus." Clin Cancer Res **14**(9): 2813-23.

Zhao, C., H. Yang, et al. (2011). "Distinct contributions of angiogenesis and vascular co-option during the initiation of primary microtumors and micrometastases." Carcinogenesis **32**(8): 1143-50.

PUBLICATIONS

NATIONAL DAY
YOUNG SCIENTISTS SESSION

ORAL COMMUNICATIONS

CLONAL SELECTION BY *IN VITRO* FRACTIONATED RADIATION IS A FEASIBLE PROCESS TO EXPLORE THE MECHANISMS INVOLVED IN TUMOR RECURRENCE AFTER RADIOTHERAPY

L.I. de Llobet[1], M. Baro[1], P. Muñoz [2], M.V. da Silva Diz[2], J. Balart[3]
[1]Laboratory of Translational Research-IDIBELL, Catalan Institute of Oncology, L'Hospitalet de Llobregat, Spain
[2]Cancer epigenetics and Biology Program-IDIBELL. Hospital Duran i Reynals, L'Hospitalet de Llobregat, Spain
[3]Department of Radiation Oncology, Hospital de la Santa Creu i Sant Pau, Barcelona, Spain
KEYWORDS: CLONAL SELECTION, RECURRENCE

Purpose: Daily standard doses (≈ 2 Gy) of fractionated radiotherapy kill, on average, 50% of carcinoma cells within a tumor during each round of radiation therapy. Surviving cells react to radiation by activating genetic and epigenetic programs to orchestrate an adaptive response. Thus, an enormous selective pressure operates on surviving cells through accumulative radiation. By the end of radiotherapy, cells may have been selected in a Darwinian-manner, conferring to the residual cancer cell population a real possibility of containing some cancer cells with proliferative advantages. Initial complete tumor regression followed by tumor rebound evidences that only a small number of cells may efficiently switch these programs on. The aim of our study was to derive a stable subset of cells through a process that mimics fractionated radiotherapy to further characterize recurrences.

Materials: A431-cultured cells were progressively treated with daily rounds of radiation starting with 0.74 Gy and ending with 3 Gy. As necessary cells were harvested and radiation stopped until 60-80 % confluence. A total dose of 85 Gy was administered over a 28-week period. Then, randomly selected single cells were left to grow as colonies, expanded and separately cryopreserved. To further characterize these cells clonogenic assay, western blot analysis and cell marker determination were performed.

Results: The process of clonal selection allows us to identify a cell population, which we named "S4", which showed a significantly increased resistance to radiation compared to A431 parental cells. While S4 cells showed a baseline cloning efficiency equivalent to A431 cells, they harbored a sustained ability to grow in huge colonies even after radiation. S4 cells displayed higher baseline and EGF-stimulated levels of the MAP kinase pERK1/2 compared with parental cells. This feature stood in stark contrast with the low levels of pAkt in S4 cells, both in baseline and EGF-stimulated conditions, indicating that different signal pathways could be favored during the selection process. We did not find differences in the expression of cancer stem cell markers CD44 and CD133 evaluated by immunofluorescence or flow cytometry techniques.

Conclusions: We conclude that clonal selection by *in vitro* fractionated radiation is a feasible process to obtain a differentiated cell population, which could be useful to explore the mechanisms involved in tumor recurrence after radiotherapy.

ESTRO

European Society for Therapeutic Radiology and Oncology

This is to certify that

LARA ISABEL DE LLOBET

is the winner of the Best Oral Communication Award during the **ALATRO, SEOR, SFRO, SPRO Young Scientists Meeting** that took place on 12 September 2010 at the ESTRO 29 Conference held in Barcelona, Spain with the abstract entitled:

CLONAL SELECTION BY IN VITRO FRACTIONATED RADIATION IS A FEASIBLE PROCESS TO EXPLORE THE MECHANISMS INVOLVED IN TUMOR RECURRENCE AFTER RADIOTHERAPY

This certificate entitles the holder to 500€ to use towards a registration to an ESTRO course of their choice. This certificate is valid for two years from the date of issue (Sunday, 12 September 2010).

SEOR President, **Ferran Guedea**
SFRO President, **Eric Lartigau**
SPRO President, **Lurdes Trigo**
ALATRO President, **Cuathemoc de la Peña**

Clin Transl Oncol (2013) 15:189–197
DOI 10.1007/s12094-012-0898-8

RESEARCH ARTICLE

Development and characterization of an isogenic cell line with a radioresistant phenotype

Lara I. de Llobet · Marta Baro · Agnès Figueras · Ignasi Modolell · Maria V. Da Silva · Purificación Muñoz · Arturo Navarro · Ricard Mesia · Josep Balart

Received: 25 January 2012 / Accepted: 22 May 2012 / Published online: 24 July 2012

Abstract
Introduction Radiation resistance is a major cause of death in cancer patients. Cancer cells react during radiotherapy by re-programming specific cell functions that may confer resistance to radiation. The understanding of this complex process is hindered due to the lack of appropriate study models. We describe an experimental development of a radioresistant isogenic cancer cell line, and its molecular characterization.

Materials and methods A431-cultured cells were irradiated for 7 month until 85 Gy. Then, a selected single cell was left to grow as stable A431-R cell line. Clonogenic assay was used to determine cell survival, the α and β parameters of the LQ model, and the mean inactivation dose. The DNA repair ability of cells was evaluated by pulsed-field electrophoresis method. Differential effect of fractionated radiation was ultimately tested in xenografts. Furthermore, we used a wound healing assay, Western blot for EGFR, AKT and ERK1/2 and ELISA test for vascular endothelial growth factor (VEGF) secretion. Finally we explored CD44 marker and cell cycle distribution.
Results The established A431-R cell line showed radiation resistance in clonogenic assays, repair of radiation-induced DNA fragmentation and xenografted tumours. The radiation resistance was associated with in vitro higher cell growth and migration, increased levels of former oncoproteins, and secretion of VEGF.
Conclusions In this model, the emergence of radiation resistance was associated with the acquisition of biological traits that support more aggressive behaviour of cancer cells. We have generated a model that will be useful for mechanistic studies and development of rational treatments against radiation resistance in cancer.

Keywords Development of isogenic cell line model · Emergence of radiation resistance · Aggressive phenotype

L. I. de Llobet · M. Baro · A. Figueras · J. Balart (✉)
Translational Research Laboratory, Catalan Institute of Oncology – IDIBELL, Avda Gran Via de l'Hospitalet, 199-203, 08907 L'Hospitalet de Llobregat, Spain
e-mail: jbalart@iconcologia.net; jbalart@santpau.cat

I. Modolell
Department of Radiophysics and Radioprotection, Catalan Institute of Oncology – IDIBELL, L'Hospitalet de Llobregat, Spain

M. V. Da Silva · P. Muñoz
Cancer Biology and Epigenetics Laboratory, IDIBELL, L'Hospitalet de Llobregat, Spain

A. Navarro
Department of Radiation Oncology, Catalan Institute of Oncology – IDIBELL, L'Hospitalet de Llobregat, Spain

R. Mesia
Department of Medical Oncology, Catalan Institute of Oncology – IDIBELL, L'Hospitalet de Llobregat, Spain

Present Address:
J. Balart
Department of Radiation Oncology, Hospital de la Santa Creu i Sant Pau, C/Sant Antoni M[a] Claret, 167, 08025 Barcelona, Spain

Introduction

In the modern era of radiation oncology, curative potential of radiotherapy has significantly increased due to new techniques in imaging diagnosis and radiation delivery. However, locoregional relapses post-radiotherapy treatments are

still a major cause of death in cancer patients. One explanation for local recurrences is the acquisition by a small proportion of cancer cells of a radioresistant pattern [1–6]. Furthermore, the cells exposed to ionizing radiation may develop adaptive molecular mechanisms to become resistant to radiotherapy [7, 8]. The primary resistance and the acquisition of effective mechanisms of resistance, together with the biological pressure of genotoxic effects of radiation, push irradiated cells through a selective process in which the most resistant genotypes will be selected in a Darwinian manner. In the end, it may enable specific genetic, as well as epigenetic programs that will confer cytoprotective properties in the cells that survive. Several observations suggest that tumour adaptation to radiotherapy induces the emergence of radiation resistance and higher malignant phenotypes that can ultimately determine the clinical outcome of recurrences after radiotherapy [9–11].

The study of the mechanisms involved in the acquisition of an aggressive resistant phenotype is complex. In part, the difficulties are due to the lack of appropriate models in which the emergence of resistance can be directly attributed to specific changes that happen during radiotherapy. In the present report, we describe the process of generating an isogenic cancer cell line that has a decreased response to radiotherapy. Furthermore, relevant novel properties of the biology of this resistant cell line are discussed.

Materials and methods

Cancer cell lines

The human epidermoid carcinoma cell line A431 from the American Type Cell Collection (LGC Promochem, Barcelona, Spain) was used in this study. Cells were maintained as a monolayer under standard cell culture conditions. We denominated them as A431-WT cells in our study. Cells growing in 100-mm plastic dishes were irradiated at room temperature (RT) using 6-MV X-rays at dose rate of 2.7 Gy/min. Cultures were progressively treated with daily rounds of radiation over a 7-month period of time, starting with 0.75 Gy/fraction and ending with 3 Gy/fraction. Irradiation was stopped, as necessary, in order to allow for cell monolayer recovery. The procedure was continued until a total of 85 Gy had been delivered. Next, single cell suspension (1,000 cells per 60-mm dishes) were plated and allowed to grow as macroscopic colonies. We next grew the cells from the colony that showed the most vigorous growth to the confluence and expanded them while the remainder of the cells was not further characterized. These selected cells were used for the present study and were denominated as A431-R and were compared to the parental A431-WT from which they were derived.

Estimation of radiosensitivity and LQ model

To determine the radiation sensitivity of the cells, clonogenic assays were performed. Briefly, cells were planted in 60-mm dishes 24 h before receiving irradiation in single doses of 0, 2, 4, 6 or 8 Gy. Cells were allowed to proliferate for 14 days and then stained with crystal violet. The respective surviving fractions (SF) were calculated as the ratio between the number of colonies following irradiation and the number of cells plated, which were then normalized by the clonogenic efficiency of non-irradiated cells. To estimate the α and β parameters of the LQ model, we used the least square regression method of the function $Y = -(\alpha D + \beta D^2)$ from the natural logarithm of surviving fractions. We evaluated differential radiosensitivity by means of the surviving fraction after 2 Gy (SF2), LQ model, and mean inactivation dose (D) between 0 and 8 Gy as described by Tucker [12].

Pulsed-field gel electrophoresis

Cell cultures were irradiated with 45 Gy, and then cells were mixed with 1 % agarose at 0, 1, 2, 4, 8 or 24 h after irradiation to form cell plugs. Cell plugs were lysed and loaded into a gel to determine residual—post-repair—radiation-induced DNA fragments using pulsed-field electrophoresis method (PFGE), as we described previously [13].

Tumour xenografts

To generate tumour xenografts, 10^6 A431-WT or 10^6 A431-R cells suspended in 100 μL of medium were injected into subcutaneous tissues on the right thigh of athymic mice. Previously, cultures were trypsinized, cells counted and properly diluted in growth medium for injection and kept on ice. Tumour growth was measured twice weekly until tumours reached 1,500 mm^3 in size. Tumour size was calculated using the formula: $\pi/6 \times$ (large diameter) $\times$ (small diameter)^2. Animal models used in this study were approved by the institutional animal care and ethics committee and in accordance with its guidelines. Six- to eight-week-old female athymic Swiss nu/nu mice were purchased from Harlan (Gannat, France) and were housed under pathogen-free conditions at our facilities (AAALAC accreditation number 1,155).

Irradiation of xenoimplanted tumours

To irradiate the tumours ($n = 5$ for A431-WT and 5 for A431-R), we used a 6-MV photon beam from a Varian Clinac 2100 linear accelerator delivering 10 fractions of 3 Gy each in 2 weeks, starting on Monday and ending on Friday. This dose of 30 Gy was delivered at 2.7 Gy/min at

the isocenter of the beam. Appropriated bolus was provided for electronic equilibrium at the entrance and the exit of beam. Radiotherapy was limited to the right thigh. In vivo dosimetry was performed by means of radiochromic films which showed less than 3 % variation in the prescribed dose. Prior to tumour irradiation, the mice were anaesthetized by an intraperitoneal injection (1 mL/kg of each solution: 50 mg/mL ketamine and 1 mg/mL medetomidine). Upon completion, 5 mg/mL atipamezole was delivered to reverse the effects of the anaesthesia [14]. A complete mock process was performed on non-irradiated mice that served as experimental controls ($n = 5$ for A431-WT and 5 for A431-R).

Wound healing assay

A431-WT and A431-R cells were seeded in 6 cm diameter plates and cultured until confluent. After 12 h of culture in foetal bovine serum (FBS)-free medium, the petri dishes were scratched with a 200 μL pipette tip to imitate a wound. After several washing and removal of floating cells, the distances between cell margins were measured at 0, 1, 2, 3, 6 and 24 h using specialized software (Leica, Wetzar, Germany). Three independent assays, done in duplicate, were conducted.

Immunoblotting

We performed a standard Western blot method to determine levels of specific proteins. Cultures were maintained without FBS for 24 h before treatment with radiation or epidermal growth factor (EGF) ligand (Sigma-Aldrich, St. Louis, MO, USA). Following treatment, equal amounts of protein (30 μg) were separated by SDS-PAGE and blotted onto nitrocellulose membranes, which were incubated with a rabbit anti-phosphorylated (Tyr992) EGFR antibody (EGFR pY992) (Sigma-Aldrich) at a 1:1,000 dilution; mouse anti-phosphorylated (Thr183 and Tyr185) MAP kinase ERK1/2 monoclonal antibody (pERK1/2) (Sigma-Aldrich) at a 1:5,000 dilution, and a rabbit anti-phosphorylated (Ser473) AKT polyclonal antibody (Cell Signaling, Danvers, MA, USA) at a 1:500 dilution in blocking solution overnight at 4 °C, as previously described [11]. Optical densitometry quantification of the Western blot protein levels was performed using Quantity One Software (Bio-Rad Laboratories, Hercules, CA, USA), then the results were represented on a histogram.

Levels of VEGF secretion

To measure the levels of vascular endothelial growth factor (VEGF) secretion, cells were plated in 6-mm dishes (1×10^6 cells per dish) and allowed to grow in a complete medium for 24 h. Next, cultures were rinsed twice with PBS buffer and incubated in FBS-free medium for 24 h. The cells were then irradiated with a single 8 Gy dose. Supernatants were collected at 0, 24 and 48 h. VEGF was determined in the supernatants by means of an enzyme-linked immunoabsorbent assay ELISA (R&D Systems Inc, Minneapolis, MN, USA) as described by Pueyo et al. [11].

CD44 determination

The cell surface marker, CD44, was determined by a standard IF process. Sterilized cover slips were put into 60-mm petri dishes, and then A431-WT or A431-R cells were seeded and cultured in full medium. After 48 h, the cells were fixed with 4 % neutral buffered formaldehyde, washed (0.1 % triton in PBS for 10 min) and incubated for 1 h with a protein-blocking solution (20 % serum goat and 20 % serum horse in 1X PBS). Next, the slides were incubated with a mouse anti-CD44 (156-3C11) monoclonal antibody (Cell Signaling) at 1:100 dilution overnight at 4 °C. To detect primary antibody, cover slips were incubated with Alexa Fluor 488-conjugated goat anti-mouse secondary antibody (Invitrogen, Carlsbad, CA, USA) at a 1:1,000 dilution for 1 h at RT. Counterstaining and fluorescence images were produced using a previously described method [13]. Additionally, CD44 detection was measured by flow cytometry using anti CD44-APC (1:12.5; BD Biosciences Pharmingen, San Diego, CA, USA) antibody in 100 μL PBS 0.5 % BSA and 2 mM EDTA. After incubation for 30 min at 4 °C, cells were washed with 0.5 % BSA 2 mM EDTA, and then the cells were re-suspended in 300 μL PBS, 2 % FBS and 2 mM EDTA. Flow cytometry quantification of CD44 positive cells was performed with a BD FACSaria III cell sorter and BD FACSDiva software (BD Biosciences Pharmingen).

Cell cycle analysis

A standard iodine propidium staining method was used to assess the cell cycle phase distribution of A431-WT and A431-R cells. Flow cytometry analysis was performed with a BD FACSCalibur cell sorter, and BD Cellquest Pro plus (BD Biosciences Pharmingen) and ModFit LT3.2 (Verity Software House, Topsham, ME, USA) softwares.

Statistics

Results were expressed as mean ± standard error (SE). Statistically significant differences in-between-group comparisons were defined using a two-tailed significance level of $p < 0.05$. The Statistical Package for Social Sciences, version 13.0 (IBM, Madrid, Spain) was used for data analysis.

Results

Fractionated irradiation and clonal selection induced radiation resistance in the A431 cell line

Radiosensitivity was significantly decreased in the new A431-R cell line. The initial shape of survival curve for A431-R cells showed a higher shoulder than parental A431-WT cells (Fig. 1a), and the mean SF2 value rose from 0.62 to 0.75 ($p = 0.024$). The potential effect of successive fractions of 2 Gy is illustrated in Fig. 1a, where the effect of a single dose of 2 Gy is repeated 4 times, assuming that no additional repair took place between fractions in either type of cells. To further evaluate variations in radiosensitivity, the α/β ratio of LQ model and the mean inactivation dose were calculated from the surviving fractions after single doses of 0, 2, 4, 6 or 8 Gy. The α/β ratio was reduced from 12 Gy for parental cells to 4.6 Gy for the resistant cells, at the expense of decreasing α-component and increasing β-component, indicating a higher ability to repair sub-lethal damage in the A431-R cells, and thus, having increased resistance to radiotherapy (Fig. 1b). The mean inactivation dose was also increased from 3 to 3.5 Gy in A431 cells.

In light of these results, and, because DNA repair is a crucial determinant of radiosensitivity, we decided to determine whether A431-R cells acquired an increased ability to repair DNA. In A431-R cells, we found a significant diminution of residual DNA fragments, measured by PFGE, indicating that in these cells the rejoining of radiation-induced DNA fragments was more efficient than A431-WT cells (Fig. 2). This functional finding provides further support to radiation resistance in A431-R cells.

Finally, to validate the in vitro findings and definitively establish relative radiation resistance in A431-R cells, we evaluated the effect of fractionated radiotherapy on the growth of xenografted tumours. Seven days after cell injection all animals exhibited tumour growth in the subcutaneous tissues of the right thigh. The average tumour size ($n = 20$) was of 51.30 ± 8.8 (in mm^3) for A431-WT cells and 30.73 ± 7.4 for A431-R cells ($p = 0.11$). At this point in time—just before radiotherapy—no significant differences were found in the size of tumours irrespectively of the treatment (non-irradiated vs. irradiated) or origin of the cells (parental vs. resistant).

Without irradiation, tumours exponentially grew as a function of time showing a similar pattern for both types of cells. At day 21, the parental tumours measured 1,120 ± 151.4 and those from resistant cells 1,092 ± 250.5. In contrast, the size of the tumours that received radiation was significantly decreased to 226.4 ± 43.6 and to 401.6 ± 53.4, respectively. This observation indicates that tumour growth was inhibited by radiation in both types of cells.

Importantly, at the ending of radiotherapy the size of resistant tumours was 1.8 (401.6/226.4) times larger than that of tumours from parental cells. This difference was maintained or increased during the follow-up, which was calculated to show statistical significance (Fig. 3). Greater growth delay and slower re-growth were observed in the parental tumours compared to tumours derived from resistant cells, although the differences in these cases did not reach a p value below 0.05 (see Fig. 3 for explanations). These results indicate that tumours derived from A431-R cells were less affected by radiation, allowing the cells to proliferate, and together with the earlier in vitro findings, there is a strong suggestion that these cells are effectively radiation resistant.

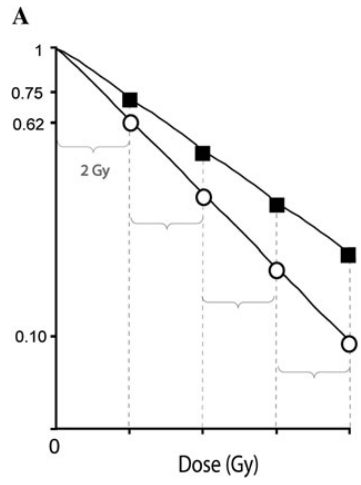

B

	A431-WT	A431-R	
Radiosensitivity			P-value*
SF2	0.62 ± 0.034	0.75 ± 0.036	0.024
α-component	0.24 ± 0.03(Gy^{-1})	0.14 ± 0.02 (Gy^{-1})	0.024
ß-component	0.02 ± 0.005(Gy^{-2})	0.03 ± 0.003(Gy^{-2})	0.490
D	3.00 ± 0.14 (Gy)	3.50 ± 0.10 (Gy)	0.015
α/ß ratio	12 (Gy)	4.6 (Gy)	

Abbreviations: SF2=Surviving Fraction after 2Gy; α- and ß-components=coefficients of the linear-quadratic equation; D=mean inactivation dose calculated as the area under clonogenic cell survival curve between 0 and 8 Gy; α/ß ratio=the dose at which cell killing participation is the same for non-reparable single hit killing and cell death due to sublethal lesion saturation.

Fig. 1 The radiosensitivity of A431-R cells was lower than A431-WT. **a** Representation of cell response to radiation after four separated doses of 2 Gy each for A431-WT cells (*circles*) and A431-R cells (*squares*). **b** Radiosensitivity of A431-WT versus A431-R cell lines. *Values* indicate the mean of nine experiments done in triplicate, and *bars* show the standard error (*$p < 0.05$; Mann–Whitney test)

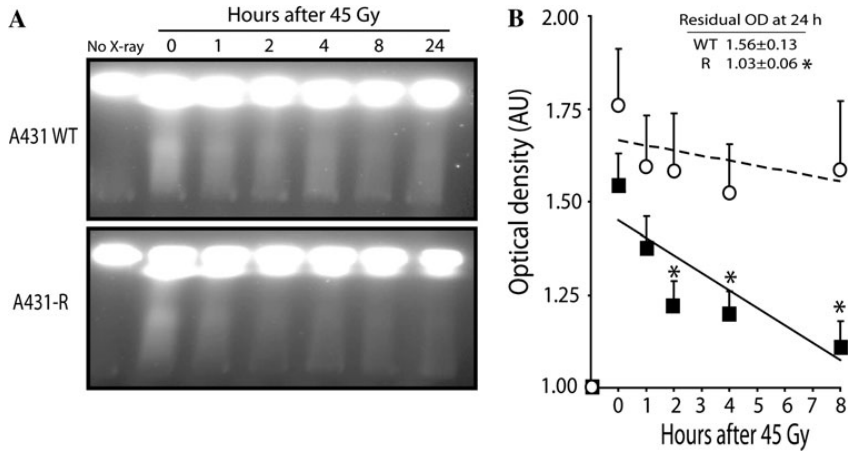

Fig. 2 The ability of rejoining radiation-induced DNA fragments was higher in A431-R cells. **a** Representative pictures from PFGE showing different degrees of DNA breakage as smears of variable intensity. To permit DNA repair, cells were cultured as adherent monolayer for 0, 1, 2, 4, 8 or 24 h after irradiation (45 Gy). **b** Rejoining was normalized to untreated cells. A431-WT cells (*circles*) versus A431-R cells (*squares*). AU stands for arbitrary units. *Values* indicate the mean of three independent experiments and *bars* show the standard error (*$p < 0.05$; Mann–Whitney test)

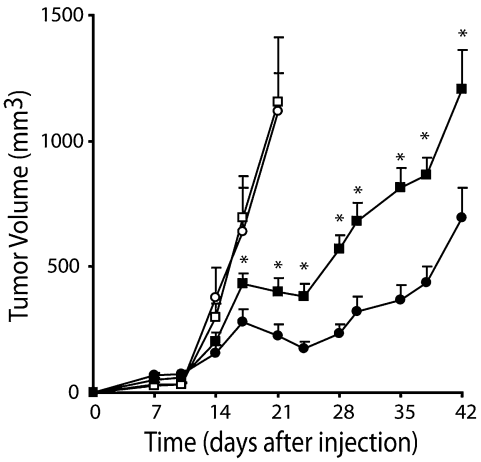

Characteristics of the growth of the tumours in mice treated with radiotherapy

	A431-WT	A431-R	P – value*
Size of tumours at the beginning of radiotherapy, at day 7 (in mm^3)	68.8 ± 10.3	50.2 ± 7.5	0.151
Size of tumours at the end of radiotherapy, at day 21 (in mm^3)	226.4 ± 43.8	401.6 ± 53.4	0.032
Growth delay(1) (in days)	7.1 ± 2.5	2.4 ± 1.5	0.222
Growth rate during the tumour re-growth(2) (in mm^3/day)	34.6 ± 6.1	45.1 ± 3.7	0.347

Explanations: (1) Growth delay was measured as time it took for tumours to reach the size they had at the end of radiotherapy.
(2) Growth rate was calculated by the least square regression method using raw data from the smallest tumour size after beginning radiotherapy to the end of follow- up (rang e 21 to 42 days after cell injection). Values are the mean± SE of 5 tumours per cellular type.

Fig. 3 The effect of radiation therapy was lower in xenografts derived from A431-R cells. Tumour growths corresponding to A431-WT cells (*circles*) and A431-R cells (*squares*) are shown for non-irradiated (*unshaded*) and irradiated tumours (*solid symbols*). 30 Gy in 2 weeks, 5 fractions of 3 Gy/week, was administered using 6 MV X-rays, from day 7 to day 21. In the growth curves, *symbols* indicate the mean of five tumours and bars show the standard error (*$p < 0.05$ compared to parental tumours; Mann–Whitney test)

Changes involved in the radioresistant phenotype of A431-R cell line

Since we observed that A431-R cells were less radiosensitive than A431-WT cells, we decided to further characterize the phenotype of these resistant cells. The baseline clonogenic efficiency of the A431-R cells was 0.19 ± 0.01 compared to 0.12 ± 0.02 of parental wild type cells (A431-WT) ($p < 0.05$; Mann–Whitney test), indicating that A431-R cells had slightly greater capacity of surviving as single cells. In addition to an increased ability to anchorage and succeed as a cell culture, the A431-R cells formed colonies of remarkable size—most of them with a lower staining, which suggested an increase in the cytoplasm rather than a greater number of cells—, as depicted in Fig. 4a, which together with clonogenic efficiency, suggested that theses cells could be potentially more aggressive than were earlier. To further explore the emergence of cellular traits that enable cells to exhibit malignant type of behaviour, we decided to determine the ability

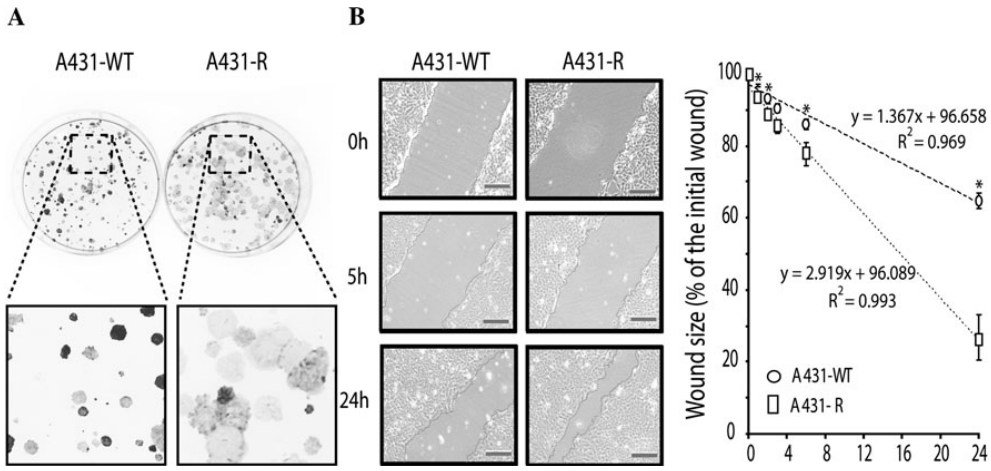

Fig. 4 In vitro, A431-R cells showed a higher growth and faster migration than the parental cells. **a** Illustrative photographs of the colonies. The *zoom* shows the size of colonies and the intensity of the staining in detail. **b** Representative microphotographs of the wound healing assay at time-points 0, 5 and 24 h (*bars* 200 μm). Distance shortening in the wound healing was normalized to the initial distance between borders of each respective wound, and was represented as the percentage of the initial wound size. *Values* indicate the mean of three independent experiments done in duplicate and *bars* show the standard error (*$p < 0.05$; Mann–Whitney test)

of migration of these A431-R cells. Experimental findings with the conventional wound healing assay confirmed that A431-R cells had acquired kinetic powers during selection process that allow them to migrate and heal the wound in a shorter period of time than the parental cells, a behaviour clearly consistent with the acquisition of an aggressive phenotype (Fig. 4b).

Due to the presence of cellular traits that are linked to sustained proliferative cell signalling, and, because, A431 parental cells overexpress the receptor of EGF, a major cell signal emitter, we looked into this cellular pathway to unravel possible changes that may be involved during the development of A431-R cell line. The most remarkable finding was that A431-R cells presented higher baseline levels of phosphorylated EGF receptor, and the AKT and ERK1/2 transducers (Fig. 5a), linchpin proteins that are involved in cell growth, mitogenesis, survival, DNA repair ability, and cell migration [15]. After cell stimulation by the presence of EGF ligand, both types of cell lines reacted by increasing levels of former oncoproteins, prominently pERK1/2. When A431-WT cells were treated with ionizing radiation, they reacted by increasing the levels of phosphorylated ERK1/2 proteins, a response that was seen irrespectively of EGF presence. However, in the A431-R cells, irradiation was not followed by a rise in the phosphorylated levels of EGFR, AKT or ERK1/2. In fact, a diminution relative to their baseline levels was observed, especially with respect to EGFR. We speculated whether A431-R cells did not need to further activate these oncoproteins which were already hyperactivated at the baseline conditions (Fig 5a).

To further evaluate distinct aspects of the radioresistant phenotype, we assessed the levels of VEGF, a crucial factor in tumour-associated angiogenesis and efficient tumour blood supply, secretion of which may also be regulated by EGFR and ionizing radiation [11, 16]. Both types of cells respond to radiation by increasing the secretion of VEGF (Fig. 5b). However, as suspected, the release of VEGF in response to radiation was more efficiently in the A431-R cells. Thus, we concluded that these cells were better adapted to resist strenuous conditions, such as the oxidative stress induced by radiotherapy, and able to promote angiogenesis to facilitate their oncogenic potential.

Recently, the cell surface antigen CD44, a putative stem cell marker, has been functionally validated as a biomarker to predict local control for early laryngeal cancer treated with radiotherapy, which suggests that this antigen could be a proper surrogate indicator for radioresistant phenotypes [17]. Nevertheless, we did not find differential expression of CD44 antigen in the two A431 cell lines (Fig. 6). Thus, this infers that this protein was constitutively expressed in the parental and, hence, its derived resistant cell line, irrespectively of their grade of radiation sensitivity.

Finally, because cell cycle distribution can influence in radiation sensitivity, the distribution of cell cycle phases was examined. We found that G1 phase was 63.1 versus 67.9 %, S phase was 28.3 versus 19.8 % and G2/M phase was 8.5 versus 12.1 %, for A431-WT and A431-R cell population, respectively, suggesting a non-relevant variation in cell cycle between cell types.

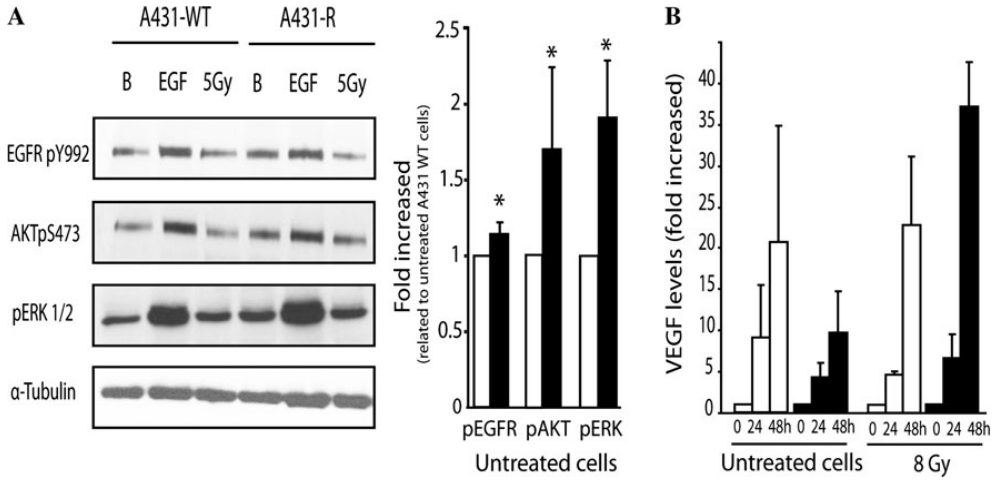

Fig. 5 A431-R sustained proliferative signalling through high levels of phosphorylated EGFR, AKT and ERK1/2 proteins and radiation-induced secretion of VEGF. **a** Proteins were determined by Western blot in cells under baseline culture conditions (B), EGF stimulation (E) or ionizing radiation (5 Gy). Before cell lysis, cells were treated with 10 ng/mL EGF for 10 min or 6 MV X-rays. α-Tubulin was used as internal control. *Bar chart* shows specific protein levels normalized by untreated A431-WT cells (*white bars*) versus A431-R cells (*black bars*). *Values* indicate the mean of three independent experiments and *bars* show the standard error ($*p < 0.05$; Mann–Whitney test). **b** VEGF was determined by the ELISA method at different interval times after 8 Gy. Cells were left to grow without FBS for 24 h before collecting supernatants at time 0, 24 and 48 h in A431-WT (*white bars*) and A431-R cells (*black bars*). VEGF values were normalized to the cell numbers per dish. Data were obtained from two independent experiments

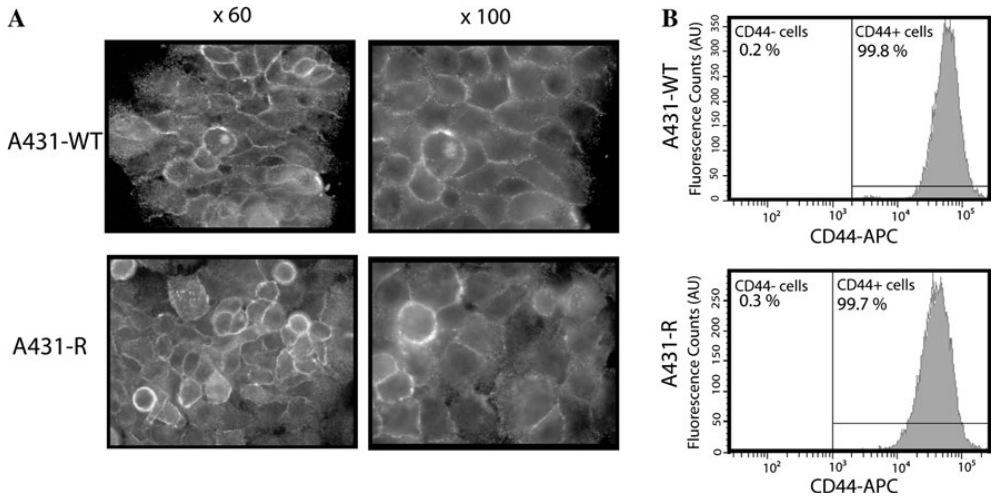

Fig. 6 CD44 antigen expression of A431-WT and A431-R cells remained unchanged. **a** Illustrative immunofluorescence microphotographs of the surface marker CD44 under baseline culture conditions. **b** Flow cytometry detection of CD44 marker. The *x* axis shows negative and positive gates for CD44 marker in both types of cells, while the *y* axis shows the number of events. AU stands for arbitrary units

Discussion

In this study, we demonstrated that, by subjecting culture cells to fractionated radiation and clonal selection, we were able to obtain a modified cohort of cells. The ultimate aim of this study was to develop an isogenic resistant cell line which could be used to identify molecular changes associated with acquired resistance to radiation and tumour aggressiveness in cancer. The identification and understanding such mechanisms is of valuable interest, not only

in overcoming radiation resistance, but also, underpinning the biology of recurrent cancer after radiotherapy. Hence, based on this knowledge, specific therapies for cancer could be devised. In this regard, our study showed that, indeed, using this model, relevant mechanisms associated with resistance to radiation were activated. We observed greater DNA repair, in vitro growth, cell migration, and oncoprotein levels, mechanisms that may provide potential targets to improve the efficacy of radiotherapy.

We developed the stable isogenic resistant A431-R cell line from parental A431 cells. The diminution of radiosensitivity in A431-R cells was found to be comparable to other published studies. Similar decreases in SF2 and α-component of LQ model were reported in radioresistant isogenic cells derived from OE33 esophagal adenocarcinoma cells. These changes were associated with an increased efficiency in DNA repair [18]. Equivalent levels of acquired tolerance to radiation were also found in the resistant version of the human lung adenocarcinoma cell line, Anip973 [19]. In these already published studies, as well as our own, radioresistant cells showed moderate levels of radiation desensitization. However, it should be taken into account that in fractionated radiotherapy a small variation in radiosensitivity could have a greater effect on the ultimate resistance than the simple difference in SF2, as shown in Fig. 2.

Besides radiation resistance, we demonstrated that A431-R cells acquired higher cloning efficiency and in vitro faster growth and migration ability; these properties were observed to be associated with remarkable baseline levels of relevant oncoproteins and elevated angiogenic capabilities. Earlier, our group described that radiation was found to induce the emergence of aggressive tumour growth in A431 cells. We identified that the addiction to EGFR was associated with this malignant phenotype and tumour-associated angiogenesis [11]. Recently, similar phenotype was elicited by radiation-induced cell signalling involving the protein encoded by *c-Met* [9]. These findings strongly suggest that cancer cells may develop adaptive responses to damaging agents, such as ionizing radiation, leading to the gain of molecular mechanisms to protect themselves from the lethal effects of these agents. Cellular stress regulates distinct genetic and epigenetic programs that may determine the acquisition of tolerance to radiation and the biology of cancer cells, as consequence, re-programming their cellular machinery. This notion is supported by new discoveries in radiation resistance. Also, the acquisition of resistance to radiation was found to be associated with increased levels of reduced state of glutathione, pointing at a better expression of genes encoding enzymes that maintain glutathione operative [18]. Similar meaning would be ascribed to the low levels of intracellular-free radical observed in isogenic resistant human non-small cell lung cancer cells [20]. In these adjustments, glutathione levels may be a reflection of re-programming energy metabolism in cancer cells leading to higher utilization of glucose and enhancing NADPH production, ready to be used in glutathione synthesis [21]. The participation of oncogenic proteins such as AKT (through mTOR), RAS or HIF1α in glycolytic fuelling as a response to oxidative stress [22, 23] gives additional support to the notion that global changes are induced by radiation, and goes beyond the idea of an isolated phenomenon of resistance.

Radiation-induced resistant cells have also revealed changes attributed to radiation in transciptome. Upregulation or downregulation of genes encoding proteins that are involved in DNA repair and anti-apoptosis, as well as in motility, invasion and angiogenesis have been reported. However, the representation of the genes involved in resistance varies, depending on the authors [19, 20, 24]. Variations in the genetic origin of cells, methods used to generate the experimental model and the technical differences to analyse gene expression may all have influenced the diversity of findings. Experimental design based on isogenic cells, such as the A431-WT and A431-R pair, could make it more suitable to directly attribute changes in gene regulation to ionizing radiation because isogenic cells have the same genetic background. However, it should be mentioned that the findings using cultured cells growing on plastic culture dishes are not influenced by factors such as tumour hypoxia, microenvironment (including tumour-stroma heterotypic interaction) and angiogenesis that occur in true oncogenesis. In this regard, these factors could have contributed to the observation that the growth of non-irradiated tumours that were derived from A431-WT cells showed similar pattern of growth as those tumours from A431-R cells, a finding that was not observed in vitro. To improve in vitro limitations, further efforts are needed to characterize in vivo experimental tumour models.

In conclusion, in this article we have presented an effective method to develop a radioresistant cell line, and showed that the emergence of tolerance to radiation was associated with the acquisition of an aggressive phenotype. In our opinion, this methodology may provide useful experimental models in order to gain insights into the biology of acquired radiation resistance.

Acknowledgments The authors would like to acknowledge the financial support of the Spanish Association against Cancer, Barcelona Committee, and the Merck KGaA company. We are grateful to Scientific Services of the University of Barcelona for cytometry assistance in cell cycle evaluation, and Jo Ellen Klaustermeier for her excellent assistance with the manuscript elaboration.

Conflict of interest None.

References

1. Bartkova J, Horejsi Z, Koed K et al (2005) DNA damage response as a candidate anti-cancer barrier in early human tumorigenesis. Nature 434:864–870
2. Abbott A (2006) Cancer: the root of the problem. Nature 442:742–743
3. Phillips TM, McBride WH, Pajonk F (2006) The response of CD24(-/low)/CD44+ breast cancer-initiating cells to radiation. J Natl Cancer Inst 98:1777–1785
4. Keith B, Simon MC (2007) Hypoxia-inducible factors, stem cells, and cancer. Cell 129:465–472
5. Rich JN (2007) Cancer stem cells in radiation resistance. Cancer Res 67:8980–8984
6. Comen E, Norton L, Massague J (2011) Clinical implications of cancer self-seeding. Nat Rev 8:369–377
7. Dittmann K, Mayer C, Fehrenbacher B et al (2005) Radiation-induced epidermal growth factor receptor nuclear import is linked to activation of DNA-dependent protein kinase. J Biol Chem 280:31182–31189
8. Toulany M, Schickfluss TA, Fattah KR et al (2011) Function of erbB receptors and DNA-PKcs on phosphorylation of cytoplasmic and nuclear Akt at S473 induced by erbB1 ligand and ionizing radiation. Radiother Oncol 101:140–146
9. De Bacco F, Luraghi P, Medico E et al (2011) Induction of MET by ionizing radiation and its role in radioresistance and invasive growth of cancer. J Natl Cancer Inst 103:645–661
10. Park CM, Park MJ, Kwak HJ et al (2006) Ionizing radiation enhances matrix metalloproteinase-2 secretion and invasion of glioma cells through Src/epidermal growth factor receptor-mediated p38/Akt and phosphatidylinositol 3-kinase/Akt signaling pathways. Cancer Res 66:8511–8519
11. Pueyo G, Mesia R, Figueras A et al (2010) Cetuximab may inhibit tumor growth and angiogenesis induced by ionizing radiation: a preclinical rationale for maintenance treatment after radiotherapy. Oncologist 15:976–986
12. Tucker SL (1986) Is the mean inactivation dose a good measure of cell radiosensitivity? Radiat Res 105:18–26
13. Balart J, Pueyo G, de Llobet LI et al (2011) The use of caspase inhibitors in pulsed-field gel electrophoresis may improve the estimation of radiation-induced DNA repair and apoptosis. Radiat Oncol 6:6
14. Baro M, de Llobet LI, Modolell I et al (2012) Development and refinement of a technique using medical radiation therapy facility to irradiate immunodeficient mice bearing xenografted human tumours. Lab Anim. doi:10.1258/la.2012.011147
15. Liang K, Ang KK, Milas L et al (2003) The epidermal growth factor receptor mediates radioresistance. Int J Radiat Oncol Biol Phys 57:246–254
16. Gorski DH, Beckett MA, Jaskowiak NT et al (1999) Blockage of the vascular endothelial growth factor stress response increases the antitumor effects of ionizing radiation. Cancer Res 59:3374–3378
17. de Jong MC, Pramana J, van der Wal JE et al (2010) CD44 expression predicts local recurrence after radiotherapy in larynx cancer. Clin Cancer Res 16:5329–5338
18. Lynam-Lennon N, Reynolds JV, Pidgeon GP et al (2010) Alterations in DNA repair efficiency are involved in the radioresistance of esophageal adenocarcinoma. Radiat Res 174:703–711
19. Xu QY, Gao Y, Liu Y et al (2008) Identification of differential gene expression profiles of radioresistant lung cancer cell line established by fractionated ionizing radiation in vitro. Chin Med J (Engl) 121:1830–1837
20. Lee YS, Oh JH, Yoon S et al (2010) Differential gene expression profiles of radioresistant non-small-cell lung cancer cell lines established by fractionated irradiation: tumor protein p53-inducible protein 3 confers sensitivity to ionizing radiation. Int J Radiat Oncol Biol Phys 77:858–866
21. Pena-Rico MA, Calvo-Vidal MN, Villalonga-Planells R et al (2011) TP53 induced glycolysis and apoptosis regulator (TIGAR) knockdown results in radiosensitization of glioma cells. Radiother Oncol 101:132–139
22. DeBerardinis RJ, Lum JJ, Hatzivassiliou G et al (2008) The biology of cancer: metabolic reprogramming fuels cell growth and proliferation. Cell Metab 7:11–20
23. Semenza GL (2010) Defining the role of hypoxia-inducible factor 1 in cancer biology and therapeutics. Oncogene 29:625–634
24. Fukuda K, Sakakura C, Miyagawa K et al (2004) Differential gene expression profiles of radioresistant oesophageal cancer cell lines established by continuous fractionated irradiation. Br J Cancer 91:1543–1550

Published online on 21 June 2012 Lab Anim, doi: 10.1258/la.2012.011147

Short Report

Development and refinement of a technique using a medical radiation therapy facility to irradiate immunodeficient mice bearing xenografted human tumours

Marta Baro[1*], Lara I de Llobet[1*], Ignasi Modolell[2], Ferran Guedea[3], Joana Visa[4] and Josep Balart[1,5]

[1]Translational Research Laboratory, Catalan Institute of Oncology and IDIBELL, Avinguda Gran Via de l'Hospitalet, 199-203, 08907 l'Hospitalet de Llobregat, Spain; [2]Medical Physics and Radioprotection Department, Catalan Institute of Oncology and IDIBELL, Avinguda Gran Via de l'Hospitalet, 199-203, 08907 l'Hospitalet de Llobregat, Spain; [3]Radiation Oncology Department, Catalan Institute of Oncology and IDIBELL, Avinguda Gran Via de l'Hospitalet, 199-203, 08907 l'Hospitalet de Llobregat, Spain; [4]Animal Facility, IDIBELL, Avinguda Gran Via de l'Hospitalet, 199-203, 08907 l'Hospitalet de Llobregat, Spain; [5]Radiation Oncology Department, Hospital de la Santa Creu i Sant Pau, Sant Antoni M Claret, 167, 08025 Barcelona, Spain

Corresponding author: J Balart. Laboratori de Recerca Translacional, Institut Català d'Oncologia-IDIBELL, Avinguda Gran Via de l'Hospitalet, 199-203, 08907 l'Hospitalet de Llobregat, Spain. Email: jbalart@iconcologia.net

Abstract

The need for using immunodeficient mice for xenoimplantation of tumours is increasing in translational research in radiation oncology. However, adverse effects of radiation and infectious diseases may ruin the experimental work, in particular when appropriate facilities are not available. In this report, we describe a procedure to deliver fractionated radiotherapy to xenoimplanted tumours in immunodeficient mice using a medical linear accelerator, a method that was devised as an alternative to the lack of facilities devoted to radiation research. The mice were irradiated under anaesthesia and aseptic conditions. Thirty Gray in 10 days using a 6 MV photon beam were delivered only to the right thigh of the mice where tumours were implanted. The mice were evaluated twice a week up to planned euthanasia. The follow-up of mice was completed without premature interruption due to toxicities or infectious diseases, an observation which demonstrates the feasibility of the method.

Keywords: Xenografted tumours, immunodeficient mice, local fractionated radiotherapy, medical linear accelerator

Laboratory Animals 2012: 1–4. DOI: 10.1258/la.2012.011147

Every year, millions of cancer patients around the world undergo radiotherapy, alone or in combination with drugs. The rise in radiotherapy use, together with an avenue of novel drugs that modulate radiotherapy action, has prompted an increased interest in radiation oncology research. An important part of this research is based on the irradiation of human tumours grown in mice.[1,2] However, such experimental models are associated with a number of difficulties that can ruin the experimental outcomes. First, it is difficult to shield radiosensitive healthy tissues from the radiation field and avoid its adverse effects in the absence of appropriate equipment to irradiate mice, such as an orthovoltage X-ray treatment machine.[3] Second, to prevent the tumour rejection mediated by a normal immune system, human tumour cells have to be implanted in immunodeficient mice which are prone to lethal infectious diseases. Third, there is a general lack of specific pathogen free (SPF) facilities to irradiate mice. Since these have to be transferred from the SPF colony to medical radiotherapy units, the risk of infectious outbreaks is greatly increased. Finally, to make matters even more complex, often experimental design requires multiple fractions of radiotherapy, which exposes mice to pathogens more frequently.

In this short report, we describe the experimental procedure and the refinements we applied to successfully deliver high doses of fractionated radiotherapy to xenoimplanted human tumours, protect radiosensitive tissues and decrease the microbiological risk when irradiating immunodeficient mice using a medical linear accelerator. Importantly, we devised this procedure as an alternative to the lack of experimental facilities devoted to radiation research in immunodeficient mice.

*Marta Baro and Lara I de Llobet contributed equally to this work and should be considered co-first authors

All experimental methods were approved in accordance with our own institutional IDIBELL guidelines for animal care and ethics. Six to eight-week-old female athymic mice (Athymic Nude-Foxn1^{nu}, Harlan, Gannat, France) were used. Complete health reports, especially the microbiological status of the animals based on the Federation of European Laboratory Animal Science Associations (FELASA) recommendations, were certified by the vendor. Tumours were generated by injecting one million human cancer cells delivered in 100 μL into the subcutaneous tissue. The mice were intraperitoneally anaesthetized (1 mL/kg of each solution: 50 mg/mL ketamine and 1 mg/mL medetomidine with 5 mg/mL atipamezole for the reversal of the anaesthesia effects) in order to precisely control the area in which the cells were to be injected and to obtain homogenous growth of tumours. We decided to inject the cells in the right thigh of the mice, which allowed us to irradiate exclusively a limited part of the body. This decision served to protect the rest of the animal body from radiation.

At a suitable tumour size, and two days before irradiation, the mice were moved from the SPF area to a quarantine room so they can adapt to the new housing conditions, and where the animals were to be permanently housed in closed autoclaved plastic cages (5 mice per cage). In this room, the mice were manipulated under a laminar flow hood using aseptic conditions. Before each radiotherapy session, they were anaesthetized, as mentioned above, and transported to the radiotherapy unit in clean autoclaved closed cages covered with a drape to conceal the animals from plain view.

Upon arrival at the radiotherapy room, the treatment table was disinfected with alcohol and covered with sterile drapes. Surgical caps, masks and sterile gloves were worn. Figure 1 shows the scheme of how an appropriate setting for selectively irradiating tumours and reducing infections in the mice was achieved. Of note is the placement of the thigh on the edge of the radiation beam to allow sufficient coverage of the tumour, while protecting the body of the mice as much as possible.

To irradiate the animals, as shown in Figure 1, a 6 MV photon beam from a Varian Clinac 2100 linear accelerator was used. A total dose of 30 Gray (Gy) in fractions of 3 Gy, separated by 24 h, excluding Saturdays and Sundays was administrated. The dose rate was 2.7 Gy per minute. In order to verify the dose that the tumours received, as well as the precision of the set-up used, an *in vivo* dosimetry was performed by means of radiochromic films (Gafchromic EBT, International Specialty Products, Wayne, NJ, USA). In total, 40 dose measurements were carried out during four separate days. Films were placed in contact with the tumour at the beam entrance. We found less than 3% variation in the doses received by different mice on the same sessions and less than 1.5% variation between different days. The mean deviation in absorbed dose in the tumours was 2.3% of the prescribed dose. The aforementioned results confirmed that our experimental set-up was homogeneous and reproducible.

The mice were evaluated twice a week. Table 1 describes the animals' health during the radiotherapy period and follow-up. Non-irradiated mice were subjected to the same procedures. No animals were excluded or had received less than 30 Gy in 10 fractions. After radiotherapy, tumours grew more slowly and took twice the time to reach a volume equivalent to non-irradiated animals. The most severe observation was always registered, whether it was reversible or not. The greatest adverse effect of

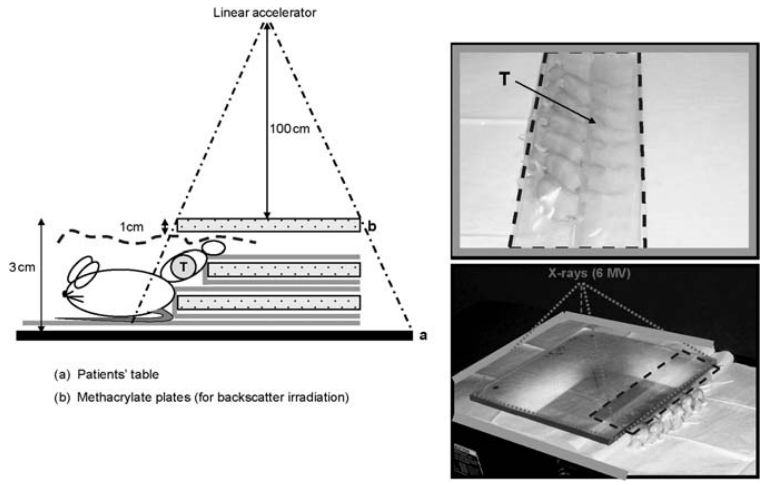

Figure 1 Scheme used for localized irradiation of xenografted tumours in multiple fractions. Tumours (T) were placed into the gap created by two polymethyl methacrylate (PMMA) plates (b), each were 35 cm × 35 cm × 1 cm in size, separated by a smaller plate (30 cm × 30 cm × 1 cm). The edge of the beam was adjusted to cover the tumour with 1 cm margin, assuring that PMMA plates were included into the beam. The thighs were kept in place using an adhesive tape, while the body of animals was maintained out of the beam. Sterile drape that cover the treatment table (a) and wrapped PMMA plates are represented by the grey lines. Dotted line illustrates the sterile transparent film put on to the mice, protecting them from the non-sterile top PMMA plate, as it can also be observed in the pictures on the right. The source-plate distance was set to 100 cm on the centre of the top plate. Note that dimensions in the diagram are not to scale

Table 1 Quality of life of the mice during and after localized irradiation in multiple fractions

	Control mice (non-irradiated)								X-ray-treated mice							
	Therapy period (n = 13)				Post-therapy period (n = 12)				Therapy period (n = 32)				Post-therapy period (n = 31)			
	Grade score (%)				Grade score (%)				Grade score (%)				Grade score (%)			
Supervision parameters	**0**	**1**	**2**	**3**	**0**	**1**	**2**	**3**	**0**	**1**	**2**	**3**	**0**	**1**	**2**	**3**
Weight loss[†]	76.9	15.4	7.7	0	83.3	8.3	8.3	0	43.8	46.9	9.4	0	61.3	35.5	3.2	0
Physical aspects[‡]	100	0	0	0	100	0	0	0	100	0	0	0	100	0	0	0
Clinical signals[¶]	100	0	0	0	100	0	0	0	100	0	0	0	100	0	0	0
Behaviour alterations[#]	100	0	0	0	100	0	0	0	100	0	0	0	87.1	12.9	0	0
Infections[††]	100	0	0	–	100	0	0	–	100	0	0	–	100	0	0	–
Stools[‡‡]	100	0	0	–	100	0	0	–	100	0	0	–	100	0	0	–
Tumour necrosis[¶¶]	100	0	–	–	91.7	8.3	–	–	100	0	–	–	100	0	–	–
Local radiation toxicity[##]	100	0	0	0	100	0	0	0	100	0	0	0	100	0	0	0

Values are the proportion of an observation expressed in grades related to the total number of animals (n) within the period of follow-up

[†]*Weight loss*. Grades: 0 no weight loss; 1 less than 10%; 2 between 10 and 20%; 3 more than 20%

[‡]*Physical appearance*. Grades: 0 normal; 1 changes in skin colour; 2 paleness and cyanosis; 3 hunching and loss of muscular mass

[¶]*Clinical signals*. Grades: 0 no presence; 1 hypothermia; 2 bleeding or mucosal secretion in any orifice; 3 abdominal strain and cachexia

[#]*Behaviour alterations*. Grades: 0 no alterations; 1 unable to move normally; 2 impossible to arrive to food/drink; 3 unconsciousness and no response to stimuli

[††]*Percentage of animals with infectious disease*. Grades: 0 no infections; 1 animals infected that survived; 2 animals infected that died. Grade 3 not evaluated (NA)

[‡‡]*Stools appearance*. Grades: 0 normal; 1 soft stools; 2 visible blood. Grade 3 NA

[¶¶]*Percentage of tumour necrosis*. Grades: 0 no tumour necrosis; 1 tumour necrosis. Grades 2 and 3 NA

[##]*Local radiation-induced toxicity*. Grades: 0 no presence; 1 erythema; 2 exudative lesion; 3 necrosis

radiation was the diminution in the initial weight, which we ascribed to the partial exposure of the inferior right hemiabdomen, which was much too close to the tumour to be completely protected from the radiation beam. However, the weight loss was not remarkable and was limited to grade 1, transitory and not associated with physical or clinical signs of disease. Also, in the irradiated group, two animals (12.9%) moved abnormally due to tumour growth, but not to local reaction because of the radiation. Interestingly, in non-irradiated mice greater weight loss was observed, which was attributable to uncontrolled tumour growth. Differences in weight loss between groups, however, were not significant (chi-square and Mann-Whitney *U* test). No infections were observed. Euthanasia using intraperitoneal pentobarbital solution (4.5 mL/kg dose of 200 mg/mL of Dolethal) was planned at day +90, or, before, in cases where more than one grade 2 or one grade 3 event was observed, or when the tumour size reached more than 1500 mm^3; however, only the last criterion had had to be applied. We applied these criteria following the international guidelines for the welfare and use of animals in cancer research.[4]

In this report, four objectives were considered during radiotherapy design. First, minimize irradiation of healthy tissues around the tumour. Second, fulfil the standard irradiation principles for human treatment.[5,6] Third, reduce time and increase efficiency by irradiating several mice at a time. Finally, be easy to reproduce and repeat on a daily basis by only two people. We demonstrated the feasibility of fractionated irradiation using immunodeficient mice to evaluate the role of radiotherapy on experimental tumours simulating a clinical setting. The major contribution of this study, however, was to demonstrate that general or local effects of irradiation did not jeopardize the tumour radiation–response observation over a long follow-up. In addition, the absence of infect–contagious diseases was particularly decisive for the success of experiments. This provided evidence that the barrier protections used accomplished the goal of preventing microbiological diseases in these animals. Since cancer patients are often immunosuppressed, concerns about zoonoses should not be ignored. Nevertheless, it should be emphasized that the potential risk of zoonoses is extremely low when good laboratory practices and healthy athymic mice are used. To our knowledge, there is no report in the medical literature about the incidence of opportunistic zoonoses in patients treated in such radiation oncology departments.

In conclusion, this study describes an effective method to irradiate human tumours implanted in immunodeficient mice which allows monitoring of tumour responses without interference from the adverse effects of radiation and infection. We demonstrate the feasibility of delivering fractionated radiotherapy using a medical accelerator when a specific experimental facility is not available for radiation research.

ACKNOWLEDGEMENT

The authors would like to acknowledge the financial support of the Spanish Association Against Cancer, Barcelona Committee.

Conflict of interest: Actual or potential conflicts of interest do not exist.

REFERENCES

1 Steel GG. How well do xenografts maintain the therapeutic response characteristics of the source tumor in the donor patient? In: Kallan RF, ed. *Rodent Tumors in Experimental Cancer Therapy*. New York: Pergamon, 1987:205–8

2 Milas L, Fang FM, Mason KA, *et al*. Importance of maintenance therapy in C225-induced enhancement of tumor control by fractionated radiation. *Int J Radiat Oncol Biol Phys* 2007;**67**:568–72

3 Medina LA, Herrera-Penilla BI, Castro-Morales MA, *et al*. Use of an orthovoltage X-ray treatment unit as a radiation research system in a small-animal cancer model. *J Exp Clin Cancer Res* 2008;**27**:57

4 Workman P, Aboagye EO, Balkwill F, *et al*. Guidelines for the welfare and use of animals in cancer research. *Br J Cancer* 2010; **102**:1555–77
5 International Commission on Radiation Units and Measurements (ICRU). *Prescribing, Recording, and Reporting Photon Beam Therapy*. ICRU Report 50. Bethesda: ICRU, 1993
6 International Commission on Radiation Units and Measurements (ICRU). *Prescribing, Recording, and Reporting Photon Beam Therapy*. ICRU Report 62 (supplement to ICRU Report 50). Bethesda: ICRU, 1999

(Accepted 30 March 2012)